



HAL
open science

Transport of critical services over unlicensed spectrum in 5G networks

Ayat Zaki Hindi

► **To cite this version:**

Ayat Zaki Hindi. Transport of critical services over unlicensed spectrum in 5G networks. Networking and Internet Architecture [cs.NI]. Institut Polytechnique de Paris, 2020. English. NNT : 2020IP-PAS022 . tel-03118924

HAL Id: tel-03118924

<https://theses.hal.science/tel-03118924>

Submitted on 22 Jan 2021

HAL is a multi-disciplinary open access archive for the deposit and dissemination of scientific research documents, whether they are published or not. The documents may come from teaching and research institutions in France or abroad, or from public or private research centers.

L'archive ouverte pluridisciplinaire **HAL**, est destinée au dépôt et à la diffusion de documents scientifiques de niveau recherche, publiés ou non, émanant des établissements d'enseignement et de recherche français ou étrangers, des laboratoires publics ou privés.



INSTITUT
POLYTECHNIQUE
DE PARIS



NNT : 2020IPPAS022

Thèse de doctorat

Transport des services critiques dans le spectre non-licencié des réseaux 5G

Thèse de doctorat de l'Institut Polytechnique de Paris
préparée à Télécom SudParis

École doctorale n°626 Ecole Doctorale de l'Institut Polytechnique de
Paris (ED IP Paris)

Spécialité de doctorat: Réseaux, Informations et Communications

Thèse présentée et soutenue à Paris, le 2 décembre 2020, par

AYAT ZAKI HINDI

Composition du Jury :

Catherine Rosenberg Professeur, University of Waterloo, Canada	Président
Antonio Capone Professeur, Politecnico di Milano, Italie	Rapporteur
Stefano Secci Professeur, Conservatoire National des Arts et Métiers, France	Rapporteur
Klaus Pedersen Professeur, Aalborg University, Denmark	Examineur
Pierre Dubois Ingénieur de recherche, Orange Labs, France	Examineur
Tijani Chahed Professeur, Télécom SudParis, France	Directeur de thèse
Salah-Eddine Elayoubi Maître de conférences, CentraleSupélec, France	Co-directeur de thèse



Transport of critical services over unlicensed spectrum in 5G networks

PhD dissertation prepared at the Institut Polytechnique de Paris, Télécom
SudParis

Presented and defended at Paris, 2 December 2020, by

AYAT ZAKI HINDI

Jury members:

Catherine Rosenberg Professor, University of Waterloo, Canada	President
Antonio Capone Professor, Politecnico di Milano, Italy	Reviewer
Stefano Secci Professor, Conservatoire National des Arts et Métiers, France	Reviewer
Klaus Pedersen Professor, Aalborg University, Denmark	Examiner
Pierre Dubois Research engineer, Orange Labs, France	Examiner
Tijani Chahed Professor, Télécom SudParis, France	Thesis supervisor
Salah-Eddine Elayoubi Associate professor, CentraleSupélec, France	Thesis co-supervisor

To my parents, for their
limitless love and support.

Abstract

We study in this thesis the transport of critical services in 5G networks, where unlicensed spectrum is advocated so as to minimize the cost and to cope with the high demand for frequency resources.

We first evaluate the performance of Ultra-Reliable Low-Latency Communication (URLLC) which has stringent requirements on reliability and delay, on the order of 99.999% and 1 ms, respectively, transported in unlicensed spectrum. We propose a model based on a Markov chain that quantifies the reliability within a delay constraint under Listen-Before-Talk (LBT) medium access procedure, and deduce the maximum number of stations that can be handled at the same time, while respecting URLLC constraints.

This analysis is then used to investigate novel methods for the joint transmission of URLLC over unlicensed and licensed spectrum. We propose three methods for the joint access to available resources, and demonstrate that the optimal method to access the resources is by using licensed ones only when unlicensed transmission fails within a given time budget. This method is then studied in the case of multiple tenants in proximity competing over the same unlicensed channel. If all tenants try to maximize their usage of unlicensed resources then everyone will end up in a tragedy of the commons type of situation. We show that at least one equilibrium point exists for this system which minimizes the cost for all tenants.

We study next the coexistence of URLLC with other 5G services, such as enhanced Mobile Broadband (eMBB), in unlicensed spectrum. eMBB has large packets and its multiplexing with URLLC may entail a large degradation in the latter's performance. We then propose a new technique to prioritize URLLC packets by transmitting them with higher power. However, high power transmission is not systematically performed so as to reduce the interference on other users and also to minimize energy consumption,

which is very important for battery-powered devices. In this case, we propose two methods to transmit with high power, as a last resort: one that is LBT-agnostic and transmits whenever the packet delay approaches time-out, and another one which respects LBT and uses high power only when transmission opportunities occur beyond a time threshold.

We then propose a decentralized implementation of the time-threshold approach. We formulate the problem as an optimization problem where transmitters are to choose the optimal policy (time threshold) which minimizes the energy consumption while preserving URLLC requirements. We then solve the optimization problem using a learning approach, which suffers from slow convergence to the optimal policy due to the fact that losses are rare events. To remedy to this, we make use of our optimization framework and the prior knowledge of the system model to accelerate this learning.

We finally study the decentralized approach for a different type of critical services which focuses on the freshness of the information, known as the Age of Information (AoI). In this context, instead of guaranteeing URLLC's reliability target within a delay, the packet must be delivered as soon as it is generated, or else it loses its value. We demonstrate that optimal policies in the AoI context tend to start aggressively, and reduce the transmission power when the age of the packet increases.

Keywords - 5G, critical services, Unlicensed spectrum, URLLC.

Résumé

La cinquième génération (5G) des réseaux mobiles est la première génération de téléphonie mobile à être conçue pour des cas d'usage autres que la voix et la donnée. Les cas d'usage de la 5G se définissent selon trois services : les communications mobiles ultra-hautes débit (eMBB), les communications entre objets (mMTC), et les communications dites critiques (URLLC), pour lesquelles la fiabilité et le temps de réponse sont primordiaux. Les communications critiques sont particulièrement intéressantes car grâce à elles, des nouveaux services vont être déployés, comme les machines et les véhicules autonomes et la chirurgie médicale par assistance robotique.

Afin d'assurer les besoins rigoureux de chaque service (eMBB, mMTC et URLLC) et particulièrement les services critiques (URLLC), il faut réserver une grande quantité de ressources sous forme de bandes de fréquences, c'est-à-dire une bonne partie des nouvelles bandes de fréquence de la 5G seront vendues aux enchères par les états aux opérateurs télécoms. Cette thèse étudie le transport des services critiques dans les réseaux 5G, où le spectre non-licencié est préconisé pour minimiser le coût et faire face à la forte demande de ressources en fréquences.

Nous évaluons d'abord les performances des services critiques type URLLC (Ultra-Reliable Low-Latency Communication) qui a des exigences strictes en matière de fiabilité et de latence, de l'ordre de 99,999% et 1 ms, respectivement, transporté dans le spectre non-licencié. Nous proposons un modèle basé sur une chaîne de Markov pour quantifier la fiabilité sous contrainte de délai, sous procédure d'accès au support Listen-Before-Talk (LBT), puis nous en déduisons le nombre maximum de stations pouvant être servies en même temps, tout en respectant l'URLLC contraintes. Cette analyse est ensuite utilisée pour étudier de nouvelles méthodes pour la transmission conjointe d'URLLC sur les spectres non-licencié et licencié. Nous proposons trois méthodes pour l'accès conjoint aux ressources disponibles et démontrons

que la méthode optimale pour accéder aux ressources consiste à utiliser des ressources licenciées, uniquement lorsque la transmission dans le système non-licencié échoue dans un budget de temps donné. Cette méthode est ensuite étudiée dans le cas de plusieurs tenants à proximité en concurrence sur le même canal non-licencié. Si tous les tenants essaient de maximiser leur utilisation des ressources non-licenciées, tout le monde se retrouvera dans une situation type “tragédie des biens communs”. Nous montrons qu’au moins un point d’équilibre existe pour ce système qui minimise le coût pour tous les tenants.

Nous étudions ensuite la coexistence d’URLLC avec d’autres services 5G, tels que le haut débit mobile amélioré eMBB (enhanced Mobile Broadband), dans le spectre non-licencié. eMBB a de grandes paquets et son multiplexage avec URLLC peut entraîner une forte dégradation des performances d’URLLC. Pour cela, nous proposons une nouvelle technique pour prioriser les paquets URLLC en les transmettant avec une puissance plus élevée. Cependant, la transmission à haute puissance n’est pas systématiquement effectuée afin de réduire les interférences sur les autres utilisateurs et aussi pour réduire la consommation d’énergie, ce qui est très important pour les appareils alimentés par batterie. Dans ce cas, deux méthodes ont été proposées pour transmettre avec une puissance élevée, en ne le laissant qu’en dernier recours. L’un est indépendant du LBT et transmet une fois le délai de paquet approche de l’expiration, tandis que l’autre respecte le LBT et n’utilise une puissance élevée que lorsque les opportunités de transmission se produisent au-delà d’un seuil de temps.

Nous proposons ensuite une mise en œuvre décentralisée de l’approche par seuil de temps décrit ci-dessus. Nous formulons le problème dans le cadre d’optimisation où les émetteurs doivent choisir la politique optimale (seuil de temps) qui minimise la consommation d’énergie tout en préservant les exigences d’URLLC. Nous résolvons ensuite le problème d’optimisation en utilisant une approche d’apprentissage et montrons une lente convergence vers la politique optimale du fait que les pertes sont des événements rares. Pour y remédier, nous utilisons le cadre d’optimisation et la connaissance préalable du système pour accélérer cet apprentissage. Nous étudions enfin l’approche décentralisée pour un type différent de services critiques qui met l’accent sur la fraîcheur de l’information, connue sous le nom d’Age de

l'Information (AoI). Dans ce contexte, au lieu de garantir une cible de fiabilité dans un délai, le paquet doit être livré dès sa génération, sinon sa valeur se dégrade. Nous démontrons que les politiques optimales dans le contexte AoI ont tendance à démarrer de manière agressive et à réduire la puissance de transmission lorsque l'âge du paquet augmente.

Mots clés - 5G, services critiques, spectre non-licencié, URLLC.

Acknowledgement

I would like to express my deepest gratitude and appreciation to my thesis supervisors, Tijani Chahed and Salah-Eddine Elayoubi, for all their guidance and support throughout the past three years. It was a great privilege and honor to work under their supervision. Their rigorous work, dynamism and their passion for research have deeply inspired me and also provided me with the tools and methodology to carry out my research. I am equally grateful for having such a great team leader at Orange, Pierre Dubois. I would like to thank him for having the confidence in me and for giving me the opportunity to conduct my work within his team.

I would like to graciously thank both Prof. Stefano Secci and Prof. Antonio Capone for reviewing my manuscript and for their useful remarks. I wish to thank as well Prof. Catherine Rosenberg and Prof. Klaus Pedersen for taking the time and the effort to be part of the jury. I enjoyed all the discussions during my PhD defense, which helped me see my work from different perspectives.

Finally, this experience would not have been the same without all the love and support from the people around me. I am extremely grateful for having someone as Ragheed by my side, especially that we were both doing our PhDs at the same time. I will never forget the precious moments that I have shared with my friends and colleagues in Orange (Abdellatif, Elkin, Felipe, Imène, Meriem, Mira, Nathalie, Rita, Romain, Stefan, Thomas, Zheng, ...). And of course, the people to whom I owe the most, my family (My mother Lina, my father Esmat, my sisters: Lama, Kinda and Afaq), who encouraged me and offered me everything without hesitation.

Contents

Résumé	x
Acknowledgement	xii
1 General Introduction	1
2 Unlicensed spectrum for URLLC service transport	5
2.1 Introduction	5
2.2 Preliminaries	6
2.2.1 Listen-Before-Talk	6
2.2.2 Bianchi model	7
2.3 URLLC traffic model	10
2.4 Delay-constrained Markov model	11
2.4.1 Stationary distribution	13
2.4.2 Transmission Reliability	14
2.5 Numerical evaluation	15
2.6 Conclusion	17
3 Joint transmission over unlicensed and licensed spectrum	19
3.1 Introduction	19
3.2 Licensed spectrum for critical services transport	20
3.2.1 Licensed medium access	20
3.2.2 System model	21
3.2.3 TTI bundling for URLLC	21
3.2.4 Numerical evaluation	23
3.3 Joint unlicensed-licensed access	25
3.3.1 Duplication method	27
3.3.2 Probabilistic system choice method	27
3.3.3 In series method	28

3.3.4	Numerical evaluation	29
3.4	Multi-tenant environment	32
3.4.1	System model	33
3.4.2	Medium access model in unlicensed spectrum	34
Fixed-point analysis		34
Closed-form analysis		35
3.4.3	Utility function	37
3.4.4	Numerical evaluation	37
3.4.5	Price of anarchy	39
3.5	Conclusion	40
4	URLLC and eMBB coexistence in unlicensed spectrum	41
4.1	Introduction	41
4.2	System model	42
4.3	Equal power transmission	43
4.3.1	URLLC medium access model	43
4.3.2	eMBB medium access model	47
4.3.3	Numerical evaluation	48
4.4	LBT-agnostic preemption	50
4.4.1	URLLC medium access model	51
4.4.2	eMBB medium access model	52
4.4.3	Numerical evaluation	53
4.5	LBT-aware time threshold policy	53
4.5.1	URLLC medium access model	54
4.5.2	eMBB medium access model	57
4.5.3	Numerical evaluation	57
4.6	Comparison and discussion	59
4.7	Conclusion	60
5	Distributed decision making for unlicensed channel access	63
5.1	Introduction	63
5.2	System model and optimization problem formulation	65
5.3	Aloha-like systems	66
5.3.1	Optimizing the policy for one station	66
5.3.2	Case of a field of transmitters	69
5.4	Listen Before Talk systems	71
5.4.1	Distribution of the number of opportunities	72

5.4.2	Optimal policy	73
5.4.3	Case of a field of transmitters	73
5.5	Learning optimal policies	74
5.5.1	MAB algorithms	74
5.5.2	MAB implementation	75
5.5.3	Performance evaluation	76
5.5.4	Model-aided learning	78
5.6	Conclusion	79
6	Revisiting transmission policies for packet age minimization objective	81
6.1	Introduction	81
6.2	Minimizing depreciation related to age	82
6.3	Policies that minimize the packet age	83
6.3.1	Formulation of the optimization objective	83
6.3.2	Solving the optimization problem	85
6.3.3	Fixed point analysis for a field of sensors	86
6.4	Conclusion	88
7	General Conclusion and Perspectives	89

List of Figures

2.1	Markov chain of Bianchi model for LBT cat4.	7
2.2	The one-step resulting states of state $\{i, j, k\}$	11
2.3	Markov chain for LBT cat3 incorporating a timer.	12
2.4	Model validation with simulation, loss rate with respect to the number of stations.	16
2.5	System capacity: the maximum number of stations respecting URLLC requirements, versus the contention window size.	18
3.1	Grant-based scheduling in licensed spectrum	21
3.2	Model validation with simulation. Loss rate with respect to number of stations for licensed system, $\delta_{max} = 8$ and $K = 10$	24
3.3	Cost with respect to the number of stations for licensed system, $\delta_{max} = 8$	25
3.4	Methods of joint unlicensed-licensed transmission. A packet is lost if none of its replicas were delivered successfully, as is the case for packet 2 of <i>Probabilistic system choice</i> method and packet 1 of <i>In series</i> method. Licensed spectrum is not necessarily used in <i>In series</i> method as for packet 3.	26
3.5	Loss rate with respect to the number of stations for standalone unlicensed and licensed systems, <i>Duplication</i> , <i>Probabilistic system choice</i> for $\mu = 0.5$ and <i>In series</i> for $\delta = 4$	30
3.6	Cost with respect to the policy μ for <i>Probabilistic system choice</i> method for $N = \{200, 250, 300\}$	31
3.7	Cost with respect to the policy δ for <i>In series</i> method for $N = \{200, 250, 300\}$	32
3.8	Cost with respect to the number of stations of: Duplication, Probabilistic system choice, In series and standalone licensed systems, at which URLLC requirements are guaranteed.	33

3.9	Validation of closed-form model with the fixed-point for unlicensed spectrum with two tenants.	38
3.10	Price of anarchy of the non-cooperative game.	39
4.1	The one-step resulting states of state $\{i, j, k\}$ of URLLC coexisting with eMBB.	43
4.2	First stage of Markov chain model for URLLC coexisting with eMBB. Example: $W = 6, \rho_e + 1 = 3(\rho_u + 1)$ and $m_u \geq 4$	44
4.3	URLLC model validation coexisting with eMBB.	49
4.4	eMBB model validation for the harmonious coexistence with URLLC.	50
4.5	URLLC model validation for the LBT-agnostic preemption approach.	53
4.6	eMBB model validation for the LBT-agnostic preemptive approach.	54
4.7	URLLC model validation for a time threshold policy $\tau = 7$	57
4.8	eMBB model validation for a time threshold policy $\tau = 7$	58
4.9	Policy and CW size effect on the performance. $N_e = 2, N_u = 100$ and $W = 4$	59
4.10	Comparison of high power utilization of the LBT-agnostic preemption and time threshold approaches. $N_e = 2, W = 4$ and $W_0 = 32$	60
5.1	Energy and loss values for different policies, $q_1 = 0.5, q_2 = 0.1, P_1 = 0.1 W, P_2 = 0.5 W, T = 1$ ms, $\alpha = 13$	68
5.2	Energy and loss values for different policies, $q_1 = 0.1, q_2 = 0.5, P_1 = 0.5 W, P_2 = 0.1 W, T = 1$ ms, $\alpha = 13$	69
5.3	Expected loss rate and energy consumption for a field of stations using Aloha. $N = 50, T = 1, P_1 = 0.1, P_2 = 0.5, \alpha = 15, \rho = 0.1, \lambda = 0.01$ (τ in ms)	71
5.4	Expected loss rate and energy consumption for a field of stations using LBT, $N = 100, W = 16, T = 1$ ms, $\rho = 7, P_1 = 0.1, P_2 = 0.5$, time slot of $9 \mu s$ (τ in slots)	74
5.5	Convergence time of the ϵ -greedy MAB algorithm for URLLC case in LBT system, $\epsilon = 0.2$	77
5.6	Convergence time of model-aided MAB	79

6.1	Energy consumption and value depreciation for Aloha and exponential value depreciation with $\beta = 2.4$, $\alpha = 5$, $P_1 = 0.5$, $P_2 = 0.1$, $q_1 = 0.1$, $q_2 = 0.5$	87
6.2	Comparing aggressive versus mild start for Aloha	87
6.3	Energy consumption, value depreciation and objective function at $\gamma = 0.3$ for LBT in a field of sensors and exponential value depreciation with $\beta = 2$	88

List of Tables

3.1	Numerical values of unlicensed and licensed system parameters.	29
3.2	Nash equilibrium illustration	38
4.1	Numerical values of the system parameters of URLLC and eMBB coexistence.	49

List of publications

Journal paper

[J1] Ayat Zaki-Hindi, Salah-Eddine Elayoubi, and Tijani Chahed. "Multi-tenancy and URLLC on unlicensed spectrum: performance and design." *Computer Networks* (2020): 107311.

Conference papers

[C1] Ayat Zaki Hindi, Salah-Eddine Elayoubi, and Tijani Chahed. "Performance evaluation of ultra-reliable low-latency communication over unlicensed spectrum." In: *ICC 2019-2019 IEEE International Conference on Communications (ICC), Shanghai, China, pp. 1-7.*

[C2] Ayat Zaki-Hindi, Salah-Eddine Elayoubi, and Tijani Chahed. "URLLC and eMBB coexistence in unlicensed spectrum: a preemptive approach". In: *Proceedings of the 16th International Wireless Communications & Mobile Computing Conference (IWCMC 2020), Limassol, Cyprus, pp. 229-234.*

[C3] Ayat Zaki-Hindi, Salah-Eddine Elayoubi, and Tijani Chahed. "Unlicensed spectrum for Ultra-Reliable Low-Latency Communication in multi-tenant environment". In: *The 10th International Conference on NETWORK Games, CONTROL and OPTimization (NETGCOOP), Corsica, France.*

[C4] Ayat Zaki-Hindi, Salah-Eddine Elayoubi, and Tijani Chahed. "Optimal preemptive retransmission strategy for URLLC in unlicensed spectrum". In: *The 2020 IEEE Global Communications Conference (GLOBECOM), Taipei, Taiwan.*

[C5] Ayat Zaki-Hindi, Salah-Eddine Elayoubi, and Tijani Chahed. "Model-Aided Learning for URLLC Transmission in Unlicensed Spectrum". In: *The MASCOTS 2020 Symposium on Modelling, Analysis, and Simulation of Computer and Telecommunication Systems, Nice, France.*

[C6] Ayat Zaki-Hindi, Salah-Eddine Elayoubi, and Tijani Chahed. "Optimal

transmission policies for critical services over wireless networks: ultra reliability versus packet age minimization". **Submitted**

Chapter 1

General Introduction

The fifth generation of mobile networks (5G) is expected to support new applications beyond those currently transported by existing 4G networks. In this context, three main services were defined: enhanced Mobile Broadband (eMBB), massive Machine-Type Communication (mMTC) and Ultra-Reliable Low-Latency Communication (URLLC) [1].

eMBB extends the 4G broadband service to support higher traffic loads with enhanced data rates that can go up to 20 Gbps [1]. Some of eMBB's use cases include web browsing, video streaming and file sharing. The second type of services, namely mMTC, involves a potentially huge number of connected objects which for instance monitor the environment and generate small packets periodically, similar to an Internet of Things (IoT) scenario. mMTC devices favor low cost and low energy consumption over high data rates and reliability requirements, which is convenient for applications such as smart buildings/cities and shipment tracking where battery-powered devices need to conserve their energy to keep reporting their status as long as possible. URLLC, which can be described as a critical machine-type communication, involves also a large number of connected objects which generate small packets for instance when a triggering event occurs. Here, the packets are expected to carry rather vital information about the system that must be conveyed to a controller that is situated in a central server in most of the cases, reliably within a small delay to avoid any failure. This service allows the existence of many promising applications such as factory automation, remote surgery and autonomous vehicles.

URLLC is considered as the most challenging service in 5G, because it has unprecedentedly stringent requirements in terms of reliability and latency, on the order of 99,999% and 1ms, respectively [2]. One of the most important

aspects of URLLC transport is the time-frequency trade-off, where restrictions in the time domain lead to requiring a large frequency bandwidth to guarantee the target reliability (without considering space or code diversity). Using licensed spectrum, as in previous generations, entails a huge cost for operators who buy at very high price the license to use certain channels for a fixed duration generally in auctions organized by the country's administrative authority responsible for spectrum allocation. To give insights about the price, the 5G spectrum auction in France took place in September 2020, it generated 2.8 billion euros to the French state from the four qualified operators [3]. Regarding the allocated bandwidth, no operator was able to get more than 100 MHz, which makes it a valuable resource that must be utilized efficiently.

The cost and scarcity of licensed spectrum calls then for the usage of unlicensed spectrum that is cheaper and available at higher quantities. The interest in unlicensed spectrum for mobile networks has begun since LTE Licensed-Assisted-Access (LTE-LAA) [4] and 5G has shown its flexibility by regulating several unlicensed bands in the 5G New Radio (NR) [5], notably the 5 GHz bands currently used by some IEEE 802.11 technologies. Furthermore, unlicensed spectrum usage is becoming popular for industrial automation (e.g., WirelessHart [6] and Multefire [7] systems), vehicular communications (e.g., IEEE 802.11p [8] and ETSI ITS G5 [9] standards) and sensor networks (e.g., LoRa [10] and Sigfox [11] systems).

In this thesis, we are interested in the transport of URLLC over unlicensed spectrum, and specifically the design of new transmission schemes for URLLC in the Medium Access Control (MAC) layer that meet the required, stringent reliability and delay constraints.

Contributions and organization

Our main contributions as well as the organization of the rest of this dissertation are as follows:

- In Chapter 2, we study the transport of URLLC over unlicensed spectrum and propose a new model based on a Markov chain that quantifies the reliability of the transmission system under delay constraints. Using this model, we derive the capacity of the standalone unlicensed

system which corresponds to the maximum number of stations verifying the URLLC Quality of Service (QoS) requirements.

- In Chapter 3, we propose the joint transmission of URLLC over unlicensed and licensed spectrum. We propose three methods for this joint transmission scheme, evaluate their performance and compare their costs, in terms of additional licensed frequency resources, to a standalone licensed system. We show that the optimal transmission scheme uses licensed resources only when the licensed system fails to transmit the packet within a fraction of the delay budget. We extend the analysis to a multi-tenant environment where tenants compete over the unlicensed resources, which may result in a tragedy of the commons type of situation. We study the equilibrium point of such a system which minimizes the cost for all tenants.
- In Chapter 4, we focus on the transport of URLLC coexisting with eMBB in unlicensed spectrum. In this case, using additional licensed resources to guarantee the requirements for both services generates a huge cost. Instead, we exploit diversity in power domain and propose two prioritization techniques for URLLC over eMBB, both based on transmitting URLLC using a higher power level. The first method makes use of pre-emption using high power transmission when the URLLC delay budget is about to expire, which does not respect Listen-Before-Talk (LBT) mechanism. The second one respects LBT and makes use of a time threshold within the delay budget after which transmission power is switched from low to high.
- In Chapter 5, we consider a decentralized setting, with no central entity to decide for the optimal policy to be followed by the URLLC stations. We focus on the time threshold method developed in the previous chapter, and analyse its performance in Aloha-like and LBT systems. We use an online learning approach to enable each station to achieve the optimal policy in a distributed manner. We also make use of our prior knowledge of the system model so as to accelerate the convergence of the learning algorithm.
- In Chapter 6, we consider a different setting, for instance monitoring of a dynamic environment, where minimization of the age of the packets,

or equivalently maximization of the freshness of information, is more valuable than meeting URLLC's strict reliability and delay constraints. We showed in the previous chapters that in the case of meeting URLLC stringent requirement, the optimal policies tend to start transmission with normal power level and then increase it as the packet delay approaches the allowed budget. However, when the objective is to minimize the delay of the packet, we show in this chapter that optimal policies favor starting at high power level, while the URLLC objective leads to a mild start followed by a power increase near the deadline expiration.

- In Chapter 7, we eventually conclude the dissertation by summarizing the contributions and indicate some future work perspectives.

Chapter 2

Unlicensed spectrum for URLLC service transport

2.1 Introduction

Unlicensed spectrum is a key enabler for 5G networks, regarding the expected huge traffic load in the future. In this chapter, we are interested in the transport of critical services, i.e. URLLC, over unlicensed spectrum in an Industry 4.0 case-study, comprised of a set of automated machines in a confined area, communicating URLLC packets to a central controller via an unlicensed access point.

The transport of critical services, and URLLC in particular, over unlicensed spectrum is rarely addressed in the literature, mainly because of the potential interference from other technologies on the same channel, besides the imposed regulations on medium access where transmitters have to perform Listen-Before-Talk (LBT) [12], which entails uncertain delays. The work in [13] reviews some physical and MAC layer mechanisms that may have a benefit to URLLC, such as multi-channel diversity and flexible frame structures. In [14], authors quantify the time spent in LBT backoff in a downlink scenario in order to demonstrate the impact of LBT on packet delay and hence URLLC requirements. As a result, LBT is shown to increase the packet delay when the traffic load is increased. The work in [15] propose a probabilistic approach to quantify the reliability within a time budget for one LTE-LAA evolved Node B (eNB) deploying LBT coexisting with several Wi-Fi stations. The results show that reliability and throughput are closely related to LTE frame duration and initial backoff window length.

In this chapter, we propose a new model which quantifies the reliability

within a delay constraint, based on Markov chains. We first start by some preliminaries about LBT and review the famous Bianchi model [16] which evaluates the performance of LBT. We show the limitation of this model for delay-constrained communications and propose a new variant of the model which takes into account the packet delay, in order to quantify the reliability under delay constraint. We also demonstrate the system capacity in terms of the maximum number of stations that can be served at the same time while URLLC requirements are still respected.

2.2 Preliminaries

2.2.1 Listen-Before-Talk

The majority of wireless access systems in unlicensed spectrum deploy LBT to guarantee fairness among stations. Several categories of LBT were defined in order to give priority to different services [17], by being more aggressive as in LBT cat1 and cat2 which do not have any backoff procedure or being less aggressive by deploying a fixed or adaptive backoff procedure as in LBT cat3 and cat4. The absence of backoff increases the chance of transmission on account of increased collision rate.

LBT with backoff guarantees fairness by the random choice of the contention window (CW) before every (re-)transmission. In every time slot, the station senses the medium and decrements its CW for idle slots only, until it hits zero at which time it transmits the packet without sensing and waits for the feedback from the receiver (the absence of response after a given time is considered as a negative feedback). In case of failure, the station repeats the previous procedure until the packet is successfully transmitted or discarded after a maximum number of trials (also called stages). In LBT cat3, $CW \in \{0, 1, \dots, W - 1\}$ for every stage where $W - 1$ is the maximum window size, while in LBT cat4, $CW \in \{0, 1, \dots, W_i - 1\}$ where $W_i - 1$ is the maximum window size in stage $i \in \{0, 1, \dots, m\}$ which increases exponentially as $W_i = 2^i W_0$ until reaching the maximum backoff stage, denoted by m .

For our system, we advise using LBT cat3 with fixed backoff because it reduces the collision probability and at the same time limits the waiting time in the backoff stages. Note that in LBT systems, packets are discarded based on their actual stage number, while in URLLC, packets are discarded based on their delay.

2.2.2 Bianchi model

We review in this section the famous Bianchi model [16] which evaluates principally the throughput of LBT cat4 based on a discrete-time Markov chain, illustrated in Figure 2.1. The key assumptions of the model are the following:

- All stations are identical, independent and saturated (always having packets to send).
- The number of stations N is finite and known.
- The channel is perfect, packet loss happens only when two or more transmissions coincide at the same time.
- The network is fully-connected, hidden-node problem does not exist.
- Packet retransmission is performed until it is successful.
- The probability of collision q is constant and does not depend on the state of the system.

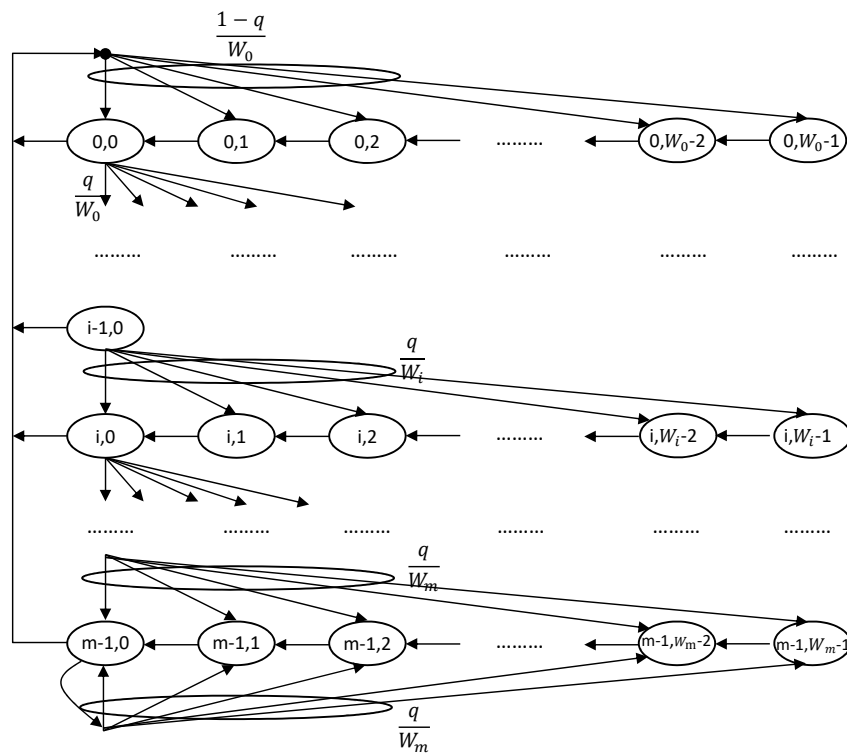


Figure 2.1: Markov chain of Bianchi model for LBT cat4.

Each state of the bi-dimensional Markov chain in Figure 2.1 is composed of two stochastic processes $\{s(t), w(t)\}$, representing the stage and CW at time t , respectively (t is discrete). The collision probability seen from the standpoint of one station in a given time slot, q , is equal to the probability that at least one of the other $N - 1$ stations is transmitting during the current time slot, expressed as:

$$q = 1 - (1 - p)^{N-1} \quad (2.1)$$

where p is the probability that a station transmits a packet in a given time slot.

Proposition 2.1. [16] *The probability that a station transmits in a given time slot is given by:*

$$p = \frac{2(1 - 2q)}{(1 - 2q)(W_0 + 1) + qW_0[1 - (2q)^m]} \quad (2.2)$$

Proof. Define $P\{i, j|i', j'\} = \mathbb{P}\{\{s(t+1), w(t+1)\} = \{i, j\} | \{s(t), w(t)\} = \{i', j'\}\}$, the one-step transition probabilities of the Markov chain, derived from Figure 2.1 as follows:

$$\begin{cases} P\{i, j|i, j+1\} = 1, & j \in \{0, \dots, W_i - 2\} \quad i \in \{0, \dots, m\} \\ P\{0, j|i, 0\} = (1 - q)/W_0, & j \in \{0, \dots, W_i - 1\} \quad i \in \{0, \dots, m\} \\ P\{i, j|i - 1, 0\} = q/W_i, & j \in \{0, \dots, W_i - 1\} \quad i \in \{1, \dots, m\} \\ P\{m, j|m, 0\} = q/W_m, & j \in \{0, \dots, W_m - 1\} \end{cases} \quad (2.3)$$

The stationary distribution represented by: $\Pi_{i,j} = \lim_{t \rightarrow \infty} \mathbb{P}\{s(t) = i, w(t) = j\}$, $i \in \{0, \dots, m\}$, $j \in \{0, \dots, W_i - 1\}$, can be derived from the following balance equations of the chain:

$$\begin{aligned} \Pi_{i,0} &= q\Pi_{i-1,0} \longrightarrow \Pi_{i,0} = q^i\Pi_{0,0}, \quad 0 < i < m \\ (1 - q)\Pi_{m,0} &= q\Pi_{m-1,0} \longrightarrow \Pi_{m,0} = \frac{q^m}{1 - q}\Pi_{0,0} \\ \Pi_{i,j} &= \frac{W_i - j}{W_i}q^i\Pi_{0,0}, \quad 0 \leq i \leq m, 0 \leq j \leq W_i - 1 \end{aligned} \quad (2.4)$$

We can finally determine $\Pi_{0,0}$ by imposing the normalization condition with the aid of equations (2.4), as follows:

$$1 = \sum_{i=0}^m \sum_{j=0}^{W_i-1} \Pi_{i,j} = \frac{\Pi_{0,0}}{2} \left[W_0 \left(\sum_{i=0}^{m-1} (2q)^i + \frac{(2q)^m}{1 - q} \right) + \frac{1}{1 - q} \right] \quad (2.5)$$

leading to:

$$\Pi_{0,0} = \frac{2(1-2q)(1-q)}{(1-2q)(W_0+1) + qW_0[1-(2q)^m]} \quad (2.6)$$

A station transmits when its CW reaches zero. This can be expressed as:

$$p = \sum_{i=0}^m \Pi_{i,0} = \frac{\Pi_{0,0}}{1-q} \quad (2.7)$$

From equations (2.6-2.7), we obtain equation (2.2), which concludes the proof. \square

Proposition 2.2. [16] *Equations (2.1-2.2) formulate a fixed-point which has a unique solution that can be determined numerically.*

Proof. Start by inverting equation (2.1): $p^*(q) = 1 - (1-q)^{1/(N-1)}$. This function is continuous and monotonically increasing, with $p^*(0) = 0$ and $p^*(1) = 1$. On the other hand, the function $p(q)$ in equation (2.2) represents a continuous and monotonically decreasing function with $p(0) = 2/(W_0+1)$ and $p(1) = 1/(1+2^m W_0)$. Since $p(0) > p^*(0)$ and $p(1) < p^*(1)$, uniqueness of the solution is hence proven. \square

Proposition 2.3. [16] *The normalized throughput of the system, denoted by S , is given by:*

$$S = \frac{\rho N p (1-p)^{N-1}}{(1-p)^N + \rho [1 - (1-p)^N]} \quad (2.8)$$

Proof. The normalized system throughput is defined as the fraction of time the channel is used for successful transmissions. In a randomly chosen time slot, the channel is:

- Empty during one time slot with probability $(1-p)^N$.
- Busy during ρ time slots with probability $1 - (1-p)^N$.
- Contains a successful transmission (during ρ time slots) when exactly one station transmits on the channel, with probability $Np(1-p)^{N-1}$.

Therefore, the normalized throughput is obtained from equation (2.8). \square

Bianchi introduces a powerful tool to evaluate the performance of LBT's random access. Nevertheless, this model is followed by many works relaxing some of the assumptions to obtain a more realistic evaluation. For instance,

the limited trials of one packet is investigated in [18]. The non-saturated buffers are studied in [19], which proposes a tri-dimensional Markov chain to capture the queuing effect on the performance; the third dimension represents the number of packets in the buffer in every state. The work in [20] extends the model in [19] by incorporating the freezing rules of backoff counters when the channel is sensed busy and the error-prone channel conditions. Authors in [21] return to the bi-dimensional Markov chain and represent the empty buffer by one additional state.

2.3 URLLC traffic model

We consider a smart-factory scenario, with the presence of N transmitting stations, representing a set of automated machines, generating packets containing urgent information that must be conveyed to a central controller via an unlicensed Access Point (AP). The packets are usually of small size and need to be received under delay and reliability constraints denoted by T and Θ , respectively. The factory area is considered confined, in the sense that interference on the transmission channel is exclusively generated from the N considered stations. The stations use LBT to access the medium and time is slotted with a unit of time slot.

In a URLLC context, the packet must be successfully transmitted within the delay budget T , or else, the packet is no longer valid and must be discarded to avoid unnecessary resource utilization.

Packet generation is triggered by events which occur independently in time. This is modeled in our work with a Poisson process of intensity λ per time slot. The Probability Mass Distribution (PMF) is expressed with $\mathbb{P}(X = k) = \frac{\lambda^k e^{-\lambda}}{k!}$, hence the probability of non-generation of a packet in a given time slot is equal to $\mathbb{P}(X = 0) = e^{-\lambda}$ leading to the probability of packet generation per time slot p_g , given in equation (2.9):

$$p_g = 1 - e^{-\lambda} \quad (2.9)$$

For URLLC applications, λ is small since the events arrive typically with low rate, otherwise ultra reliability cannot be ensured. Consequently, no queuing is considered in this work for the same device.

We assume that a packet transmission requires exactly ρ time slots from the beginning of transmission until its reception. The acknowledgment feedback is considered instantaneous.

2.4 Delay-constrained Markov model

The Bianchi model and its variants are able to evaluate the throughput, the average delay and the packet drop probability for a system constrained by a number of stages. However, imposing constraints on the packet delay and evaluating its impact on the system performance have never been studied before. We hence extend in this chapter the Markov chain to incorporate the packet delay and the imposed constraint.

We assume that every packet is tagged with a timer from the moment of its generation, once the timer reaches the delay budget T , the packet is no longer useful and is discarded. This timer is added to the Markov chain as a third dimension, and now every state is composed of the tuple $\{s(t), w(t), d(t)\}$, where $s(t)$, $w(t)$ and $d(t)$ are the stochastic processes representing the stage, CW and the packet delay, respectively. $d(t)$ is either incremented by one for idle slots or by ρ for busy ones since any transmission is considered to last ρ consecutive time slots.

Note that during a transmission, all stations (other than the transmitting ones) are in backoff, hence at the end of every transmission, all stations sense at least one idle slot before any other transmission begins, this can be seen as an inevitable increment of the delay by $\rho + 1$ time slots every time the medium is sensed busy. Figure 2.2 illustrates the one-step resulting states of $\{s(t), w(t), d(t)\} = \{i, j, k\}$ where $j > 0$.

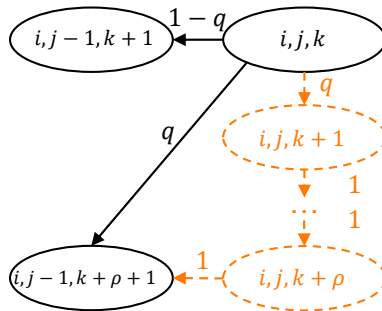


Figure 2.2: The one-step resulting states of state $\{i, j, k\}$.

The existence of two possible increments of $d(t)$ generates a huge number of states for practical values of CW , T and ρ , rendering the solution prohibitive. However, we notice that by neglecting the one time slot increment in $d(t)$ for idle slots, the resulting states can be combined with the ones from the previous contention window, as $d(t)$ values become multiples of $\rho + 1$. The complete approximate Markov chain for LBT cat3 with fixed CW size of W is illustrated in Figure 2.3, where $d(t)$ is expressed as a multiple of $\rho + 1$ and $m = \lfloor T/(\rho + 1) \rfloor$. Note that when $m > W$, T is not always attained in the first stages and the chain must be modified accordingly.

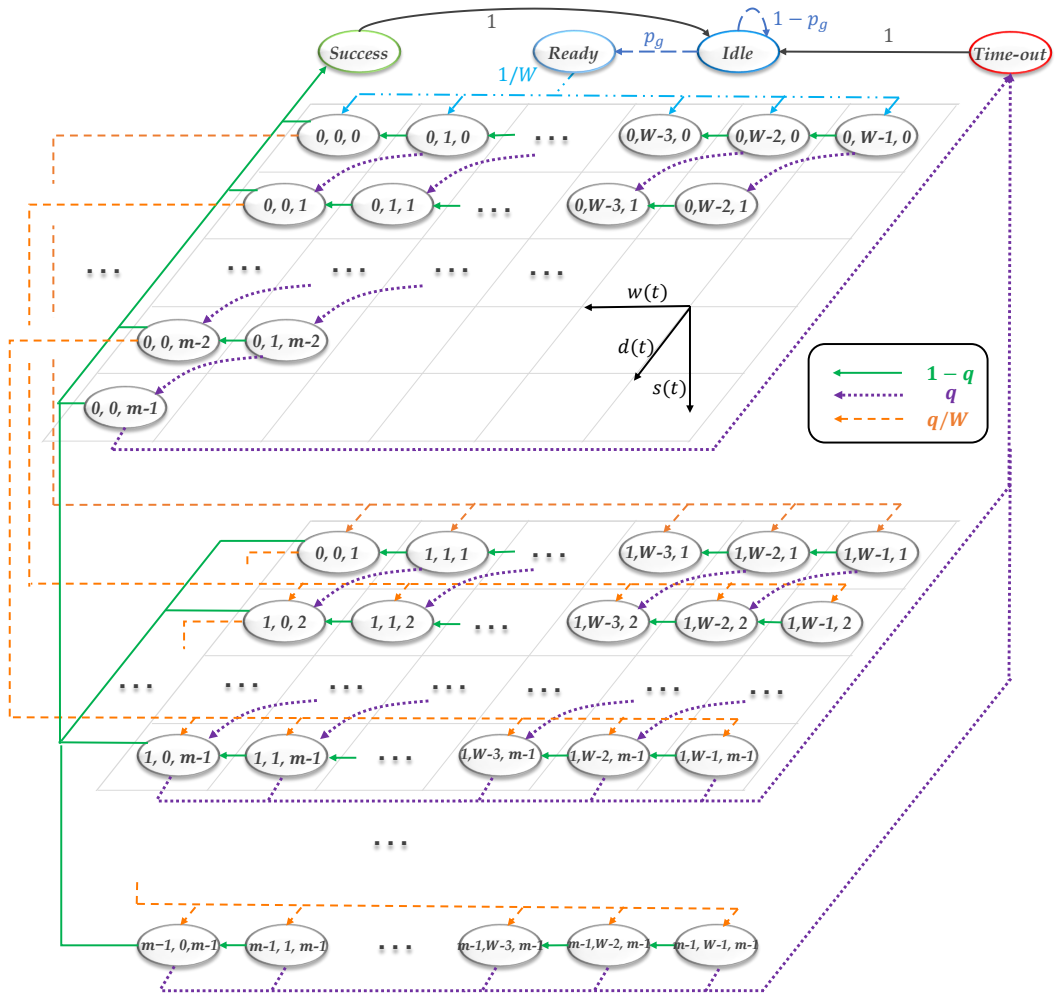


Figure 2.3: Markov chain for LBT cat3 incorporating a timer.

To suit our context, we added the following:

- State *Idle*, due to the sporadic packet generation, where a packet is generated with probability p_g .

- State *Ready*, representing the generation of the packet and the beginning of LBT process.
- State *Success*, representing the system after a successful transmission, which leads to the idle state where the system is waiting for a new packet generation.
- State *Time-out*, representing the system when the delay of the packet reaches constraint T and the packet is discarded. The system again enters the idle state waiting for new packets.

2.4.1 Stationary distribution

To evaluate the stationary distribution, it is still important to assume that q is constant and independent of the state of the system. To facilitate the notation, states *Ready*, *Success* and *Time-out* are all merged into state *Idle*.

The balance equations of the chain are described in a recursive manner row by row starting from the columns with higher $w(t)$, as follows:

$$\begin{aligned}
\Pi_{0,W-1,0} &= p_g \frac{\Pi_{Idle}}{W} \\
\Pi_{0,W-j,0} &= p_g \frac{\Pi_{Idle}}{W} + (1-q) \Pi_{0,W-j+1,0}, \quad 2 \leq j \leq W \\
\Pi_{0,W-k-1,k} &= q \Pi_{0,W-k,k-1}, \quad 1 \leq k \leq m-1 \\
\Pi_{0,W-j,k} &= (1-q) \Pi_{0,W-j+1,k} + q \Pi_{0,W-j+1,k-1}, \quad \begin{array}{l} 1 \leq k \leq m-1, \\ k+2 \leq j \leq W \end{array}
\end{aligned} \tag{2.10}$$

$$\begin{aligned}
\Pi_{i,W-1,k} &= \frac{q}{W} \Pi_{i-1,0,k-1}, \quad 1 \leq i \leq m-1, \quad i \leq k \leq m-1 \\
\Pi_{i,W-j,k} &= \frac{q}{W} \Pi_{i-1,0,k-1} + (1-q) \Pi_{i,W-j+1,k} + q \Pi_{i,W-j+1,k-1}, \quad \begin{array}{l} 1 \leq i \leq m-1, \\ i \leq k \leq m-1, \\ 2 \leq j \leq W \end{array}
\end{aligned}$$

All states can be written as a function of Π_{Idle} and q , hence Π_{Idle} can be determined by applying the normalization condition:

$$\Pi_{Idle} + \sum_{i=0}^{m-1} \sum_{j=0}^{W-1} \sum_{k=0}^{m-1} \Pi_{i,j,k} = 1 \tag{2.11}$$

We obtain Π_{Idle} numerically, and hence the rest of the states. In this case, the probability of transmission in one time slot is given by:

$$p = \sum_{i=0}^{m-1} \sum_{k=0}^{m-1} \Pi_{i,0,k} \quad (2.12)$$

We use equation (2.1) to determine q numerically with the aid of equation (2.12), where a unique solution of the fixed-point equations (2.1-2.12) exist similarly to classical Bianchi model.

Remark 2.4. A simple method to compensate for the neglected idle time slots in the model above is obtained by adding a certain value to the delay after every backoff stage. The additional value depends on W and will be discussed later in the numerical evaluation section. In this case, instead of starting the next stage from $d(t) + 1$ of the previous stage, a new value must be added to $d(t)$ according to the chosen compensation.

2.4.2 Transmission Reliability

We use the hitting probability to quantify the reliability of transmission under the system described in Figure 2.3. The hitting probability from state i to state j , denoted by h_j^i , is the probability of ever reaching state j starting from initial state i . Hence the transmission reliability can be described by the hitting probability of state *Success* from state *Ready*, $h_{Success}^{Ready}$.

We develop the hitting probabilities of the Markov chain illustrated in Figure 2.3 as follows:

$$\begin{aligned}
h_{0,W-1,0}^{Ready} &= \frac{1}{W} \\
h_{0,W-j,0}^{Ready} &= p_g \frac{1}{W} + (1-q) h_{0,W-j+1,0}^{Ready}, \quad 2 \leq j \leq W \\
h_{0,W-j,k}^{Ready} &= q h_{0,W-j+1,k-1}^{Ready}, \quad 1 \leq k \leq m-1, \quad j = k+1 \\
h_{0,W-j,k}^{Ready} &= (1-q) h_{0,W-j+1,k}^{Ready} + q h_{0,W-j+1,k-1}^{Ready}, \quad \begin{array}{l} 1 \leq k \leq m-1, \\ k+2 \leq j \leq W \end{array} \quad (2.13) \\
h_{i,W-1,k}^{Ready} &= \frac{q}{W} h_{i-1,0,k-1}^{Ready}, \quad 1 \leq i \leq m-1, \quad i \leq k \leq m-1 \\
h_{i,W-j,k}^{Ready} &= \frac{q}{W} h_{i-1,0,k-1}^{Ready} + (1-q) h_{i,W-j+1,k}^{Ready} + q h_{i,W-j+1,k-1}^{Ready}, \quad \begin{array}{l} 1 \leq i \leq m-1, \\ i \leq k \leq m-1, \\ 2 \leq j \leq W \end{array} \\
h_{Success}^{Ready} &= (1-q) \sum_{i=0}^{m-1} \sum_{k=0}^{m-1} h_{i,0,k}^{Ready}
\end{aligned}$$

By a numerical solution of equations (2.13), we evaluate the reliability of the system $h_{Success}^{Ready}$. We can easily verify that the loss rate is $h_{Time-out}^{Ready} = 1 - h_{Success}^{Ready}$. In the sequel, we denote the loss rate within a time budget T in unlicensed transmission by $P_{loss}^U(T)$. For simplicity, we consider the notation P_{loss}^U when the parameter is T , otherwise, it is specified.

$$P_{loss}^U = 1 - h_{Success}^{Ready} \quad (2.14)$$

2.5 Numerical evaluation

We consider similar numerical values to the ones defined in latest IEEE 802.11 standards [22], notably a time slot duration of $T_s = 9\mu s$ and a bit rate of $R_b = 100 Mbps$. Small URLLC packets are considered of length $L_u = 32 Bytes$ and the feedback of length $L_f = 14 Bytes$. We also consider guard periods $SIFS = 16\mu s$ and $DIFS = 34\mu s$ which are important to determine the end of a transmission. The transmission duration ρ is calculated as: $\rho = \lceil (L_u/R_b + SIFS + L_f/R_b + DIFS)/T_s \rceil = 6$ time slots. The fixed-size contention window of LBT cat3 is considered $W = 16$ for model validation. We assume URLLC stations generate on average one packet every 10 ms following a Poisson process, hence $\lambda = 0.001$ and $p_g = 1 - e^{-0.001}$. The

considered target delay and reliability are $T = 1 \text{ ms} = 111$ time slots and $\Theta = 1 - 10^{-5}$, respectively.

The evaluation is performed considering one channel, where multiple simultaneous transmissions lead to the loss of all transmitted packets, which is not the case in the presence of Dynamic Frequency Selection (DFS) mechanism.

We develop a system-level Monte-Carlo simulator of a station contending for the wireless access using LBT protocol under delay constraint. Every generated packet is tagged with a timer and a CW, chosen randomly from zero to $W - 1$. At every time slot, the station senses the medium busy with probability q calculated from the Markov chain in Figure 2.3 for the given number of stations N . When CW reaches zero, the packet succeeds with probability $1 - q$ or else the station re-attempts transmission with a new CW, as long as the delay constraint is respected.

We validate our analytical model against simulations in Figure 2.4 by evaluating the loss rate. We also implement error compensation as in Remark 2.4. The model with no error compensation is validated against a simulation which similarly discards idle time slots from the delay. The accurate simulation without discarding idle slots is then compared to an error compensation of $W/2$ and W .

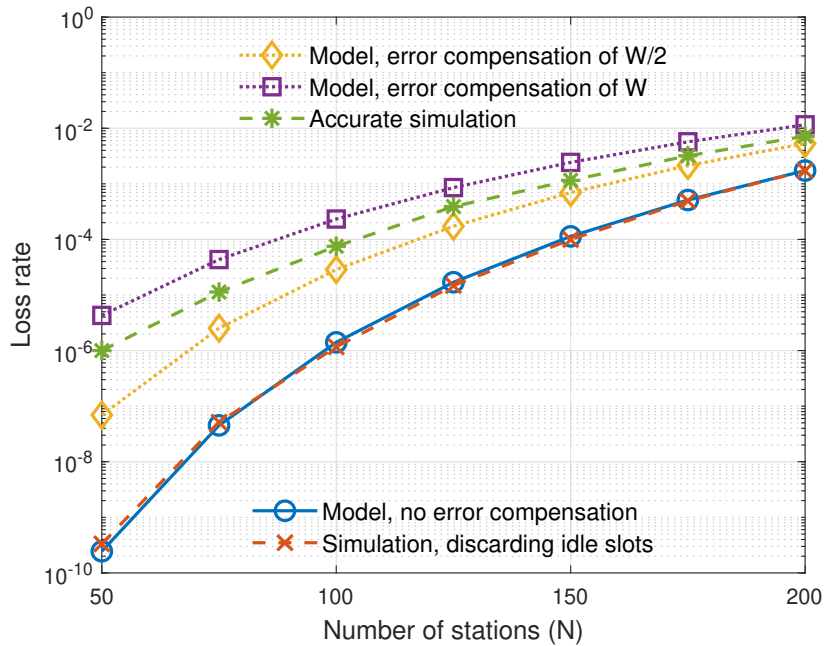


Figure 2.4: Model validation with simulation, loss rate with respect to the number of stations.

Observing Figure 2.4, the accurate simulation lays between the maximum and the average values of error compensation, W and $W/2$, respectively. Neglecting idle slots generates a considerable error in evaluation the loss rate of the system.

Considering the accurate simulation as a baseline, we can deduce the capacity of the system denoted by the maximum number of stations, at which reliability and delay requirements are fulfilled, $N_{max} = 75$ when $W = 16$.

An important parameter of the system is the CW size, which impacts directly the delay of the packet. In general, reducing CW size reduces the waiting time in backoff stages but also increases the chance of collisions with other transmissions, especially for dense traffic scenarios. We show in Figure 2.5 the effect of different CW sizes on the system capacity under delay and reliability constraints. For this evaluation, we used the model with error compensation of $W/2$.

Figure 2.5 suggests that reducing W increases the system capacity, and the maximum capacity, $N_{max} \approx 180$, is reached when $W = 1$ which corresponds to LBT cat2 without random backoff. In this case, the randomness introduced by the packets arrival process is sufficient to guarantee fairness among stations.

For the rest of the thesis, we choose $W = 4$ or $W = 16$ depending on the context.

2.6 Conclusion

We developed throughout this chapter an analytical tool based on Markov chains to quantify the reliability of delay-constrained transmissions, in a confined industrial area, using LBT cat3. We validated the model against simulations, then studied the effect of the contention window size on the performance. We deduced that decreasing the CW size increases the maximum number of stations that can be served at the same time, while preserving URLLC requirements.

In the following chapter, we aim to dimension the capacity of unlicensed system by exploiting the joint transmission schemes of unlicensed and licensed systems.

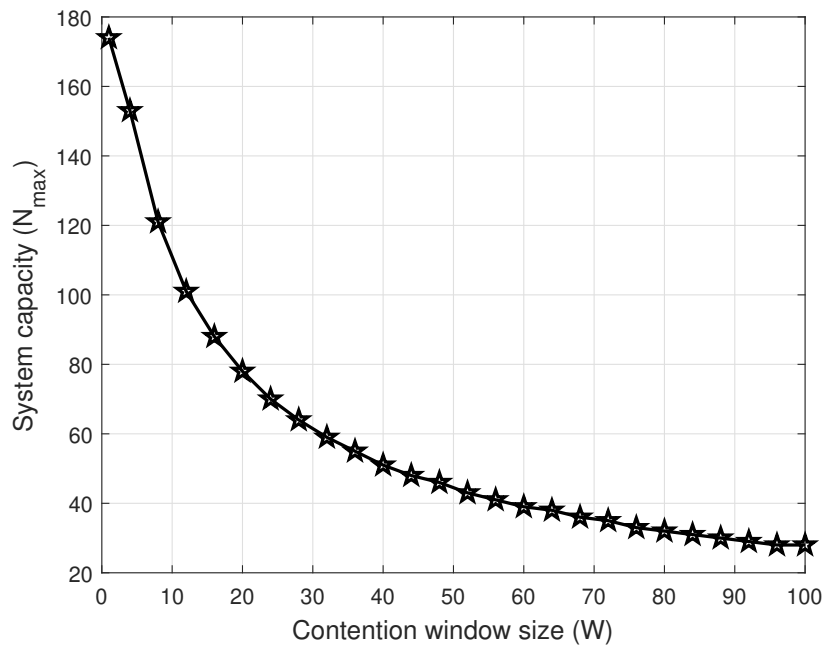


Figure 2.5: System capacity: the maximum number of stations respecting URLLC requirements, versus the contention window size.

Chapter 3

Joint transmission over unlicensed and licensed spectrum

3.1 Introduction

The transport of URLLC over standalone unlicensed system reduces the cost of the network. However, unlicensed resources can be easily saturated when the traffic increases, which violates URLLC constraints. To remedy this, we explore in this chapter the joint usage of unlicensed and licensed systems for URLLC transmission.

The joint usage of unlicensed and licensed spectrum is particularly addressed in heterogeneous networks context, deploying multiple radio access technologies [23]. This joint access by one technology is initiated by LTE LAA where unlicensed spectrum is used as an anchor to the licensed one to offload part of the traffic. Note that all devices are equipped with both communication systems. The legacy LTE LAA is introduced in 3GPP release 13 [4], and was first proposed in the downlink only, to be followed by the enhanced LAA (eLAA) for uplink and downlink in release 14 [2].

The work in [24] proposes a joint access scheme for URLLC transmission in Industry 4.0 scenario, where unlicensed spectrum is used for the first attempt of transmission performing LBT. If the unlicensed channel is sensed busy or the packet transmission has failed its first attempt, then the station toggles its transmission to the licensed system, increasing by that its chance of success. This scheme results in frequent switches to the licensed system in case of high traffic loads, leading to a resembling performance to the one of standalone licensed system. Thus, the benefit of unlicensed system is not sufficiently exploited.

In this chapter, we propose three methods for the joint unlicensed-licensed transmission and compare their performance. We then consider the case where multiple tenants compete over the unlicensed spectrum, and show the resulting equilibrium point in terms of the amount of licensed spectrum each tenant has to use.

3.2 Licensed spectrum for critical services transport

3.2.1 Licensed medium access

Time is slotted into intervals called Transmission Time Intervals (TTIs), during which transmissions take place. Stations must be synchronised and if a packet arrives to the system in the middle of a TTI then its transmission begins in the next one. In 4G systems, TTI duration is fixed to 1 ms , but 5G shows more flexibility concerning the duration selection from a wider range, in order to adapt to various applications, among which URLLC. We consider the radio interface to have a channel bandwidth denoted by BW , divided into K sub-channels, each has a bandwidth of BW_{SC} . The intersection of one TTI-sub-channel represents a Resource Block (RB).

Existing methods for uplink transmission in licensed spectrum are Grant-based (GB) scheduling and Grant-free (GF) on a common pool. GB scheduling is the traditional method used in cellular systems: when a station has a packet to transmit, it sends a scheduling request to the base station through a random access channel. Once the BS receives the request, it allocates one or more RBs to the station according to its demand and transmits back to the station the positions of the allocated RBs in time and frequency. This approach offers very high reliability and spectral efficiency since the resources are managed by one central unit. On the other hand, the resource reservation process is time consuming and unsuitable for delay constrained applications as every step consumes one TTI, i.e., in a best-case scenario, a packet transmission requires at least eight TTIs as illustrated in Figure 3.1, ignoring the delay from packet generation until next TTI, which can go up to one TTI. Other factors may impact the packet delay, such as RB request loss in the random access channel or a delayed allocated RB due to high demand. In this case, even when the smallest TTI duration is considered, 0.125 ms , a single transmission consumes at least 1 ms , making it difficult to meet the delay constraint.

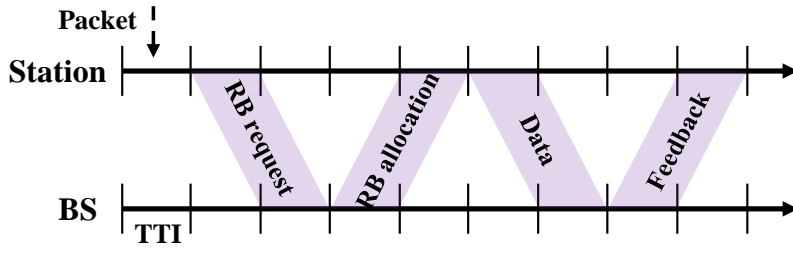


Figure 3.1: Grant-based scheduling in licensed spectrum

In GF transmission, RBs are accessible without prescheduling, similar to slotted Aloha protocol, which minimizes the delay on account of reliability degradation. Assuming that stations are synchronized in time, when a station has a packet to transmit, it does so immediately at the beginning of the following TTI using a randomly chosen RB from the K available ones in that TTI, as advocated by [25]. If the delay budget T is still respected, then more replicas in the following TTIs can be sent, without waiting for feedback from the BS so as to reduce the delay. In the following, we adopt this mechanism which is standardized and called TTI bundling for URLLC [26] and evaluate the performance of the system.

3.2.2 System model

We consider a smart factory scenario, with the presence of N stations generating URLLC packets that must be conveyed to a central controller under delay and reliability constraints, denoted by T and Θ , respectively. This time, licensed spectrum is used and the stations communicate their packets to a Base Station (BS) of a mobile network operator covering the factory as a relay for the packets back to the controller.

3.2.3 TTI bundling for URLLC

We are interested in evaluating the cost of deploying such a system under strict delay and reliability constraints. For that, we first quantify the loss rate within a time budget T for a given number of required RBs per TTI, K , then we use it to deduce the minimum K which enables the system to meet the imposed constraints.

Assuming packets are generated following a Poisson process of intensity λ_{TTI} per TTI, then the probability of packet generation per station per TTI is

given by:

$$p_{gen} = 1 - e^{-\lambda_{TTI}} \quad (3.1)$$

We denote by δ_{max} the maximum number of allowed replicas, given by $\delta_{max} = \lfloor T/TTI \rfloor$. For one station deploying the blind replication mechanism, it transmits either a fresh packet with probability p_{gen} or a replica of it in the next $\delta_{max} - 1$ TTIs with the same probability. Therefore, the probability of not having any transmission in a given TTI is equal to $(1 - p_{gen})^{\delta_{max}}$, and hence the probability of transmission in one TTI knowing δ_{max} can be expressed by:

$$p_{tr}(\delta_{max}) = 1 - e^{-\lambda_{TTI} \delta_{max}} = 1 - e^{-\lambda_T} \quad (3.2)$$

where we denote $\lambda_{TTI} \delta_{max}$ by λ_T , as it represents the intensity of packet generation during time T .

For simplicity, we (most of the time) drop the function parameter notation when the parameter is δ_{max} .

We assume that all of the N stations are identical and deploy the same mechanism with the same δ_{max} . A transmitted packet can be damaged if other packets are being sent over the same RB because of high interference, and this will be considered as the only source of packet loss in our analysis.

Proposition 3.1. *The loss rate within time budget T in TTI bundling for URLLC is given by:*

$$P_{loss}^L = \left[1 - \left(\frac{e^{-\lambda_T} + K - 1}{K} \right)^{N-1} \right]^{\delta_{max}} \quad (3.3)$$

Proof. We start by computing the probability of collision in one TTI from the standpoint of one transmitting station. The station of interest chooses one RB uniformly with probability $1/K$. Accordingly, another active station does not choose the same RB in the same TTI with probability $1 - 1/K$.

Let A_n be the event of having n transmissions other than the one under study in one TTI; $n \in \{0, 1, \dots, N-1\}$. Let B denote the event of no collision with other active stations in one TTI. Hence the probability of event B is calculated by applying the following chain rule:

$$\mathbb{P}(B) = \sum_{n=0}^{N-1} \mathbb{P}(B|A_n) \mathbb{P}(A_n) \quad (3.4)$$

where:

$$\mathbb{P}(A_n) = \binom{N-1}{n} p_{tr}^n (1 - p_{tr})^{N-1-n} \quad (3.5)$$

$$\mathbb{P}(B|A_n) = \left(1 - \frac{1}{K}\right)^n \quad (3.6)$$

We replace $p_{tr}(\delta_{max})$ by p_{tr} for simplicity. We now obtain the probability of collision in one TTI as [25]:

$$\begin{aligned} P_{col} &= 1 - \sum_{n=0}^{N-1} \binom{N-1}{n} p_{tr}^n (1-p_{tr})^{N-1-n} \left(1 - \frac{1}{K}\right)^n \\ &= 1 - \left[p_{tr} \left(1 - \frac{1}{K}\right) + 1 - p_{tr} \right]^{N-1} \\ &= 1 - \left(\frac{e^{-\lambda T} + K - 1}{K} \right)^{N-1} \end{aligned} \quad (3.7)$$

and using the Binomial identity:

$$(x + y)^N = \sum_{n=0}^N \binom{N}{n} x^n y^{N-n} \quad (3.8)$$

The packet is lost if and only if all its δ_{max} replicas are in collision with other transmissions, expressed by $(P_{col})^{\delta_{max}}$, leading to the expression in equation (3.3). \square

Proposition 3.2. *The minimum number of sub-channels required to guarantee the delay and reliability constraints in licensed system is given by:*

$$K^{licensed} = \frac{1 - e^{-\lambda T}}{1 - [1 - (1 - \Theta)^{1/\delta_{max}}]^{1/(N-1)}} \quad (3.9)$$

Proof. Equation (3.9) is obtained directly from equation (3.3) by replacing P_{loss}^L with $1 - \Theta$ and isolating K . \square

$K^{licensed}$ represents the cost of using licensed spectrum for URLLC transport for a given number of stations, which means that a share of bandwidth $BW = K^{licensed} \times BW_{SC}$ must be reserved for this purpose.

3.2.4 Numerical evaluation

We assume that a URLLC packet fits in one RB of TTI= 0.125 ms and a sub-channel bandwidth $BW_{SC} = 180$ KHz. In LTE, every sub-channel is composed of 12 subcarriers with carrier spacing of 15KHz. Reliability and delay

constraints are taken as $\Theta = 1 - 10^{-5}$ and $T = 1\text{ms}$, respectively, which correspond to $\delta_{max} = 8$. For a packet generation rate of 1 packet per 10 ms, we have $\lambda_{TTI} = 0.0125$ and $\lambda_T = 0.1$.

We simulate the TTI bundling mechanism in a system-level Monte-Carlo simulator considering the above numerical values. At every TTI, the number of generated packets is a Poisson random variable of parameter λ_T , and the used RBs are selected uniformly. We designate one station and compute its loss rate, where packet loss happens when all the δ_{max} replicas of a packet collide with other transmissions.

We compare the results obtained from the analytical model with simulation in Figure 3.2, for $K = 10$. The curves show a good match which validates our model.

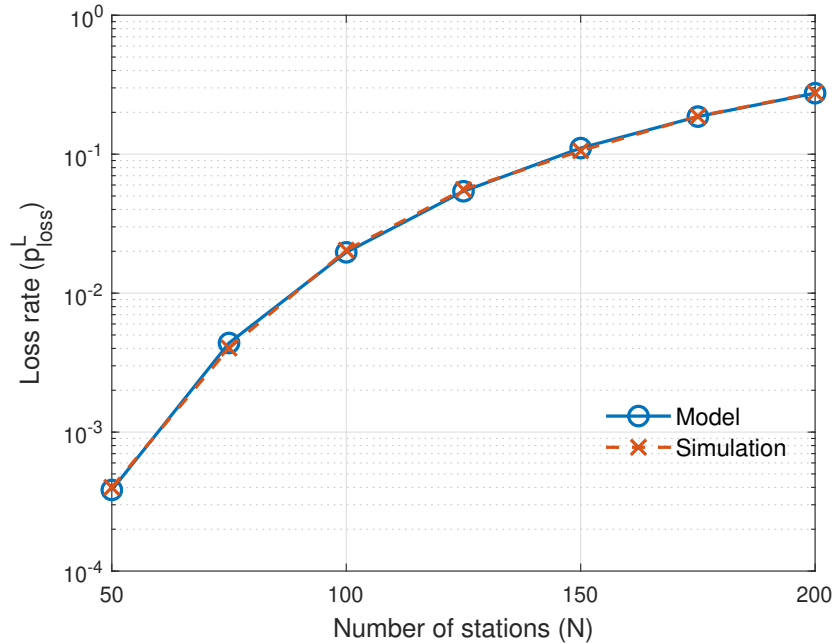


Figure 3.2: Model validation with simulation. Loss rate with respect to number of stations for licensed system, $\delta_{max} = 8$ and $K = 10$.

We notice that for $K = 10$, URLLC reliability constraint cannot be guaranteed even for small density of stations. For this reason, we evaluate the cost $K^{licensed}$ with respect to the number of stations, shown in Figure 3.3.

We observe that the minimum cost is a linearly increasing function of the number of stations. The effective cost is calculated by multiplying $K_{licensed}$ by BW_{SC} , for instance, $N = 200$ corresponds to $K_{licensed} = 70$ and a bandwidth $BW = 13\text{MHz}$, considering the subcarrier spacing between sub-channels.

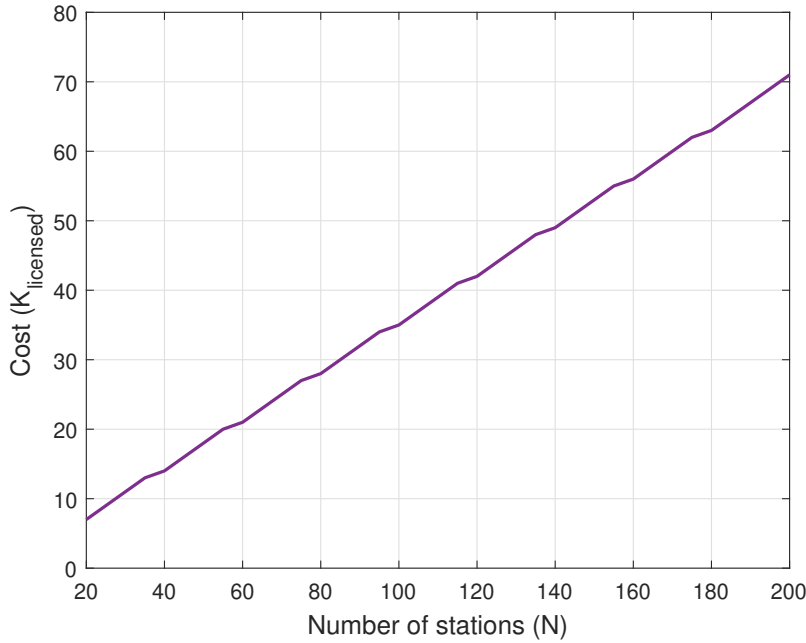


Figure 3.3: Cost with respect to the number of stations for licensed system, $\delta_{max} = 8$.

3.3 Joint unlicensed-licensed access

In the previous section, we calculated the frequency bandwidth needed to respect the requirements for a given traffic load (i.e., number of stations) and demonstrated that the transport of URLLC over licensed spectrum can be very pricey in terms of frequency resources. We also showed earlier that URLLC transport over unlicensed spectrum can meet the stringent delay and reliability constraints, but to a certain limit of traffic load, after which the system cannot meet these constraints. However, unlicensed transmission is considered to be cheap compared to the licensed one and can thus help reduce the overall transmission cost when used cooperatively with the licensed one, and this is the object of our present study.

Assuming that all stations are equipped with both unlicensed and licensed transmission systems, multiple methods for the joint use of these two types of resources can be considered, as listed below and illustrated in Figure 3.4.

- Duplication: send a copy of the packet over both links and it is enough to receive correctly one of the copies to consider it as a successful transmission.

- Probabilistic system choice: send the packet over one of the links, chosen randomly with a given probability after the packet generation. The selection probability must be chosen so that the cost is minimized.
- In series: we assume that generated packets are first transmitted over the unlicensed link, but if a packet is not served within some delay budget (smaller than the delay constraint T), it stops attempting over the unlicensed link and switches to the licensed one for the remaining time. Here also, the switching time between unlicensed and licensed systems plays a role in minimizing the cost.

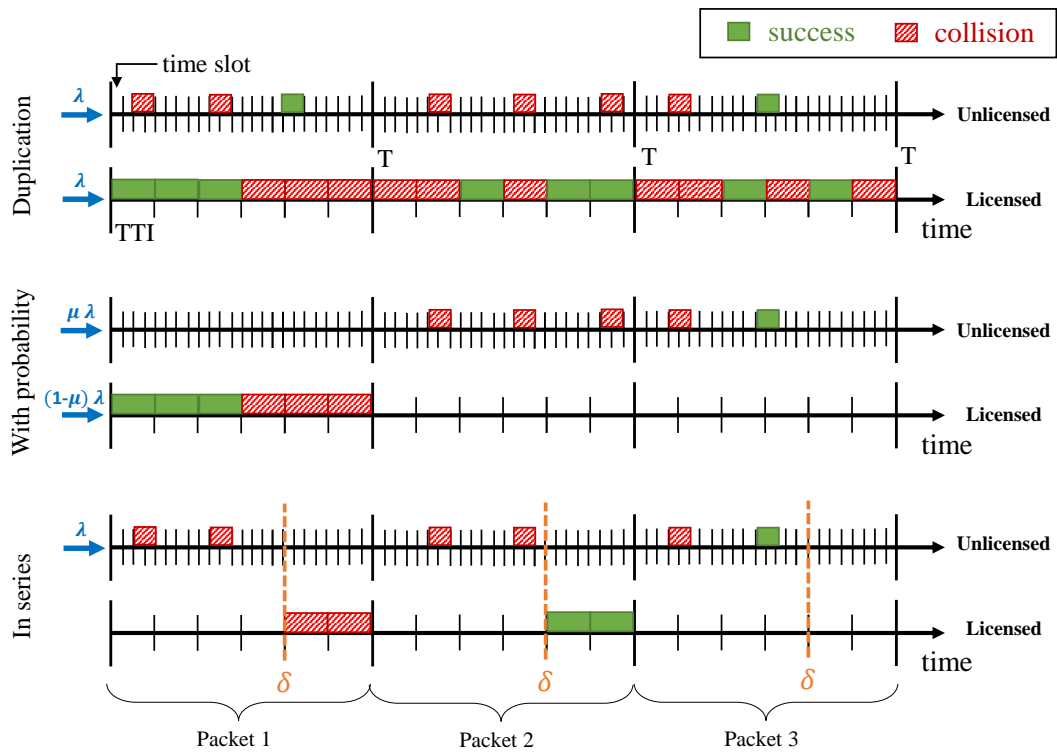


Figure 3.4: Methods of joint unlicensed-licensed transmission. A packet is lost if none of its replicas were delivered successfully, as is the case for packet 2 of *Probabilistic system choice* method and packet 1 of *In series* method. Licensed spectrum is not necessarily used in *In series* method as for packet 3.

We do not consider the “Inverse in series” method where the licensed link is used before the unlicensed one, as we aim to minimize the overall cost and hence reduce as much as possible the use of licensed resources.

We consider the same confined smart factory scenario with N stations generating URLLC traffic following Poisson process with intensity λ per time slot or equivalently λ_{TTI} per TTI. Every station is equipped with unlicensed

and licensed transmission systems and uses them according to the chosen method.

3.3.1 Duplication method

In this method, the packet generation rate in both links is equal to the one of the station. The main drawbacks of this method are doubling the load of the system and increasing the overall energy consumption of the station. The loss probability of the unlicensed link, P_{loss}^U , is as calculated equation (2.14) and for licensed one in equation (3.3). The packet is lost if and only if the transmission fails in both links, leading to an overall probability of loss:

$$P_{loss}^{duplication} = P_{loss}^U \times P_{loss}^L \quad (3.10)$$

For a target loss rate of $1 - \Theta$, the required loss rate for licensed transmission to guarantee this target is computed as:

$$P_{loss}^{L*} = \frac{1 - \Theta}{P_{loss}^U} \quad (3.11)$$

Note that this expression is only valid when $P_{loss}^U \geq 1 - \Theta$, otherwise, licensed resources are not needed. This leads us to formulate the minimum cost as:

$$K_{duplication} = \frac{1 - e^{-\lambda T}}{1 - \left[1 - \left(\frac{1 - \Theta}{P_{loss}^U} \right)^{1/\delta_{max}} \right]^{1/(N-1)}} \quad (3.12)$$

3.3.2 Probabilistic system choice method

We denote by $\mu \in [0, 1]$ the probability of choosing unlicensed link for a given packet, hence licensed link is chosen with probability $1 - \mu$. In this case, the packet generation intensity in the selected link is proportional to the probability of selecting it, i.e., $\mu \lambda$ per time slot for unlicensed system and $(1 - \mu) \lambda_{TTI}$ per TTI for licensed one. The total loss rate of the system for a given μ corresponds to the sum of loss rates of each system multiplied by the probability of choosing it, expressed by:

$$P_{loss}^{with\ probability}(\mu) = \mu P_{loss}^U(\mu \lambda) + (1 - \mu) P_{loss}^L((1 - \mu) \lambda_{TTI}) \quad (3.13)$$

We note that when $\mu P_{loss}^U(\mu \lambda) > 1 - \Theta$, the system cannot guarantee the reliability constraint, as $(1 - \mu) P_{loss}^L((1 - \mu) \lambda_{TTI})$ is a positive quantity. To calculate the minimum required cost for a given μ that verifies $\mu P_{loss}^U(\mu \lambda) \leq 1 - \Theta$, we have:

$$K_{with\ probability}(\mu) = \frac{1 - e^{-(1-\mu)\lambda T}}{1 - \left[1 - \left(\frac{1-\Theta - \mu P_{loss}^U(\mu \lambda)}{1-\mu}\right)^{1/\delta_{max}}\right]^{1/(N-1)}} \quad (3.14)$$

Here we have μ as a parameter to optimize in order to minimize the cost function. We designate by μ the policy and study later the function $K_{with\ probability}(\mu)$ numerically, since $P_{loss}^U(\mu \lambda)$ does not have an explicit expression that allows us to study the function analytically. We denote the optimal policy which minimizes the cost by μ^* .

3.3.3 In series method

When combining the two systems, we have to keep in mind that the unlicensed system time unit (time slot) is smaller than its licensed counterpart (TTI). The choice of the time budget to spend in both systems determines the cost. We denote by T_U and T_L the time budget allocated to unlicensed and licensed systems, respectively, where $T = T_U + T_L$, and we denote by z the number of time slots in one TTI. We choose $T_U = \delta z$ time slots where $\delta \in \{1, 2, \dots, \delta_{max} - 1\}$, assuming that packets are generated and then conveyed to licensed system when unlicensed transmission fails at the beginning of TTIs, to avoid the extra delay before starting licensed transmission. Recall that $\delta_{max} = \lfloor T/TTI \rfloor$.

The packet generation rate for unlicensed system remains λ per time slot and the corresponding packet loss rate per time slot is calculated for its allowed time budget and corresponds to $P_{loss}^U(T_U)$ from equation (2.14). For licensed system, packets arrive after being generated and failed to be transmitted in unlicensed system with probability $(1 - e^{-\lambda}) P_{loss}^U(T_U)$ per time slot. The licensed time budget allows $(\delta_{max} - \delta)$ replicas, therefore, the probability of having no transmission in $(\delta_{max} - \delta)$ TTIs equals $\left[1 - (1 - e^{-\lambda}) P_{loss}^U(T_U)\right]^{(\delta_{max} - \delta)z}$

From this, we can compute respectively the loss rate and the cost of this method for a given δ , in equations (3.15) and (3.16). Here too we designate

by δ the policy which can be optimized to minimize the cost.

$$P_{loss}^{in\ series}(\delta) = \left[1 - \left(\frac{[1 - (1 - e^{-\lambda}) P_{loss}^U(T_U)]^{(\delta_{max}-\delta)z} + K - 1}{K} \right)^{N-1} \right]^{(\delta_{max}-\delta)} \quad (3.15)$$

$$K_{in\ series}(\delta) = \frac{1 - [1 - (1 - e^{-\lambda}) P_{loss}^U(T_U)]^{(\delta_{max}-\delta)z}}{1 - [1 - (1 - \Theta)^{1/(\delta_{max}-\delta)}]^{1/(N-1)}} \quad (3.16)$$

The optimal policy δ^* is the one which minimizes the function in equation (3.16), which can be determined numerically. Nevertheless, we can have some insights of δ^* from the following reasoning: when δ is relatively small then $P_{loss}^U(T_U)$ is (relatively) large since the unlicensed system cannot ensure packet delivery in a small time budget. On the other hand, licensed system benefits from a larger number of replicas, reducing its need for frequency resources. For a relatively large δ , unlicensed system can handle more traffic and leads to smaller $P_{loss}^U(T_U)$, but the licensed one demands more and more resources to cope with the reliability constraint in a small number of replicas. This indicates that the optimal policy must lay somewhere in the middle of the δ range so as to allow enough time for each system to perform properly, depending also on the traffic load.

3.3.4 Numerical evaluation

We recall in Table 3.1 the numerical values used earlier in the numerical application of unlicensed and licensed systems.

Table 3.1: Numerical values of unlicensed and licensed system parameters.

T	111 time slots	W	16	λ	0.001
ρ	6 time slots	K	10	λ_{TTI}	0.0125
z	13 time slots	δ_{max}	8	Θ	$1 - 10^{-5}$

We compare in Figure 3.5 the loss rate of the three proposed methods of joint unlicensed-licensed transmission, along with standalone unlicensed and licensed systems, for the same offered licensed resources: $K = 10$. When using the Markov model from Chapter 2 to evaluate the unlicensed system

loss rate, we take for example an error compensation of $W/2$. The selection probability of “Probabilistic system choice” method is $\mu = 0.5$ and the switching time for “In series” method is $\delta = 4$.

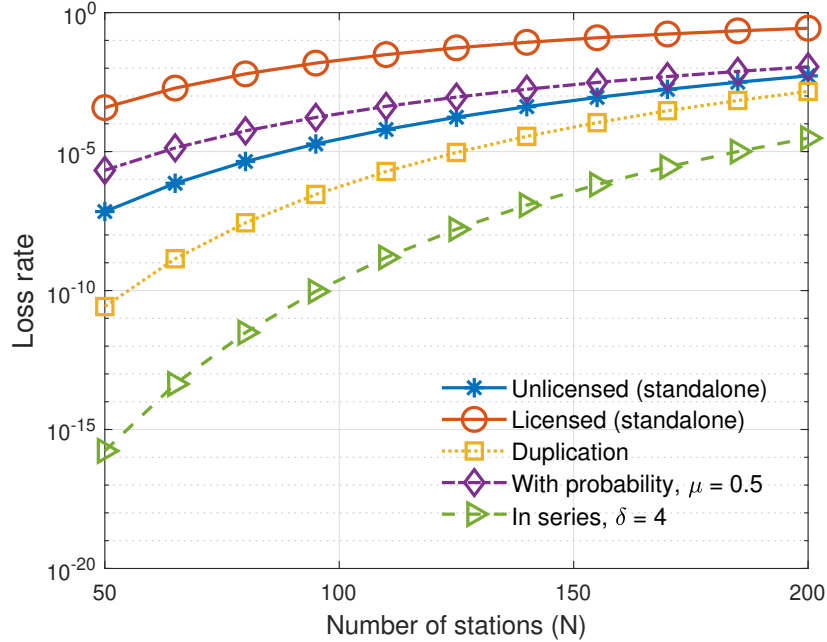


Figure 3.5: Loss rate with respect to the number of stations for standalone unlicensed and licensed systems, *Duplication*, *Probabilistic system choice* for $\mu = 0.5$ and *In series* for $\delta = 4$.

We observe from Figure 3.5 the following:

- The loss rate of “Duplication” method is always below the one of both standalone systems and shows an enhancement between 10^3 to 10^6 times compared to standalone licensed system for the same offered resources. The system capacity increases from $N \approx 85$ to $N = 135$ compared to standalone unlicensed system.
- “Probabilistic system choice” method enhances the loss rate of the licensed system by a constant proportion of approximately 100 times. In spite of the equally shared traffic between the links, $\mu = 0.5$, the overall loss rate remains worse than the one of unlicensed system, due to the poor performance of the licensed system when $K = 10$.
- “In series” method shows a considerable enhancement on the performance when compared to the standalone licensed system, estimated

between 10^4 and 10^{10} times. This also shows that this method outperforms the two other proposed methods because it utilizes licensed resources only when needed.

We study now the optimization of μ in “Probabilistic system choice” method. We plot in Figure 3.6 the cost with respect to the used policy μ for high-load regime with $N = \{200, 250, 300\}$. We assume that $K = 100$ is the maximum number of available resources and $K^* = 100$ means that the system is not respecting URLLC constraints.

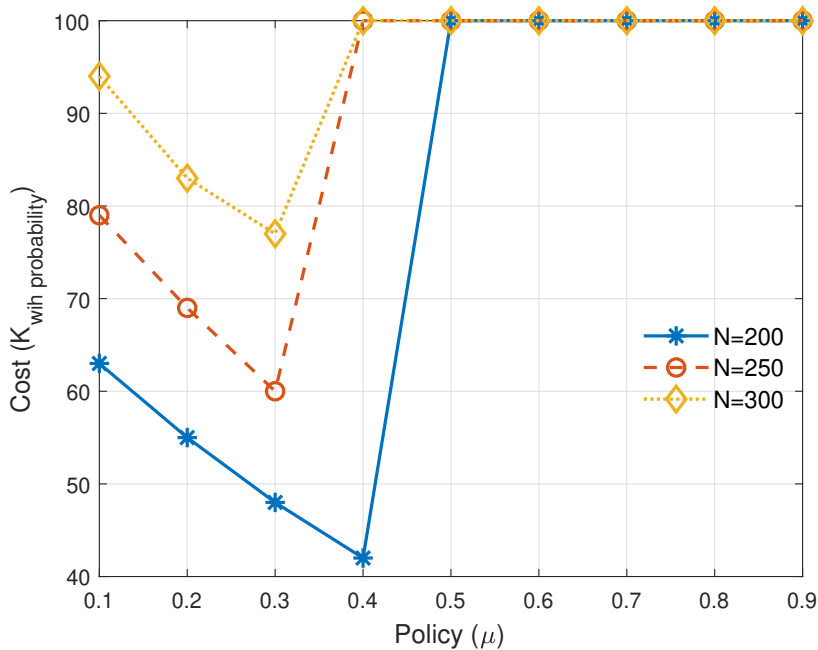


Figure 3.6: Cost with respect to the policy μ for *Probabilistic system choice* method for $N = \{200, 250, 300\}$.

We notice that increasing μ up to a certain level decreases the need for licensed resources, as it utilizes the unlicensed system more often. However, after this level the system cannot handle the offered load, as we discussed earlier in subsection 3.3.2, that when $P_{loss}^U > 1 - \Theta$, it is impossible for the system to attain URLLC requirements. From Figure 3.6, we deduce the optimal policy for $N = \{200, 250, 300\}$ as $\mu^* = \{0.4, 0.3, 0.3\}$ corresponding to costs $K^* = \{42, 60, 87\}$.

We now move to “In series” method. We plot in Figure 3.7 the cost with respect to policy δ for the same high-load regime of $N = \{200, 250, 300\}$.

We notice the effect of small and large δ on the performance as discussed in subsection 3.3.3, where the performance is best in the middle of the range.

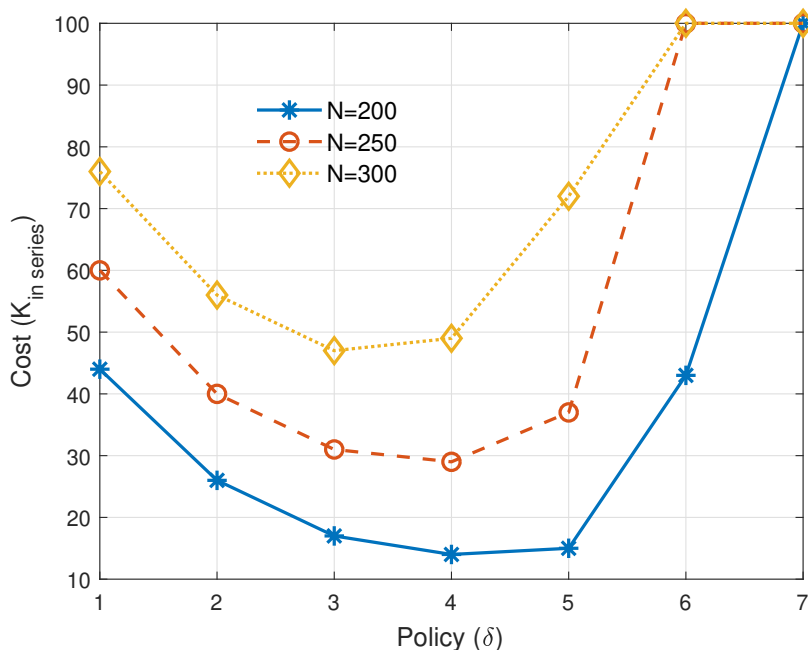


Figure 3.7: Cost with respect to the policy δ for *In series* method for $N = \{200, 250, 300\}$.

However, when N increases, δ^* tends to take smaller values since the unlicensed system becomes more saturated and it is better to utilize the licensed one more often. The optimal policies for $N = \{200, 250, 300\}$ are $\delta^* = \{4, 4, 3\}$ corresponding to costs $K^* = \{4, 30, 58\}$, which are smaller than the ones of “Probabilistic system choice” method.

Finally, we compare in Figure 3.8 the cost with respect to the number of stations for the three proposed methods deploying their optimal policies, alongside to standalone licensed system.

We observe the same result as in Figure 3.5, that the “In series” method outperforms considerably the other methods, followed by Duplication and Probabilistic system choice methods, respectively. This demonstrates the interest of the joint unlicensed-licensed transmission and the “In series” method in particular.

3.4 Multi-tenant environment

Our previous study considered a confined smart-factory scenario operated by one tenant only which aims to minimize the cost of network deployment. However, in a real-life situation, an industrial area may include several smart factories in vicinity, creating non-negligible interference from one to another.

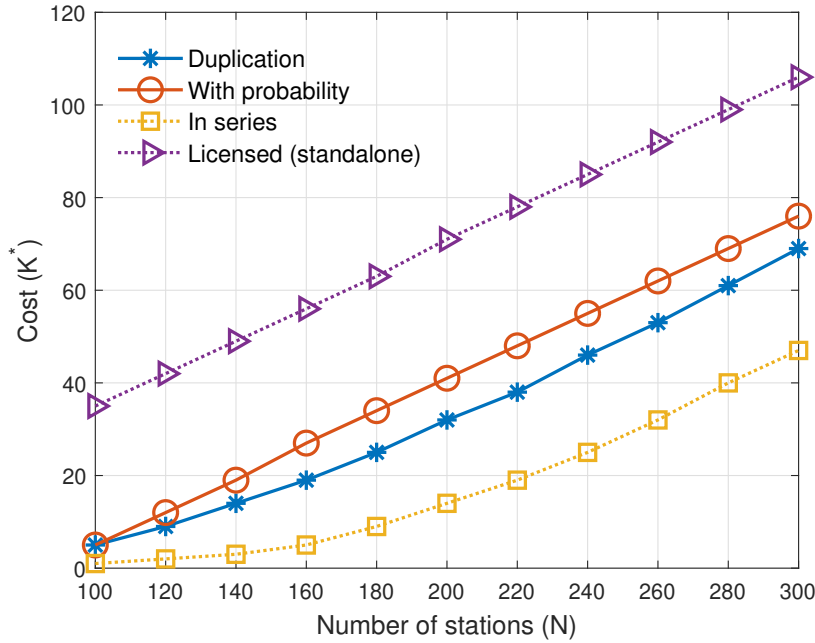


Figure 3.8: Cost with respect to the number of stations of: Duplication, Probabilistic system choice, In series and standalone licensed systems, at which URLLC requirements are guaranteed.

If all factories are operated by one tenant then this interference can be managed rather easily, but usually it is not the case: factories are operated by different tenants and unlicensed spectrum is no longer confined.

Assuming the existence of M tenants operating in proximity, deploying the “In series” mechanism to transport their URLLC traffic, then if every tenant tries to use unlicensed resources selfishly (without considering neighbouring interfering stations) then the overall interference could increase and the gain from using the unlicensed system will be reduced, which may result in the tragedy of the commons like situation. In the following, we study this multi-tenant scenario and compare it to our previous one-tenant study. We assume that licensed resources are private for every tenant, i.e., with no interference.

3.4.1 System model

We denote a given tenant by v_i (v is for vertical) and we evaluate its system performance under interference from other tenants, $i \in \{1, \dots, M\}$. We denote by N_i the number of stations of tenant v_i .

We assume that each vertical's coverage includes all N stations transmitting in the uplink, where $N = N_1 + N_2 + \dots + N_M$. We assume that all stations share the same properties and constraints, i.e., the same λ, W, T and Θ .

Each tenant v_i deploys a URLLC transmission strategy $\delta_i; i \in \{1, \dots, M\}$, $\delta_i \in \{1, \dots, \delta_{max} - 1\}$.

This situation can be represented by a non-cooperative game, similar to work in [27], with the triplet $G = (V, \{S_i\}_{i \in V}, \{u_i\}_{i \in V})$ where $V = \{v_1, v_2, \dots, v_M\}$ is the finite set of players, S_i is the set of strategies of v_i represented by $\delta_i \in \{1, \dots, \delta_{max} - 1\}$ and u_i is the utility function of v_i which is the inverse of its cost function represented by the required licensed resources to satisfy the reliability and delay requirements, equivalent to $K_i(\delta_1, \dots, \delta_M)$, where K_i is the cost of licensed resources for tenant v_i .

In non-cooperative games, each player aims to maximize its own utility over its strategy set, thus player i chooses the strategy s_i which maximizes its utility u_i for a given vector of strategies $\vec{s} = (s_1, \dots, s_M)$. Thereafter, player i waits for others to change/keep their strategies, and then changes/keeps its strategy accordingly. If there exists a vector of strategies $\vec{s}^* = (s_1^*, \dots, s_M^*)$ which satisfies $\forall i \in V, \forall s_i' \in S_i, u_i(s_i^*, \vec{s}_{-i}^*) \geq u_i(s_i', \vec{s}_{-i}^*)$ where \vec{s}_{-i}^* refers to the set of strategies of all players except player i , then the game has Nash equilibria [28].

Our game can be considered as finite since it has finite sets of players and strategies. Nash showed in [29] that at least one equilibrium point exists in finite games. However, this proves the existence of mixed-strategy Nash equilibria only and not pure ones. In the following, we prove the existence of at least one pure-strategy Nash equilibrium by studying the concavity of the utility function, where a concave utility function of a game indicates the existence of pure strategies.

3.4.2 Medium access model in unlicensed spectrum

We study in the following the effect of tenants interference in unlicensed spectrum on the loss probability of each tenant.

Fixed-point analysis

We focus here on tenant v_1 . Using the proposed Markov model in section 2.4 for the multi-tenant case, where the effect of other stations on the one being studied is present in q calculation, which we denote here by q_1 referring

to the collision probability calculated by v_1 .

Different policies δ_i suggest having different number of stages m_i , $i \in \{1, \dots, M\}$, then the probability of transmission in equation (2.12) becomes:

$$p_i(\delta_i) = \sum_{j=0}^{m_i-1} \sum_{k=0}^{m_i-1} \Pi_{j,0,k}, \quad i \in \{1, \dots, M\} \quad (3.17)$$

Equation (2.1) is rewritten similarly for all tenants as:

$$q_i(\delta_1, \dots, \delta_M) = 1 - (1 - p_g p_i(\delta_i))^{N_i-1} \times \sum_{\substack{j=0 \\ j \neq i}}^M (1 - p_g p_j(\delta_j))^{N_j} \quad (3.18)$$

Numerically, we can assess the impact of interfering stations from other tenants on v_1 by solving the set of fixed-point Equations (3.17) and (3.18), then plugging q_1 into Equation (2.14) to get the loss probability for v_1 denoted in the following by $P_1^U(\delta_1, \dots, \delta_M)$.

Solving the fixed point does not allow us to have a closed-form expression for the Nash equilibrium points of $P_1(\delta_1, \dots, \delta_M)$. We propose next an approximate way to obtain such an expression, which will help us next to study its concavity and hence the existence of pure strategies.

Closed-form analysis

For this purpose, we go back to the classical Bianchi model illustrated in Figure 2.1. Since the arrival of packets is random and the arrival rate p_g is assumed to be small, the random backoff process can be reduced to the arrival process only, and hence a time slot is busy if one or more packets arrive at the same time. q_1 is then expressed as follows:

$$q_1 = 1 - (1 - p_g)^{N-1} \approx 1 - [1 - (N-1)p_g] = (N-1)p_g \quad (3.19)$$

q_1 depends also on the number of stages a packet goes through, because the actual number of packets in the system depends on their arrival and whether they were successfully transmitted or are still in backoff. Assuming

that all tenants deploy the same W , we estimate the average number of stages a packet goes through, denoted by \bar{m}_i , in a time budget equal to $T_U^i = \delta_i z$ as:

$$\bar{m}_i = \frac{\delta_i z}{\bar{D}_{stage} + \rho + 1} - 1, \quad (3.20)$$

where \bar{D}_{stage} represents the average time spent in one stage, composed of (on average) $(W - 1)/2$ busy or idle periods with probabilities q_i and $1 - q_i$, respectively, calculated by:

$$\bar{D}_{stage} = \frac{(W - 1) \times [q_i \rho + (1 - q_i)]}{2}. \quad (3.21)$$

The probability of going through \bar{m}_i stages without success is $(q_i)^{\bar{m}_i}$, and so staying in the backoff phase has a probability of $1 - (q_i)^{\bar{m}_i}$. The actual number of packets that are still in backoff phase \tilde{N}_i can be approximated by:

$$\tilde{N}_i = N_i(1 - (q_i)^{\bar{m}_i}), \quad i \in \{1, \dots, M\} \quad (3.22)$$

$$\tilde{N} = \tilde{N}_1 + \tilde{N}_2 + \dots + \tilde{N}_M \quad (3.23)$$

We inject \tilde{N} into equation (3.19), and we obtain a more accurate value of q_i knowing that \tilde{N} depends on q_i :

$$q_i' = 1 - (1 - p_g)^{\tilde{N}-1} \approx (\tilde{N} - 1)p_g \quad (3.24)$$

The probability of failure of v_1 equals to the probability of going through \bar{m}_1 stages without success:

$$P_1^U(\delta_1, \dots, \delta_M) = (q_1')^{\bar{m}_1} \quad (3.25)$$

And hence we obtain a closed-form formula for P_1^U .

In this approach, we are using the fact that p_g is very small to perform the approximations in equations (3.19) and (3.24). However, when p_g tends to grow, this approximation is no longer valid and we cannot use this approach anymore.

3.4.3 Utility function

The utility function of tenant v_1 is, as described earlier, the inverse of the cost function K_1 , illustrated in equation (3.16) and adapted for the multi-tenant case as follows:

$$u_1(\delta_1, \dots, \delta_M) = \frac{1 - \left[1 - (1 - \Theta)^{1/(\delta_{max} - \delta_1)}\right]^{1/(N_1 - 1)}}{1 - \left[1 - (1 - e^{-\lambda}) P_1^U(\delta_1, \dots, \delta_M)\right]^{(\delta_{max} - \delta_1)z}} \quad (3.26)$$

This function is twice differentiable on $\delta_1 : 1 \leq \delta_1 < \delta_{max}$ and its second derivative is positive for the practical values that correspond to our URLLC scenario, leading to the proof of its concavity and the existence of pure-strategy Nash equilibria. The equilibrium points correspond to the roots of the first derivative of u_1 with respect to δ_1 . Since the set of possible values of δ_1 is limited, the simplest way to identify the equilibrium points is by brute force search of the points which maximize u_1 .

In our case, we can replace the utility function maximization by the penalty (cost) function minimization, since we considered the utility as the inverse of the penalty. The penalty notion is more comprehensible in our context and in the numerical evaluation. In fact, the penalty function K is convex and meets the pure-strategy Nash equilibria condition.

3.4.4 Numerical evaluation

We consider the case of two tenants v_1 and v_2 with: $N_1 = 3N/4$ and $N_2 = N/4$. To illustrate the effect of different policies, we choose $\delta_1 = 5$ and $\delta_2 = 3$.

We first validate the approximate model (closed-form) of unlicensed probability of collision and loss rate with the ones of the Markov model (fixed-point) in Figure 3.9. We consider an error compensation of $W/2$ for the Markov model for more accuracy.

We observe from Figure 3.9 that the approximation error is negligible for the two measures, and the two loss rate curves share the same behaviour, which validates the closed-form model and hence the proof of concavity of the utility function.

We next illustrate Nash equilibria by evaluating the penalty of all possible combinations of the pair of policies (δ_1, δ_2) . The evaluation is done using the closed-form model. We first consider v_1 as the tenant of interest with

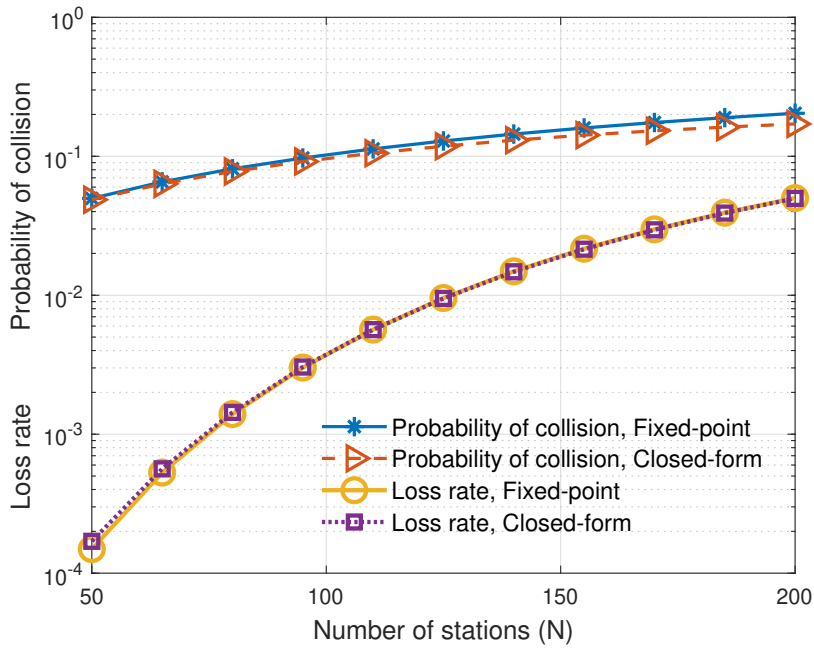


Figure 3.9: Validation of closed-form model with the fixed-point for unlicensed spectrum with two tenants.

$N = 200$: $N_1 = 150$ and $N_2 = 50$, then we consider v_2 as the tenant of interest with $N_2 = 150$ and $N_1 = 50$, which yields to a symmetrical scenario for both tenants. We illustrate in Table 3.2 the resulting penalty matrix $(K_1(\delta_1, \delta_2), K_2(\delta_1, \delta_2))$, computed with the aid of equation (3.26). Note that 99 RBs is the maximum offered number of RBs, which also indicates that the reliability target is not reached and further resources should be allocated to guarantee the required QoS.

We observe from Table 3.2 the existence of a unique equilibrium point, which corresponds to the pure-strategy Nash equilibrium: $(\delta_1^*, \delta_2^*) = (5, 5)$.

Table 3.2: Nash equilibrium illustration

$\delta_2 \backslash \delta_1$	1	2	3	4	5	6	7
1	61, 61	61, 48	61, 20	61, 11	61, 9	61, 14	61, 99
2	48, 61	50, 50	53, 21	54, 12	54, 10	54, 16	54, 99
3	20, 61	21, 53	24, 24	25, 15	26, 12	26, 23	26, 99
4	11, 61	12, 54	15, 25	16, 16	17, 14	17, 26	17, 99
5	9, 61	10, 54	12, 26	14, 17	14, 14	14, 27	15, 99
6	14, 61	16, 54	23, 26	26, 17	27, 14	28, 28	28, 99
7	99, 61	99, 54	99, 26	99, 17	99, 15	99, 28	99, 99

If the game arrives to this point, then it is not in the interest of either player to change their strategy because it does not improve its payoff (minimizes its cost). Table 3.2 illustrates the fact that decreasing the time budget in unlicensed system for one player (decreasing its δ_i) improves the performance for the other player. By this, we conclude that our game has pure-strategy Nash equilibria, and a unique one for the given numerical example.

3.4.5 Price of anarchy

It is interesting to discuss the notion of *price of anarchy* in non-cooperative games, which measures the efficiency deterioration of the system in the presence of multiple non-cooperative players, compared to a cooperative system.

We evaluate in Figure 3.10 the cost for the case of one player with N stations versus the case of two players with $N/2$ stations each; the cost in the second case is $K_1 + K_2$. Figure 3.10 confirms that a cooperative setting achieves higher gain than a non-cooperative one.

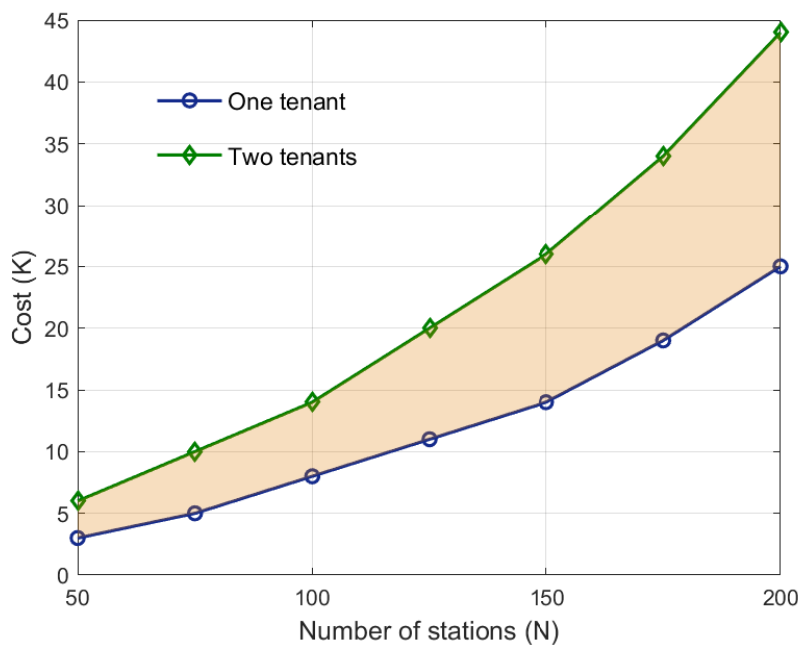


Figure 3.10: Price of anarchy of the non-cooperative game.

3.5 Conclusion

We studied in this chapter the joint unlicensed and licensed transport of URLLC. We were mainly interested in estimating the cost of different transmission schemes in terms of licensed bandwidth. The proposed “In series” method, where packets are first transmitted over unlicensed system during a given time budget and only unsuccessful packets toggle to the licensed system for the remaining time, requires the minimum cost compared to other proposed methods since licensed resources are only used when needed. We considered a multi-tenant scenario where different tenants share the same unlicensed resources and deploying “In series” method. We illustrated the existence of at least one equilibrium point, at which all tenants minimize their cost.

We focus in next chapter on the transport of URLLC in the presence of eMBB. In this case, using licensed resources as an anchor to unlicensed ones may entail a substantial cost due to the increased load. For that, we investigate the use of different power levels for URLLC transmission, in order to compete with eMBB while ensuring its stringent constraints.

Chapter 4

URLLC and eMBB coexistence in unlicensed spectrum

4.1 Introduction

The coexistence of URLLC with other services, notably eMBB, is inevitable in future networks deployment. For instance, eMBB traffic can be generated from a simple usage of a personal smartphone, but this traffic have a substantial effect on other users of the network. In this chapter, we focus on the coexistence of URLLC and eMBB in a standalone unlicensed system for the uplink transmission in a smart-factory scenario.

The basic method for solving the problem of heterogeneous services on the same resources is by network slicing, or orthogonal multiple access (OMA) [30]. In this method, distinct radio resources are reserved for different services and it can be deployed for downlink and uplink. However, this method suffers from poor spectral efficiency since allocated frequency bandwidth is not adapted to the load of each service, especially for URLLC, which demand a large bandwidth to guarantee its requirements, as demonstrated in previous chapter. Non-Orthogonal Multiple Access (NOMA) [31] allows multiplexing simultaneous transmissions on the same resources, e.g., using different power levels. In fact, NOMA requires high computational power to implement real-time power allocation and successive interference cancellation algorithms.

Other techniques are based on prioritizing URLLC over eMBB by puncturing ongoing eMBB transmissions to schedule the urgent URLLC packets, as proposed in [32] and [33] for downlink. The work in [34] proposes using

unlicensed spectrum as an anchor to serve the punctured eMBB packets for the downlink as well.

Nevertheless, URLLC and eMBB coexistence in standalone unlicensed system has never been discussed before. This can be related to the recent interest in unlicensed spectrum for URLLC. Our proposed technique to prioritize URLLC over eMBB is by increasing its transmission power level, which gives it a better chance of being decoded by the receiver even in case of collision with other “lower” power level transmission. In this context, optimal power control for URLLC is studied in [35] for uplink grant-free transmission in licensed spectrum, in order to enhance the reliability of URLLC against noisy channels.

In this chapter, we first model the medium access for both services coexisting in unlicensed spectrum at the same power level and evaluate their performance metrics: reliability within a delay budget for URLLC and throughput for eMBB. The results show that URLLC requirements cannot be met even for low eMBB traffic load. In order to cope with this, we explore a preemptive approach where URLLC packets are transmitted with a higher power when their delay approaches the delay constraint, increasing their chance of being successfully received. This approach is LBT-agnostic, hence we propose another approach which respects LBT and allows high power transmissions after a certain time threshold.

4.2 System model

In the smart-factory scenario where a number of automated machines communicate URLLC traffic using unlicensed spectrum, there might exist other users generating other types of traffic, for instance eMBB, and transport it over the same unlicensed channel as URLLC. This scenario is very likely to happen when workers inside the factory are using the available access point to browse the internet on their personal devices for example.

When an eMBB user is active, we assume it generates traffic constantly (saturated source), as is the case of video streaming or file transfer. We consider a fixed number of active eMBB stations, denoted by N_e , which can be variable over the long term but considered constant over the studied time interval. eMBB packets are usually bulky and require more time slots for transmissions than URLLC ones. We denote the number of required time

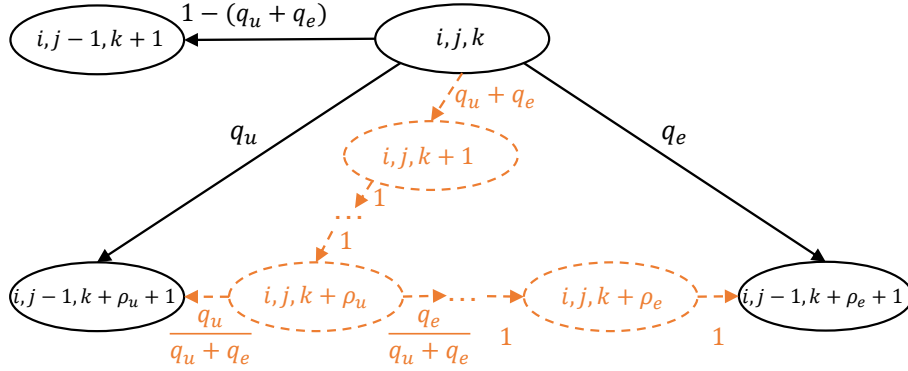


Figure 4.1: The one-step resulting states of state $\{i, j, k\}$ of URLLC coexisting with eMBB.

slots for URLLC and eMBB transmissions by ρ_u and ρ_e , respectively. We further denote the number of URLLC stations by N_u (instead of N as we did previously) to better distinguish the variables.

4.3 Equal power transmission

In this section, we model the medium access of both types of traffic coexisting in unlicensed system under LBT.

4.3.1 URLLC medium access model

URLLC stations deploy LBT cat3 with a fixed CW size, denoted by W . Here also, we are interested in quantifying the loss rate within a time budget, as we did in previous chapters. The system can be modeled with a three-dimensional Markov chain with states $\{s(t), w(t), d(t)\}$ representing the stochastic processes of stage, CW and packet delay, respectively.

When coexisting with eMBB, URLLC stations now sense the medium busy during different periods, ρ_u or ρ_e . This is illustrated in Figure 4.1, where q_u and q_e denote the probability of sensing the medium busy during $\rho_u + 1$ and $\rho_e + 1$ time slots from the standpoint of one URLLC station, respectively. q_u and q_e represent also the probability of collision with a transmission of duration $\rho_u + 1$ and $\rho_e + 1$, for a transmitting URLLC station, respectively.

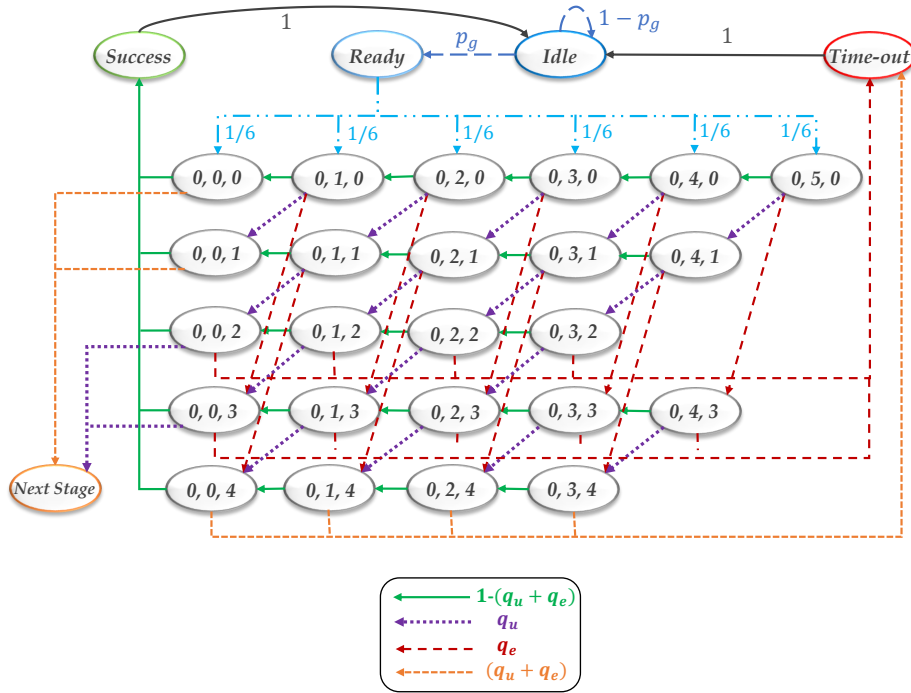


Figure 4.2: First stage of Markov chain model for URLLC coexisting with eMBB. Example: $W = 6$, $\rho_e + 1 = 3(\rho_u + 1)$ and $m_u \geq 4$.

The fact of having three possible next states for every state generates a huge number of states and renders the solution of the balance equations prohibitive. For that, we apply the same approximation as in section 2.4 to reduce the number of states. The approximation is based on neglecting the one-time-slot increment in $d(t)$ when sensing the medium idle. We also assume that $\rho_e + 1 = c(\rho_u + 1)$ with $c \in \mathbb{N}$, which further simplifies the chain. Denoting the maximum allowed number of stages by m_u : $m_u = \lfloor T/(\rho_u + 1) \rfloor$, we propose a toy example to illustrate the first stage of the chain for $W = 6$, $\rho_e + 1 = 3(\rho_u + 1)$ and $m_u \geq 4$, in Figure 4.2.

URLLC packet generation is modeled with a Poisson process of intensity λ per time slot and the packet generation probability per time slot is denoted by p_g and is given by $p_g = 1 - e^{-\lambda}$.

The states *Idle*, *Ready*, *Success* and *Time-out* represent four different states the station can be in: waiting for a packet, starting LBT process for a generated packet, after a successful transmission and discarding the packet when its delay reaches the constraint T , respectively. The state *Next stage* indicates the following stages of LBT when the packet is still respecting the delay constraint.

We assume q_u and q_e to be constant and independent from the state. We derive from Figure 4.1 the balance equations of the Markov chain for the general case, organized in the set of equations (4.1) and described in a recursive manner row by row starting from the columns with higher $w(t)$. The states *Success*, *Ready*, *Idle* and *Time-out* are reduced accordingly to one state, denoted by *Idle*.

$$\begin{aligned}
\Pi_{0,W-1,0} &= p_u \frac{\Pi_{Idle}}{W} \\
\Pi_{0,W-j,0} &= p_u \frac{\Pi_{Idle}}{W} + (1 - q_u - q_e) \Pi_{0,W-j+1,0}, \quad 2 \leq j \leq W \\
\Pi_{0,W-k-1,k} &= \begin{cases} q_u \Pi_{0,W-k,k-1}, & 1 \leq k \leq c-1 \\ q_e \Pi_{0,W-k,k-c}, & c \leq k \leq m_u - 1 \end{cases} \\
\Pi_{0,W-j,k} &= \begin{cases} (1 - q_u - q_e) \Pi_{0,W-j+1,k} + q_u \Pi_{0,W-j+1,k-1}, & 1 \leq k \leq c-1 \\ (1 - q_u - q_e) \Pi_{0,W-j+1,k} + q_u \Pi_{0,W-j+1,k-1} + q_e \Pi_{0,W-j+1,k-c}, & k+2 \leq j \leq W \\ & c \leq k \leq m_u - 1 \\ & k+2 - \lfloor \frac{k}{c} \rfloor (c-1) \leq j \leq W \end{cases} \\
\Pi_{i,W-1,k} &= \begin{cases} \frac{q_u}{W} \Pi_{i-1,0,k-1}, & 1 \leq i \leq m_u - 1, \quad i \leq k \leq i+c-1 \\ \frac{q_u}{W} \Pi_{i-1,0,k-1} + \frac{q_e}{W} \Pi_{i-1,0,k-c}, & 1 \leq i \leq m_u - 1, \\ & i+c \leq k \leq m_u - 1 \end{cases} \quad (4.1) \\
\Pi_{i,W-j,k} &= \begin{cases} \frac{q_u}{W} \Pi_{i-1,0,k-1} + q_u \Pi_{i,W-j+1,k-1} + q_e \Pi_{i,W-j+1,k-c}, & 1 \leq i \leq m_u - 1, \\ & 2 \leq j \leq W, \\ & i \leq k \leq i+c-1 \\ \frac{q_u}{W} \Pi_{i-1,0,c+i-1} + \frac{q_e}{W} \Pi_{i-1,0,c+i-c} + q_u \Pi_{i,W-j+1,c+i-1} \\ & + q_e \Pi_{i,W-j+1,c+i-c}, & 1 \leq i \leq m_u - 1, \\ & 2 \leq j \leq W, \\ & k = i+c \\ \frac{q_u}{W} \Pi_{i-1,0,k-1} + \frac{q_e}{W} \Pi_{i-1,0,k-c} + q_u \Pi_{i,W-j+1,k-1} + q_e \Pi_{i,W-j+1,k-c} \\ & + q_e \Pi_{i,W-j+1,k-c}, & 1 \leq i \leq m_u - 1, \\ & 2 \leq j \leq W, \\ & i+c+1 \leq k \leq m_u - 1 \end{cases}
\end{aligned}$$

We apply the normalization condition to calculate the value of Π_{Idle} which can be obtained numerically, leading to the probability of transmission in one

time slot p_u given by:

$$p_u = \sum_{i=0}^{m_u-1} \sum_{k=0}^{m_u-1} \Pi_{i,0,k} \quad (4.2)$$

We denote by p_e the transmission probability of an eMBB station (it will be evaluated in the next subsection). q_u corresponds to having at least one URLLC transmission in the absence of eMBB ones and is given by equation (4.3) and q_e corresponds to the probability of having at least one eMBB transmission regardless of URLLC ones since they have a smaller duration and is given by equation (4.4).

$$q_u = [1 - (1 - p_u)^{N_u-1}] (1 - p_e)^{N_e} \quad (4.3)$$

$$q_e = 1 - (1 - p_e)^{N_e} \quad (4.4)$$

Equations (4.2-4.3-4.4) along with equations (4.8-4.7) derived in the next subsection, formulate a set of fixed-point equations which can be jointly solved to obtain q_u and q_e .

To quantify the reliability, we calculate the hitting probability of state *Success* from state *Ready*, denoted by $h_{Success}^{Ready}$. It is shown in equation (4.5) where the hitting probabilities $h_{i,j,k}^{Ready}$ can be deduced from the balance equations (4.1), similar to equations (2.13).

$$h_{Success}^{Ready} = (1 - q_u - q_e) \sum_{i=0}^{m_u-1} \sum_{k=0}^{m_u-1} h_{i,0,k}^{Ready} \quad (4.5)$$

Thus, the loss rate, denoted by P_{loss} , is also obtained from $h_{Time-out}^{Ready}$ and is given by:

$$P_{loss} = 1 - h_{Success}^{Ready} \quad (4.6)$$

4.3.2 eMBB medium access model

We suppose that eMBB packets have less priority than URLLC ones, since eMBB users do not have as stringent QoS requirements as URLLC ones. Therefore, eMBB users deploy LBT cat4 with adaptive CW. However, a minimum throughput must be guaranteed to them, we denote it by S_{target} .

To quantify the throughput of eMBB users when coexisting with URLLC ones, we use the Bianchi model shown in section 2.2.2.

We denote the adaptive CW by $\{W_0, W_1, \dots, W_{m_e}\}$ where m_e is the maximum CW size. The probability of collision seen from the standpoint of one eMBB station, denoted by q_{embb} , is obtained from solving the set of fixed-point equations (4.2-4.3-4.4-4.7-4.8).

$$q_{embb} = 1 - (1 - p_e)^{N_e - 1} (1 - p_u)^{N_u} \quad (4.7)$$

$$p_e = \frac{2(1 - 2q_{embb})}{(1 - 2q_{embb})(W_0 + 1) + q_{embb}W_0[1 - (2q_{embb})^{m_e}]} \quad (4.8)$$

Equation (4.7) represents the collision probability seen from the standpoint of one transmitting eMBB station among the N_e ones, and the packet is in collision if it encounters at least one other packet (URLLC or eMBB). The transmission probability of an eMBB station shown in equation (4.8) is derived from Bianchi model, as in equation (2.2). Hence, we describe eMBB throughput in equation (4.9), similar to equation (2.8).

$$S_e = \frac{P_{success}^e \rho_e}{P_{idle} + P_{\rho_u} \rho_u + P_{\rho_e} \rho_e} \quad (4.9)$$

where $P_{success}^e$ is the probability of having a successful eMBB transmission, P_{idle} is the probability of sensing an idle time slot, P_{ρ_u} and P_{ρ_e} are the probabilities of sensing the medium busy during ρ_u and ρ_e time slots, respectively. These probabilities are expressed as follows:

$$\begin{cases} P_{success}^e = N_e p_e (1 - p_u)^{N_u} (1 - p_e)^{N_e - 1} \\ P_{idle} = (1 - p_u)^{N_u} (1 - p_e)^{N_e} \\ P_{\rho_u} = [1 - (1 - p_u)^{N_u}] (1 - p_e)^{N_e} \\ P_{\rho_e} = 1 - (1 - p_e)^{N_e} \end{cases} \quad (4.10)$$

4.3.3 Numerical evaluation

We consider the same numerical values of URLLC system as previously, repeated in Table 4.1. W is chosen smaller than the conventional 16 to give URLLC stations more priority over eMBB ones.

For eMBB, we consider that their packets require three times the time to transmit one URLLC packet, $c = 3$, which means that $\rho_e = 20$. For LBT cat4, $W_0 = 16$ and $m_e = 4$ are considered, leading to a maximum window size of 256. The target normalized throughput is $S_{target} = 0.5$, which indicates

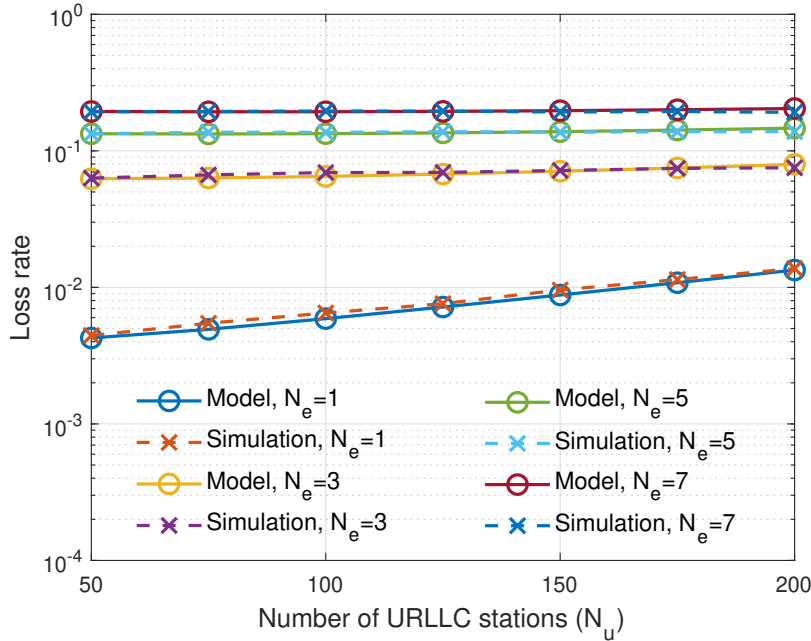


Figure 4.3: URLLC model validation coexisting with eMBB.

that over a given horizon of time, the channel must be utilized by successful eMBB transmissions for at least half of the time. We organize the ensemble of the numerical values in Table 4.1.

Table 4.1: Numerical values of the system parameters of URLLC and eMBB coexistence.

T	111 time slots	W	8	λ	0.001
ρ_u	6 time slots	W_0	16	m_e	4
ρ_e	20 time slots	S_{target}	0.5	Θ	$1 - 10^{-5}$

We validate our analytical model against simulations by evaluating the loss rate for different values of N_u and N_e . The results, shown in Figure 4.3, show a good match between model and simulation for $N_e = \{1, 3, 5, 7\}$. As predicted, the loss rate increases considerably compared to a URLLC-only situation, even when coexisting with one eMBB station. This indicates that the reliability constraint cannot be assured for URLLC coexisting “harmoniously” with eMBB. We notice that the impact of N_e is more obvious than N_u , the loss rate is almost constant when changing N_u for the same N_e .

We evaluate the throughput of eMBB and show in Figure 4.4 the results obtained by the analytical model and compare them to those obtained through simulation.

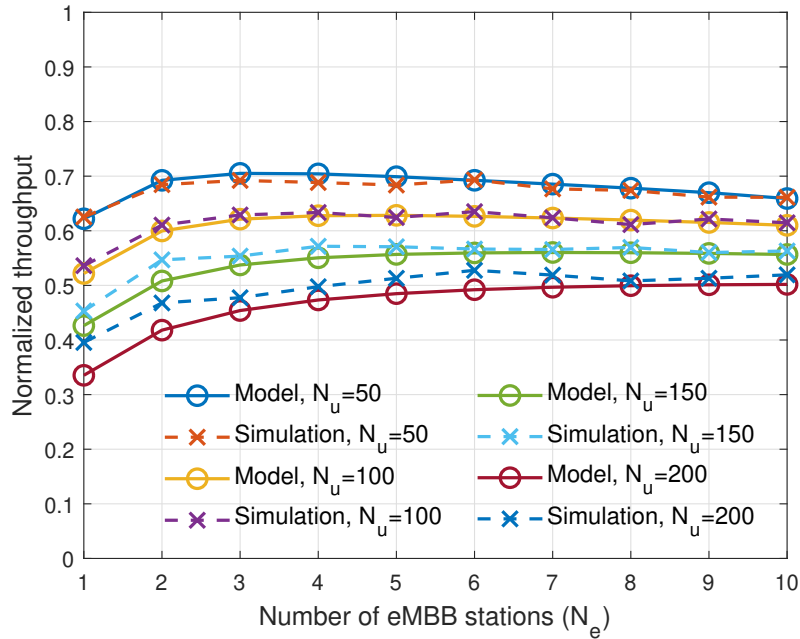


Figure 4.4: eMBB model validation for the harmonious coexistence with URLLC.

We observe that the results obtained by the model and simulations are very close which validates the former; the difference between analysis and simulations is due to modeling URLLC transmissions by their arrival process, which does not incorporate their LBT process. We notice that the target throughput of 0.5 is respected almost all the time, when $N_u \leq 150$. Increasing the number of eMBB stations decreases slightly the throughput. When $N_e = 1$, the throughput is generally small since only one eMBB station utilizes the channel.

4.4 LBT-agnostic preemption

As illustrated in the previous section, the coexistence of URLLC with eMBB, both transmitting at the same power level, degrades considerably the performance of URLLC due to its strict constraints on delay and reliability, leading to requiring more resources to guarantee QoS for both. We propose here a new approach to improve the reliability of URLLC, by making use of preemption at the transmission power level. We study the effect of this approach on eMBB performance too, so as to determine its feasibility.

The preemption scheme we propose is that when the delay of the active

URLLC packet approaches its deadline, i.e., the remaining time budget allows one URLLC packet transmission, then this packet will be transmitted with high power, which increases its chance of being decoded by the receiver. This very packet will be lost only if it is transmitted simultaneously with another high-power URLLC packet. We call this scheme “LBT-agnostic preemption”. This scheme violates the process of LBT, it results in interrupting an ongoing eMBB transmission, decreasing thus its throughput. However, the high-power usage should be kept minimal and used only when needed, i.e., when the URLLC delay budget is about to expire.

4.4.1 URLLC medium access model

We make use of the Markov chain illustrated in Figure 4.2. We suppose that the URLLC station decides to preempt the channel when the given packet delay reaches $T - \rho_u$ and that it only has one attempt to transmit before timeout, which corresponds to the states with $d(t) = m_u - 1$. We note that states with $d(t) < m_u - 1$ could arrive to the state $d(t) = m_u - 1$ and then to the state *Time-out* when the medium is sensed busy for ρ_e time slots, which is illustrated in Figure 4.1.

In this case, a state, e.g., *Preemption*, replaces state *Time-out* to represent the high-power transmission, and leads to states *Time-out* and *Success* with respective probabilities of q_h and $1 - q_h$; q_h expresses the probability of collision with another high-power transmission. Hence, reliability is increased as a new path to the state *Success* is created.

The stationary distribution equations (4.1) from the last section are still valid here, but for the fixed-point equations, we introduce the probability of a preemptive transmission, p_h , defined as the probability that a URLLC station transmits with high power, and given by:

$$p_h = \sum_{i=0}^{m_u-1} \sum_{j=0}^{W-1} \Pi_{i,j,m_u-1} + \sum_{i=0}^{m_u-1} \sum_{j=0}^{W-1} \sum_{k=m_u-c+1}^{m_u-2} \Pi_{i,j,k} \quad (4.11)$$

The first term: $\sum_{i=0}^{m_u-1} \sum_{j=0}^{W-1} \Pi_{i,j,m_u-1}$, corresponds to the sum of all states with $d(t) = m_u - 1$. The second term of the expression corresponds to the implicit states when the medium is busy for ρ_e time slots.

We then compute the probability of collision with another high-power transmission, q_h , as:

$$q_h = 1 - (1 - p_h)^{N_u - 1} \quad (4.12)$$

We obtain the new values of q_u , q_e and q_{emmb} in addition to q_h by solving the fixed-point equations (4.3-4.4-4.8-4.7-4.12), with the new expression of p_u in equation (4.13).

$$p_u = \sum_{i=0}^{m_u-1} \sum_{k=0}^{m_u-1} \Pi_{i,0,k} + p_h \quad (4.13)$$

We denote the new hitting probabilities for states *Success* and *Time-out* from state *Ready* by $\tilde{h}_{Success}^{Ready}$ and $\tilde{h}_{Time-out}^{Ready}$, respectively. Using equation (4.5), we obtain:

$$\tilde{h}_{Success}^{Ready} = h_{Success}^{Ready} + (1 - q_h) \times (1 - h_{Success}^{Ready}) \quad (4.14)$$

$$\tilde{h}_{Time-out}^{Ready} = 1 - \tilde{h}_{Success}^{Ready} \quad (4.15)$$

and hence we obtain the reliability and loss rate of URLLC for the LBT-agnostic preemption method.

4.4.2 eMBB medium access model

We indicated in the last subsection that the new probability of collision q_{embb} is obtained by solving the new set of fixed-equations (4.3-4.4-4.8-4.7-4.12-4.13).

We evaluate now the new value of throughput, denoted by \tilde{S}_e , using the expression in equation (4.9) with the new values of p_u , p_e and $P_{success}^e$. The latter denotes now the probability of not being transmitted simultaneously with other eMBB or URLLC transmissions, and no preemptive URLLC transmission occurs in any of its remaining $c - 1$ parts, given by equation (4.17).

$$\tilde{S}_e = \frac{\tilde{P}_{success}^e \rho_e}{P_{idle} + P_{\rho_u} \rho_u + P_{\rho_e} \rho_e} \quad (4.16)$$

$$\tilde{P}_{success}^e = N_e p_e (1 - p_e)^{N_e - 1} (1 - p_u)^{N_u} (1 - p_h)^{N_u(c-1)} \quad (4.17)$$

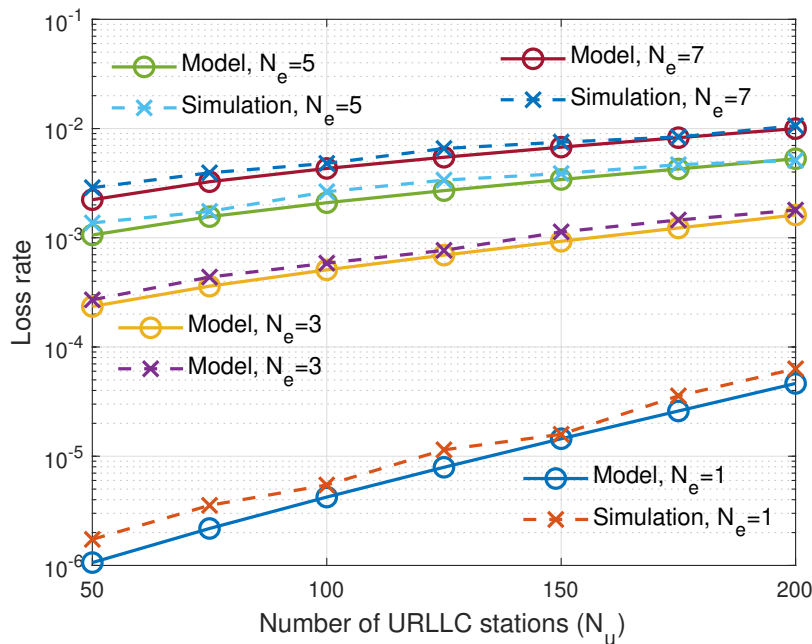


Figure 4.5: URLLC model validation for the LBT-agnostic preemption approach.

4.4.3 Numerical evaluation

We validate the model of the LBT-agnostic preemption approach against simulations, using the numerical values in Table 4.1. The results, shown in Figures 4.5 and 4.6, indicate a good match between models and simulation. We observe that the loss rate of URLLC decreases by an order of a thousand to ten thousands, compared to the coexistence with no preemption. URLLC performance is now closer to the target, and yet can be ensured for small traffic loads, i.e., $N_e = 1$ and $N_u \leq 150$.

Regarding eMBB performance, the throughput has slightly decreased compared to the case of coexistence with no preemption, especially when N_u grows. However, the target throughput remains feasible for most of N_u and N_e values, as for the case with no preemption.

4.5 LBT-aware time threshold policy

We propose a new transmission scheme based again on preemption using high power, but this time the latter is activated starting from a given switching time which depends on the packet delay. In this scheme, the station selects a time threshold $\tau \in \{0, 1, \dots, T\}$, when $d(t) < \tau$ the station transmits

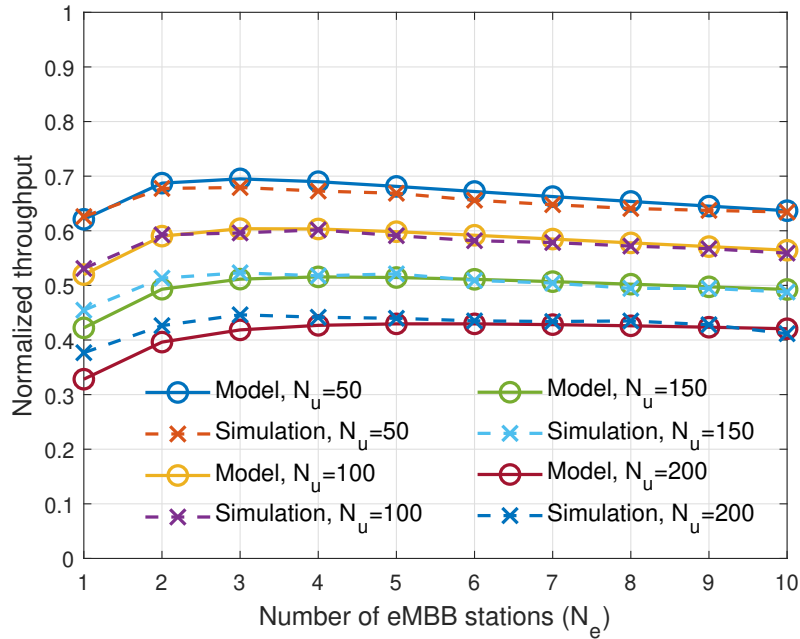


Figure 4.6: eMBB model validation for the LBT-agnostic preemptive approach.

when CW hits zero using normal power, else, it transmits using high power. τ here expresses a transmission policy which changes the performance of the system.

This scheme has several benefits over the LBT-agnostic preemptive approach, such as avoiding LBT violation which causes eMBB packet preemption, and the flexibility in choosing τ which allows more transmissions using high power and hence increases the packet success rate. In this case, if all URLLC stations transmit with a higher power than eMBB ones, then URLLC packets have a higher chance to pass successfully since collisions with eMBB packets are removed, at the same time, eMBB stations are not affected by this scheme since a collision with the same or a higher power transmission results in the same packet loss.

In the following, we study URLLC performance following this approach and how it is used to dimension the network.

4.5.1 URLLC medium access model

Here also, we add a state called *Preemption* to the Markov chain illustrated in Figure 4.2, to represent the high-power transmission. For simplicity, we consider policies spaced by $\rho_u + 1$ time slots, which allows us to use the Markov

chain directly to assess the performance of the system. The new set of policies are expressed by $\tau \in \{0, 1, \dots, m_u - 1\}$.

For a given policy τ , when transmitting using normal power, we denote the probability of collision with a respective duration of ρ_u and ρ_e by q_u and q_e . When transmitting using high power, the same probabilities are denoted by $q_u^h(\tau)$ and $q_e^h(\tau)$, respectively. Note that q_u and q_e do not depend on the policy τ . Here, it is important to distinguish between the two probabilities of collision. When transmitting with high power, in case of collision with at least another high power transmission and a simultaneous eMBB packet, then the transmitting URLLC stations have to wait for the rest of the eMBB packet to resume their LBT process.

The stationary distribution in this case is slightly different from equation (4.1), where for the first stage it remains the same, i.e., when $i = 0$. For the following stages, the balance equations are modified as follows:

$$\Pi_{i,W-1,k} = \begin{cases} \frac{q_u^{prev}}{W} \Pi_{i-1,0,k-1}, & 1 \leq i \leq m_u - 0, \quad i \leq k \leq i + c - 1 \\ \frac{q_u^{prev}}{W} \Pi_{i-1,0,k-1} + \frac{q_e^{prev}}{W} \Pi_{i-1,0,k-c}, & 1 \leq i \leq m_u - 1, \\ & i + c \leq k \leq m_u - 1 \end{cases} \quad (4.18)$$

$$\Pi_{i,W-j,k} = \begin{cases} \frac{q_u^{prev}}{W} \Pi_{i-1,0,k-1} + q_u \Pi_{i,W-j+1,k-1} + q_e \Pi_{i,W-j+1,k-c}, & 1 \leq i \leq m_u - 1, \\ & 2 \leq j \leq W, \\ & i \leq k \leq i + c - 1 \\ \frac{q_u^{prev}}{W} \Pi_{i-1,0,c+i-1} + \frac{q_e^{prev}}{W} \Pi_{i-1,0,c+i-c} & 1 \leq i \leq m_u - 1, \\ + q_u \Pi_{i,W-j+1,c+i-1} + q_e \Pi_{i,W-j+1,c+i-c}, & 2 \leq j \leq W, \\ & k = i + c \\ \frac{q_u^{prev}}{W} \Pi_{i-1,0,k-1} + \frac{q_e^{prev}}{W} \Pi_{i-1,0,k-c} + q_u \Pi_{i,W-j+1,k-1} & 1 \leq i \leq m_u - 1, \\ + q_e \Pi_{i,W-j+1,k-c} + q_e \Pi_{i,W-j+1,k-c}, & 2 \leq j \leq W, \\ & i + c + 1 \leq k \leq m_u - 1 \end{cases}$$

where

$$q_u^{prev} = \begin{cases} q_u, & k \geq \tau \\ q_u^h(\tau), & \text{elsewhere} \end{cases}$$

$$q_e^{prev} = \begin{cases} q_e, & k - c \geq \tau \\ q_e^h(\tau), & \text{elsewhere} \end{cases}$$

The expressions of q_u and q_e are still valid from equations (4.3-4.4) with the aid of equations (4.2-4.8), applied to the new stationary distribution. We calculate the probability of transmitting using high power, denoted by $p_h(\tau)$, which corresponds to the sum of all states with $w(t) = 0$ and $d(t) \geq \tau$, and is given by:

$$p_h(\tau) = \sum_{i=0}^{m_u-1} \sum_{k=\tau}^{m_u-1} \Pi_{i,0,k} \quad (4.19)$$

We then deduce $q_u^h(\tau)$ and $q_e^h(\tau)$ as follows:

$$q_u^h(\tau) = \left[1 - (1 - p_h(\tau))^{N_u-1} \right] (1 - p_e)^{N_e} \quad (4.20)$$

$$q_e^h(\tau) = \left[1 - (1 - p_h(\tau))^{N_u-1} \right] \left[1 - (1 - p_e)^{N_e} \right] \quad (4.21)$$

The probabilities q_u , q_e , $q_u^h(\tau)$ and $q_e^h(\tau)$ can be obtained by solving the fixed point equations (4.3-4.4-4.2-4.8-4.7-4.19-4.20-4.21)

The hitting probabilities of states *Success* and *Time-out* from state *Ready*, denoted by $h_{Success}^{Ready}(\tau)$ and $h_{Failure}^{Ready}(\tau)$, respectively, are given by:

$$h_{Success}^{Ready}(\tau) = \begin{cases} (1 - q_u^h(\tau) - q_e^h(\tau)) \sum_{i=0}^{m_u-1} \sum_{k=0}^{m_u-1} \Pi_{i,0,k}, & \tau = 0 \\ (1 - q_u - q_e) \sum_{i=0}^{m_u-1} \sum_{k=0}^{\tau-1} \Pi_{i,0,k} \\ + (1 - q_u^h(\tau) - q_e^h(\tau)) \sum_{i=0}^{m_u-1} \sum_{k=\tau}^{m_u-1} \Pi_{i,0,k}, & \tau > 0 \end{cases} \quad (4.22)$$

$$h_{Time-out}^{Ready}(\tau) = 1 - h_{Success}^{Ready}(\tau) \quad (4.23)$$

We obtain hence the loss rate and reliability of this time-threshold approach.

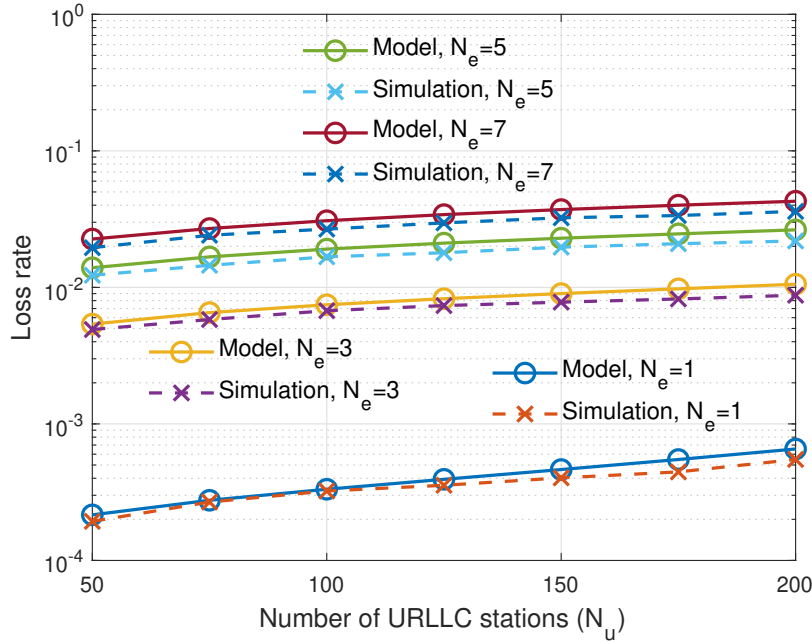


Figure 4.7: URLLC model validation for a time threshold policy $\tau = 7$.

4.5.2 eMBB medium access model

For eMBB, this transmission scheme is not different from the first coexistence case where all stations transmit always at the same power level. The throughput is calculated using equation (4.9) for the new values of p_u and p_e obtained after solving the previously mentioned fixed-point equations (4.3-4.4-4.2-4.8-4.7-4.19-4.20-4.21).

4.5.3 Numerical evaluation

We validate the analytical model against simulations using the numerical values in Table 4.1, for $\tau = 7$.

We show, respectively, in Figures 4.7 and 4.8 the loss rate for URLLC and normalised throughput for eMBB with respect to increasing respective number of stations. All URLLC stations are considered to deploy the same policy.

We notice that URLLC loss rate has been enhanced compared to the case of coexistence with no preemption by an order higher than ten times. The reliability approaches its target but still does not attain it.

Figure 4.8 confirms the fact that this approach does not affect eMBB performance as the results are identical to the ones in the first studied case.

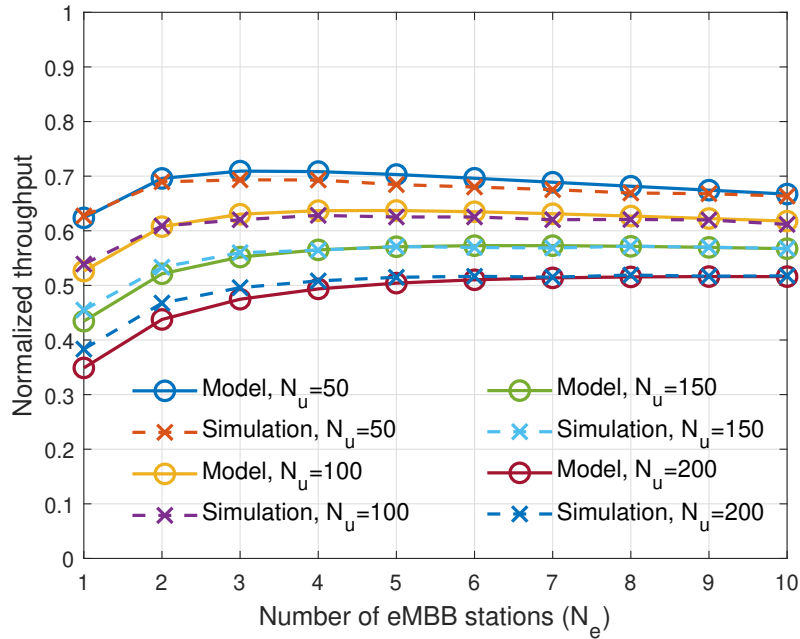


Figure 4.8: eMBB model validation for a time threshold policy $\tau = 7$.

We study now the effect of choosing different thresholds $\tau = 7$ on URLLC's loss rate and eMBB's throughput. We show in Figure 4.9 the two metrics as a function of τ for $N_e = 2$ and $N_u = 100$. We also demonstrate the importance of CW size in attaining the target QoS, especially for URLLC, and illustrate the cases of $W = 4$ and different $W_0 = \{16, 32, 64\}$, while maintaining the maximum window size of eMBB to 256.

We observe from Figure 4.9 the convexity of the loss rate as a function of τ . This is due to the increased collision rate with other high-power transmissions when τ is small, and to the collisions with eMBB transmissions when τ is large. In some cases, several policies verify the loss rate condition, e.g., for $W_0 = 32$, the set of admitted policies is $0 < \tau < 9$. However, we aim also to minimize the energy consumption, which indicates to us that the optimal policy is the one which verifies the QoS constraints and minimizes the energy consumption at the same time. This corresponds to the maximum τ from the set of admitted policies, i.e., $\tau = 8$ for the previous example.

Regarding CW size, increasing eMBB's CW size decreases URLLC's loss rate while decreasing eMBB's throughput as well. This introduces a compromise when calibrating CW. For the given example, setting $W_0 = 32$ leads to the optimal solution, where both URLLC and eMBB requirements are respected (for a given τ).

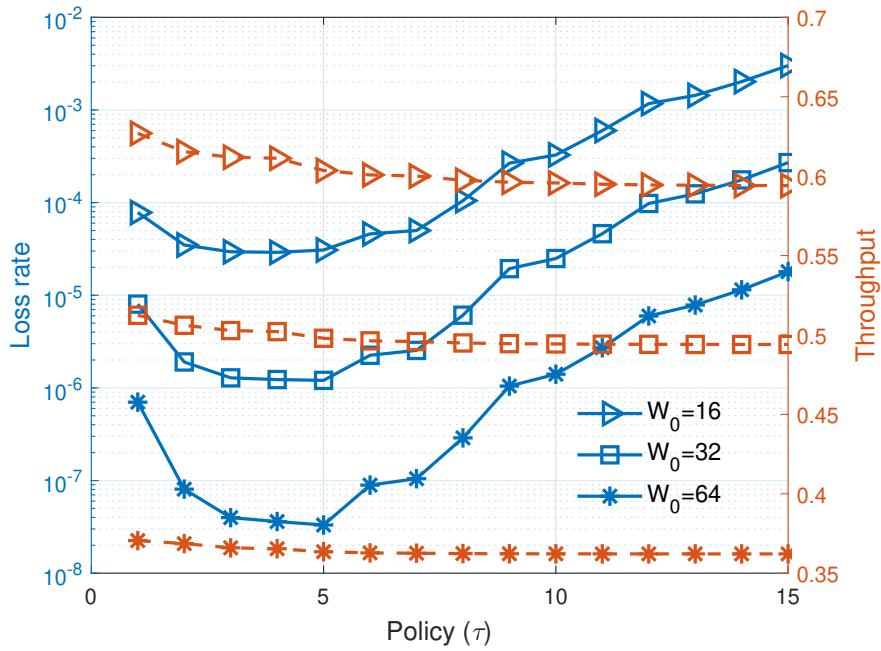


Figure 4.9: Policy and CW size effect on the performance. $N_e = 2$, $N_u = 100$ and $W = 4$.

4.6 Comparison and discussion

In this section, we compare the overall performance of the LBT-agnostic preemptive approach with the time threshold one. The evaluation takes into account both achieving URLLC and eMBB requirements and the energy consumption of the two methods.

We illustrate in Figure 4.10, the utilization rate of high power for both approaches, considering $N_e = 2$, $W = 4$ and $W_0 = 32$, for the optimal policy τ which verifies the constraints with a minimum energy consumption. It actually corresponds to the hitting probability of state *Preemption* from state *Ready* in both cases. It reflects the excess energy consumption due to high power usage, while normal power transmissions are inevitable.

We conclude from Figure 4.10 the predicted result: the LBT-agnostic preemptive approach consumes less energy than the time threshold one. However, the fact that the former violates LBT renders it less favorable and sometimes infeasible due to the regulations on the spectrum. With careful calibration of the time threshold method, we are able to attain the services requirements, albeit an added cost of energy consumption.

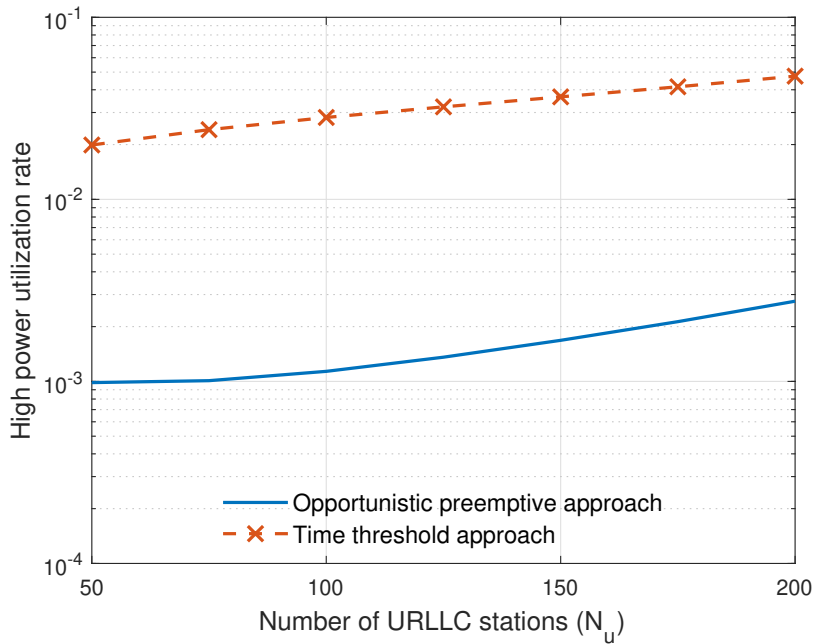


Figure 4.10: Comparison of high power utilization of the LBT-agnostic preemption and time threshold approaches. $N_e = 2$, $W = 4$ and $W_0 = 32$.

4.7 Conclusion

We studied in this chapter the coexistence of URLLC and eMBB services in unlicensed spectrum in a smart-factory scenario and illustrated the performance deterioration of both services with respect to the traffic load if both transmit at the same power level.

We then proposed two approaches based on high-power transmission, to enhance the performance of URLLC. High power transmissions are used by URLLC stations to prioritize their packets. The first one, *the LBT-agnostic preemptive approach*, uses high power only when the delay of the packet approaches the delay constraint, interrupting by that the LBT process and hence the ongoing eMBB transmissions. The second one, termed *time threshold approach*, selects a time threshold within the delay budget and starts after which transmitting at high power transmission, without violating LBT.

Comparing the two methods, we showed that with a good calibration of the time threshold and CW size, we can attain the performance requirements, with some additional cost in terms of energy consumption.

In next chapter, and based on the time threshold method, we propose an

online learning approach which allows URLLC stations to adapt their optimal policy in a distributed manner, where the system parameters such as the number of transmitting stations and their transmission probabilities are unknown and each station adapts its policy by collecting information about the environment through interactions.

Chapter 5

Distributed decision making for unlicensed channel access

5.1 Introduction

In the previous chapters, we considered the existence of a central entity which decides the optimal policy of transmission with a total knowledge of the environment, i.e., the number of stations with optimal channel conditions. In the presence of many stations or devices, it is quite prohibitive for a central entity to determine the optimal transmission policy, especially when the channel conditions are different for each one of them. In this chapter, we propose to make use of online learning to enable each transmitter to achieve its optimal policy, in a distributed manner.

We consider a time-threshold multi-level transmission power scheme, similar to the one proposed in chapter 4 and formulate an optimization framework where the transmitter adapts its transmission power with time so as to reach its performance objective while minimizing its energy consumption, for both Aloha-like and LBT systems. This analysis is environment agnostic and considers interference and collision rate as an input. This does not require solving a Markov chain nor a set of fixed-point equations.

We then employ online learning in our context to allow stations to adapt their policies in a distributed manner. The idea of learning is that the learner attempts to identify the action(s) which maximizes a certain expected reward over a time horizon depending on the feedback from the environment to that action. When the action causes the environment to change (move to another state), then the learning process can be solved using *reinforcement learning* (RL) for instance, which involves mainly solving a Markov Decision Process

(MDP) [36]. However, solving complex MDPs is unnecessary in many cases (similar to ours) where the feedback of the environment is not very dependent on the learner's actions, due to the large number of devices. In this case, *Multi-Armed Bandit* (MAB) becomes the best candidate to solve such problems.

Stochastic MAB is a special case of RL (it is equivalent to a one-state MDP), where each action is denoted by an *arm* and is associated to a reward distribution that is unknown to the learner. In our case, the action is represented by the transmission policy (switching moment between low and high power regimes). In every round, i.e., at each packet generation, the learner picks an arm and receives an observation from the reward distribution of that arm; it refines its knowledge about the arm by selecting it for a sufficient number of times. At the same time, the learner desires to identify the best arm as soon as possible in order to maximize its cumulative reward over a horizon of rounds. MAB illustrates the famous learning trade-off between *exploration versus exploitation*.

For applications where some measures are linked to rare events, as does reliability in our case (it has to remain below 10^{-5}), it is hard to estimate efficiently the reward, which renders the learning process very slow, i.e., the exploration phase requires a very large number of rounds to collect accurate estimates of the reward distribution for all arms. This drawback originates from the fact that MAB (and learning in general) deals with the environment as a black box, and the observations in one round are exclusive to the picked arm. One possibility for accelerating the learning process that we adopt in this chapter is to exploit our knowledge of the environment and the system to model the metrics that are hard to assess, and incorporate them in the learning algorithm.

Learning in wireless communications has become a hot topic recently, especially in 5G networks where it can offer efficient solutions for existing problems such as optimal resource allocation schemes [37, 38]. Using machine learning (ML) techniques in the context of URLLC has also attracted many researchers, for instance [39–41]. In [39], a Q-learning approach is proposed for adaptive power and frequency resource allocation for URLLC in downlink scheduling. This approach is shown to improve the queuing delay and the inter-cell interference. The work in [40] inspects also the downlink scheduling problem of URLLC, but this time using eMBB puncturing where

a deep RL approach is proposed with the aid of a defined optimization problem in order to improve the performance of both services and reduce eMBB puncturing. The work in [41] deals with uplink URLLC scenario and proposes a distributed risk-aware ML approach for optimal radio resource management of scheduled and non-scheduled URLLC traffic.

Regarding the rare events problem, the work in [42] uses importance sampling to capture the rare events in a system simulator, in the context of RL. However, a rare event in [42] represents a state in the MDP which has a small probability to be reached. This is different from our problem since we do not have an MDP and our rare event is related to the policy itself. Using prior knowledge of the environment model is considered in [43] for the case of RL so as to accelerate the learning speed by accelerating the solution of the MDP albeit increasing the computation complexity.

5.2 System model and optimization problem formulation

In the smart-factory setting, a transmitting station shares the medium with other devices in a contention-based manner, where opportunities for transmissions arrive following a stochastic process. As long as a packet is not correctly decoded by the receiver, the packet is retransmitted when a next transmission opportunity arises. In general, the transmission power is included in some interval $[P_{min}, P_{max}]$, and transmission with power P_i leads to a loss probability $L(P_i)$ that is a decreasing function of P_i . Formally, we define policy π and associated actions $P^{(\pi)}(t)$ as the transmission power if a transmission opportunity arrives at time t after the generation of the packet. We define Π as the set of all possible policies.

The objective of the transmitter is to keep its success rate above a threshold Θ . One policy might be to use the highest power to transmit the packet and its potential replicas. However, this has two drawbacks. First, it results in a high energy consumption for devices that are, in general, battery-powered, and second, it increases the level of interference to other devices that share the same radio resources. We then seek policies that ensure the latency and reliability targets while minimizing the energy consumption.

Let n be the number of transmission opportunities within the interval $[0, T]$ and t_i the arrival moment of opportunity number i after the generation of the packet. The optimal transmission policy is the solution of the following stochastic optimization problem:

$$\min_{\pi \in \Pi} \mathbb{E}_{\{n, t_1, \dots, t_n\}} [P^{(\pi)}(t_1) + \sum_{j=2}^n P^{(\pi)}(t_j) \prod_{i=1}^{j-1} L(P^{(\pi)}(t_i))] \quad (5.1)$$

subject to:

$$\mathbb{E}_{\{n, t_1, \dots, t_n\}} [\prod_{i=1}^n L(P^{(\pi)}(t_i))] \leq 1 - \Theta \quad (5.2)$$

Equation (5.1) indicates that the expected energy is to be minimized, subject to constraint (5.2) that indicates that the expected packet loss has to be smaller than a target.

Without loss of generality, we consider in the rest of this chapter two levels of power, P_1 and P_2 , with corresponding loss probabilities q_1 and q_2 , respectively ($q_1 > q_2$ if $P_1 < P_2$ and vice versa). We consider only monotonic policies, in the sense that the transmission starts with power P_1 and then, after a time τ , it switches to power P_2 . A policy π reduces to a switching time $\tau \leq T$ so that $P^{(\pi)}(t) = P_1 \mathbb{1}_{t \leq \tau} + P_2 \mathbb{1}_{t > \tau}$. Intuitively, as the objective is to minimize the energy consumption, we consider policies with “mild start” ($P_1 < P_2$). We then show, using numerical analysis, that this intuition is indeed correct.

5.3 Aloha-like systems

In many applications involving battery-powered stations (e.g., LoRa), Aloha-like protocols are used as sensing the channel would be very costly otherwise. In this case, the transmitter backs off for an exponential time before (re-)transmitting, so the transmission opportunities occur following a Poisson process of parameter α (the interval between transmissions is exponentially distributed with mean $1/\alpha$). We start by the case of one station, and then extend our study to multiple stations.

5.3.1 Optimizing the policy for one station

When the transmitter has a reliability objective and is latency-constrained, we have the following result:

Lemma 5.1. *The optimal policy in the exponential inter-opportunity case is the one that minimizes the following average energy function:*

$$\bar{P}(\tau) = \frac{P_1(1 - e^{\alpha(q_1-1)\tau})}{1 - q_1} + e^{\alpha(q_1-1)\tau} \frac{P_2(1 - e^{\alpha(q_2-1)(T-\tau)})}{1 - q_2} \quad (5.3)$$

in the interval $[0, \tau^*]$ for a mild start ($P_1 < P_2$, $q_1 > q_2$), with optimal switching time

$$\tau^* = \frac{\ln(1 - \Theta) + \alpha(1 - q_1)T}{\alpha(q_1 - q_2)} \quad (5.4)$$

Proof. The numbers of arrivals in $[0, \tau]$ and in $(\tau, T]$, n_1 and n_2 , are independent Poisson variables of averages $\alpha\tau$ and $\alpha(T - \tau)$, respectively.

Knowing n_1 , the probability for moving to the second stage is $q_1^{n_1}$. The power consumption knowing a realization of the process of transmission opportunities is given by:

$$\begin{aligned} & \mathbb{E}[P^{(\tau)}(t_1) + \sum_{j=2}^n P^{(\tau)}(t_j) \prod_{i=1}^{j-1} L(P^{(\tau)}(t_i)) | n_1, n_2] \\ &= P_1 \sum_{i=1}^{n_1} q_1^{i-1} + P_2 q_1^{n_1} \sum_{j=1}^{n_2} q_2^{j-1} = P_1 \frac{1 - q_1^{n_1}}{1 - q_1} + P_2 q_1^{n_1} \frac{1 - q_2^{n_2}}{1 - q_2} \end{aligned}$$

Averaging over the Poisson distributions of n_1 and n_2 , we compute the expected energy consumption $\bar{P}(\tau)$ in (5.3).

We now move to the loss calculation. Knowing n_1 and n_2 , the loss probability is equal to $q_1^{n_1} q_2^{n_2}$. Averaging over the Poisson distributions of n_1 and n_2 , we get the expected loss probability under policy τ , $\bar{L}(\tau)$:

$$\bar{L}(\tau) = e^{-\alpha\tau(1-q_1)} e^{-\alpha(T-\tau)(1-q_2)} \quad (5.5)$$

leading to the inequality $\tau \leq \tau^*$. □

We now discuss the derivation of the optimal policy in practical cases, where the loss rates (q_1, q_2) are in general small and the power is increased by several dB. We start by computing the derivative of the energy function to minimize (5.3). It has the same sign as the function:

$$f(\tau) = P_1 - P_2 \frac{1 - q_1}{1 - q_2} + P_2 \frac{q_2 - q_1}{1 - q_2} e^{-\alpha(T-\tau)(1-q_2)} \quad (5.6)$$

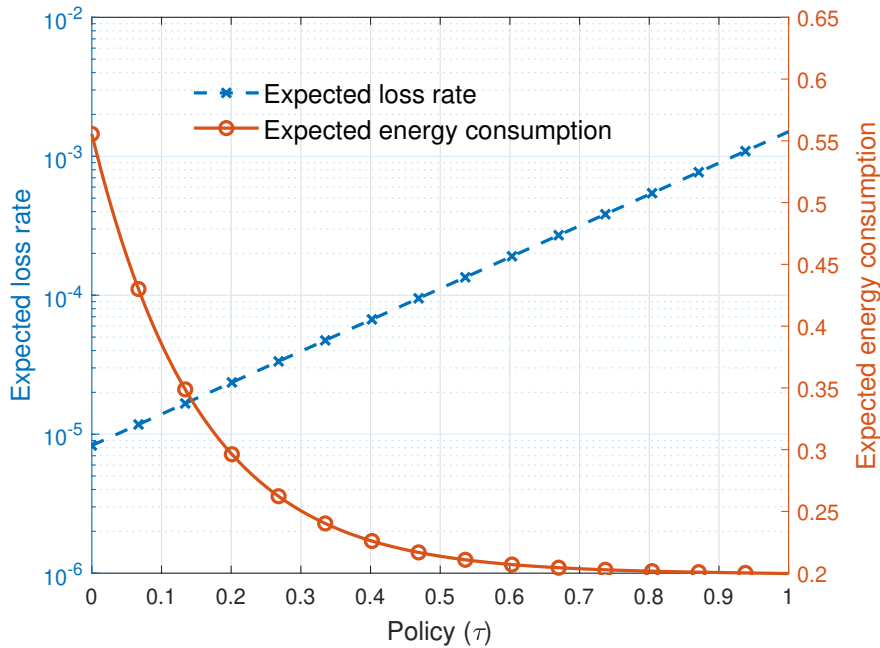


Figure 5.1: Energy and loss values for different policies, $q_1 = 0.5$, $q_2 = 0.1$, $P_1 = 0.1$ W, $P_2 = 0.5$ W, $T = 1$ ms, $\alpha = 13$.

In the mild start case ($P_1 < P_2$), this function is decreasing with τ , and its maximal value at $\tau = 0$ is negative in the practical cases stated above. The solution of the minimization problem is thus $\tau = \tau^*$, given by (5.4).

Figure 5.1 shows the evolution with τ of the energy and loss functions, as derived in lemma 1. We observe that the energy consumption effectively decreases while the loss rate increases with τ , and the optimal policy here is the one which corresponds to the maximal loss (e.g., 10^{-4}).

We now move to the validation of the intuition that suggests a mild start as opposed to an aggressive one. We consider a policy with an aggressive start ($P_1 > P_2$, $q_1 < q_2$). Using the same arguments as before, we can see that the loss rate in equation (5.5) is now a decreasing function of τ , meaning that the feasible region is now $[\tau_{aggressive}^*, T]$, with

$$\tau_{aggressive}^* = \frac{-\ln(1 - \Theta) - \alpha(1 - q_2)T}{\alpha(q_2 - q_1)} \quad (5.7)$$

The average energy given by equation (5.3) can also be shown to be an increasing function with τ in practical cases, as illustrated in Figure 5.2, meaning that the best policy in the aggressive start case corresponds to $\tau_{aggressive}^*$. We made a comparison between this best aggressive policy and the optimal “mild start” policy of lemma 1 and observed that the aggressive policy leads

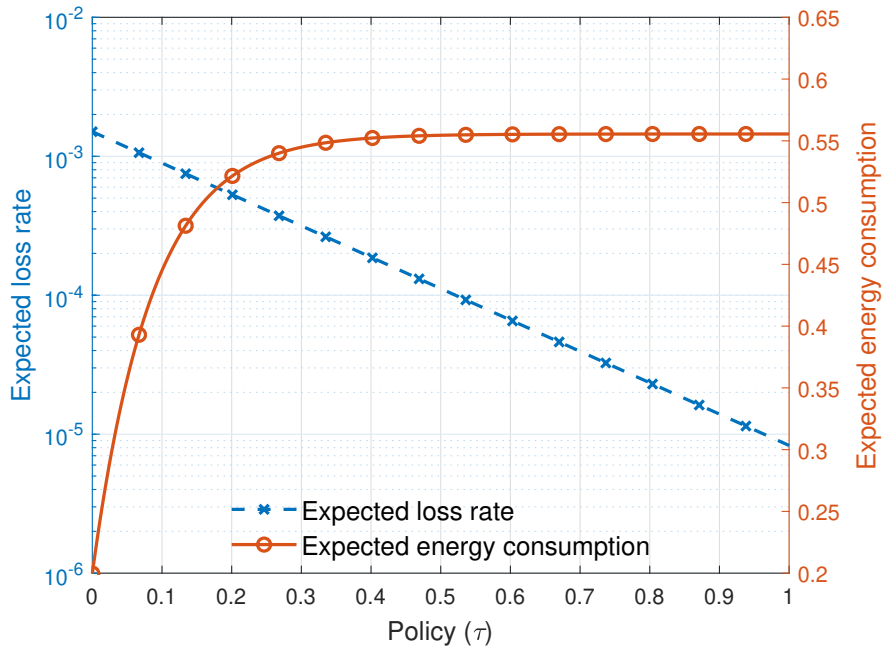


Figure 5.2: Energy and loss values for different policies, $q_1 = 0.1$, $q_2 = 0.5$, $P_1 = 0.5$ W, $P_2 = 0.1$ W, $T = 1$ ms, $\alpha = 13$.

to an increase of the average energy consumption by 50% to 200% for values of q_i 's ranging between 0.1 and 0.5. And so, it is better to start with a low power and increase it when the delay deadline approaches to its limit and the packet is not yet received. τ^* of lemma 1 is thus the optimal policy among the monotonic ones.

5.3.2 Case of a field of transmitters

The above analysis was performed considering one transmitter that conveys packets to a receiver. The derivation of the optimal policy in lemma 1 holds only in the case where the station is playing against exogenous noise/interference phenomena (e.g., a fading channel or interference from other systems). We now move to the more common case where several stations are deployed in a field and contend to the channel while having similar URLLC objectives.

We namely consider N identical stations, each generating small packets of equal transmission time ρ , following a Poisson process of intensity λ and seeking to reach its reliability and delay targets while minimizing its energy consumption. The loss of a packet occurs if it collides with another packet of equivalent or superior power, i.e., a low power packet is always lost when in collision, while a high power packet is lost only if it collides with another

high power packet. In this case, q_1 and q_2 are not exogenous parameters but depend on the traffic conditions and the policies of the stations. We study the system equilibrium when all the stations follow the same policy τ .

From the standpoint of one station, the probability that a given packet transmitted using P_1 will be repeated can be approximated by:

$$q_1 = 1 - e^{-2\lambda(\bar{n}_1 + \bar{n}_2)(N-1)\rho} \quad (5.8)$$

where \bar{n}_1 (resp. \bar{n}_2) represents the average number of repetitions of a packet with power P_1 (resp. P_2). Indeed, each new packet generates a series of $\bar{n}_1 + \bar{n}_2$ repetitions, separated by exponential times of average $1/\alpha$. Each station generates thus a process of packets of average intensity $\lambda(\bar{n}_1 + \bar{n}_2)$. We make the assumption that the superposition of $N - 1$ stochastic processes of this type can be approximated by a Poisson process of intensity $(N - 1)\lambda(\bar{n}_1 + \bar{n}_2)$.

For high power transmissions, the packet is repeated if it encounters other high power transmissions only, and so:

$$q_2 = 1 - e^{-2\lambda\bar{n}_2(N-1)\rho} \quad (5.9)$$

We now compute the average number of retransmissions knowing q_1 and q_2 . For a given number of transmission opportunities during τ , n_1 , the average number of effective retransmissions is given by:

$$(1 - q_1) + \dots + (n_1 - 1)q_1^{n_1-2}(1 - q_1) + n_1q_1^{n_1-1} = \frac{1 - q_1^{n_1}}{1 - q_1}$$

Averaging over the Poisson distribution of n_1 , we get:

$$\bar{n}_1 = \frac{1 - e^{-\alpha\tau(1-q_1)}}{1 - q_1} \quad (5.10)$$

Similarly, we obtain:

$$\bar{n}_2 = e^{-\alpha\tau(1-q_1)} \frac{1 - e^{-\alpha(T-\tau)(1-q_2)}}{1 - q_2} \quad (5.11)$$

where $e^{-\alpha\tau(1-q_1)}$ is the probability that the packet has moved to power P_2 .

For a field with homogeneous stations of identical objectives, the common optimal policy τ^* can be obtained using a fixed point approach, where

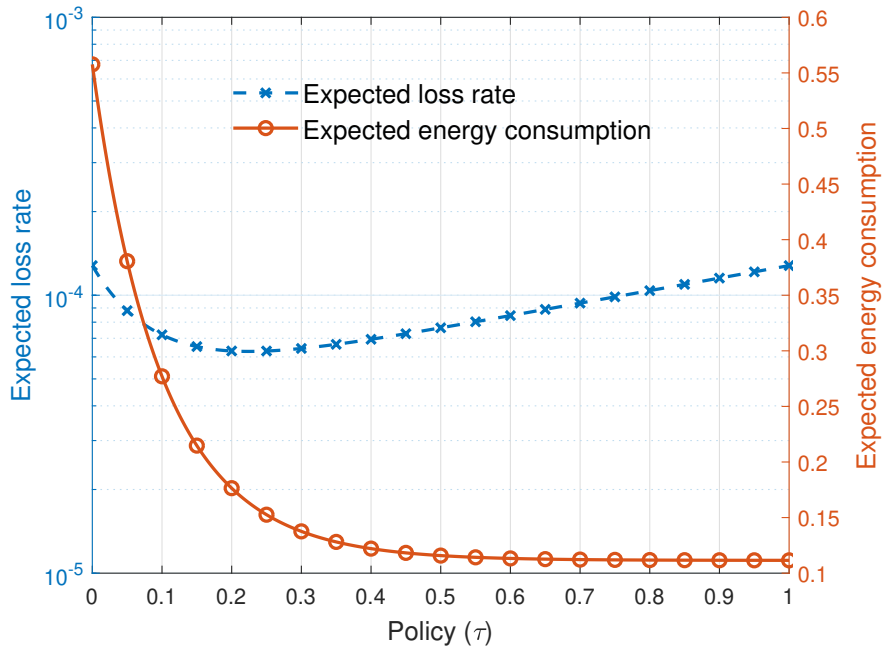


Figure 5.3: Expected loss rate and energy consumption for a field of stations using Aloha. $N = 50$, $T = 1$, $P_1 = 0.1$, $P_2 = 0.5$, $\alpha = 15$, $\rho = 0.1$, $\lambda = 0.01$ (τ in ms)

the loss probabilities q_1 and q_2 are calculated from solving the fixed point equations (5.8-5.9-5.10-5.11) then plugged in equation (5.4).

Figure 5.3 shows the performance (energy consumption and loss) for a field of stations using the same strategy τ . Unlike the single station case competing against noise, the loss rate is not monotonically increasing with τ . It is large when the high power is used by a large proportion of interfering packets (small τ) or when it is not sufficiently used to ensure high reliability (large τ). There may be two policies that ensure the same URLLC target, in this case the largest τ is chosen as energy consumption decreases with τ .

5.4 Listen Before Talk systems

In the majority of wireless access systems using unlicensed spectrum, LBT is used. The inter-opportunity arrival distribution is not exponential as for the Aloha case and hence the number of opportunities within a time interval does not follow Poisson law anymore. Therefore, we derive in the following these distributions for the LBT case which will allow us to derive the optimal transmission policy.

5.4.1 Distribution of the number of opportunities

Let θ denote the random variable (rv) representing the time spent in one stage (which depends on CW), and let W , ρ and q_1 denote the CW size, the packet transmission time and the probability of sensing the medium busy, respectively.

The Cumulative Density Function (CDF) of θ , denoted by F_θ is given by equation (5.12), following the derivation proposed in [44]:

$$F_\theta(z) = \frac{1}{W} \sum_{i=0}^{W-1} \sum_{\substack{j=0 \\ j \leq i}}^{\max(0, \lfloor \frac{z-i}{\rho} \rfloor)} \binom{i}{j} q_1^j (1 - q_1)^{i-j} \quad (5.12)$$

From the standpoint of one station competing to access the medium, the end of every stage can be seen as a future opportunity of transmission. As the inter-opportunity time is no more exponentially distributed, we make use of renewal theory to derive the associated distribution of the number of arrivals within a given time interval [45].

We denote by $\theta_m = \sum_{i=1}^m \theta$, the sum of m i.i.d. rvs $\sim f_\theta$, the Probability Mass Function (PMF) of $\theta_m \sim f_m$ where f_m is the m -fold convolution of f_θ . Note that the CDF is calculated as:

$$F_2(z) = (F_\theta * f_\theta)(z), \quad F_3(z) = (F_2 * f_\theta)(z), \quad \dots \quad (5.13)$$

Let n_1 and n_2 denote the number of transmission opportunities during time intervals $[0, \tau]$ and $(\tau, T]$, respectively, then according to renewal theory, we have the following:

$$n_1 \geq m \Leftrightarrow \theta_m \leq \tau, \quad n_2 \geq m \Leftrightarrow \theta_m \leq T - \tau$$

Taking into account the packet transmission time ρ after every opportunity, a corresponding sum must be subtracted from θ_m . The PDF of n_1 and n_2 is thus given by equations (5.14) and (5.15), respectively.

$$\begin{aligned} f_{n_1}(m) &= \mathbb{P}(n_1 = m) \\ &= F_m(\tau - (m - 1)\rho) - F_{m+1}(\tau - m\rho) \end{aligned} \quad (5.14)$$

$$f_{n_2}(m) = F_m(T - \tau - (m - 1)\rho) - F_{m+1}(T - \tau - m\rho) \quad (5.15)$$

5.4.2 Optimal policy

Assuming n_1 and n_2 to be independent rvs since the LBT process is random, then knowing n_1 and n_2 , the expected loss rate is given by $q_1^{n_1} q_2^{n_2}$. Averaging over the distributions f_{n_1} and f_{n_2} , we obtain the expected loss rate $\bar{L}(\tau)$ under policy τ :

$$\bar{L}(\tau) = \mathbb{E}_{n_1, n_2}(q_1^{n_1} q_2^{n_2}) = \sum_{i=1}^{\infty} f_{n_1}(i) q_1^i \times \sum_{j=1}^{\infty} f_{n_2}(j) q_2^j \quad (5.16)$$

$\bar{L}(\tau)$ can be calculated numerically and τ^* is determined as the largest τ which verifies: $\bar{L}(\tau) \leq (1 - \Theta)$, based on the hypothesis that $P_1 < P_2$. The average energy consumption $\bar{P}(\tau)$ under policy τ is given by:

$$\bar{P}(\tau) = \frac{P_1}{1 - q_1} \left[1 - \sum_{i=1}^{\infty} f_{n_1}(i) q_1^i \right] + \frac{P_2}{1 - q_2} \left[1 - \sum_{j=1}^{\infty} f_{n_2}(j) q_2^j \right] \sum_{i=1}^{\infty} f_{n_1}(i) q_1^i \quad (5.17)$$

5.4.3 Case of a field of transmitters

We now consider a field of transmitters using LBT and show how to derive the equilibrium point. Similarly to the Aloha case, q_1 and q_2 are given by:

$$q_1 = 1 - e^{-\lambda(\bar{n}_1 + \bar{n}_2)(N-1)} \quad (5.18)$$

$$q_2 = 1 - e^{-\lambda \bar{n}_2(N-1)} \quad (5.19)$$

where q_1 and q_2 are expressed here per time slot, and:

$$\bar{n}_1 = \frac{1 - \mathbb{E}_{n_1}(q_1^{n_1})}{1 - q_1} \quad (5.20)$$

$$\bar{n}_2 = \mathbb{E}_{n_1}(q_1^{n_1}) \frac{1 - \mathbb{E}_{n_2}(q_2^{n_2})}{1 - q_2} \quad (5.21)$$

The equilibrium point of the system can thus be obtained, as for the Aloha case, by solving the fixed point equations (5.18-5.19-5.20-5.21) then τ^* is deduced with the aid of equations (5.16-5.17).

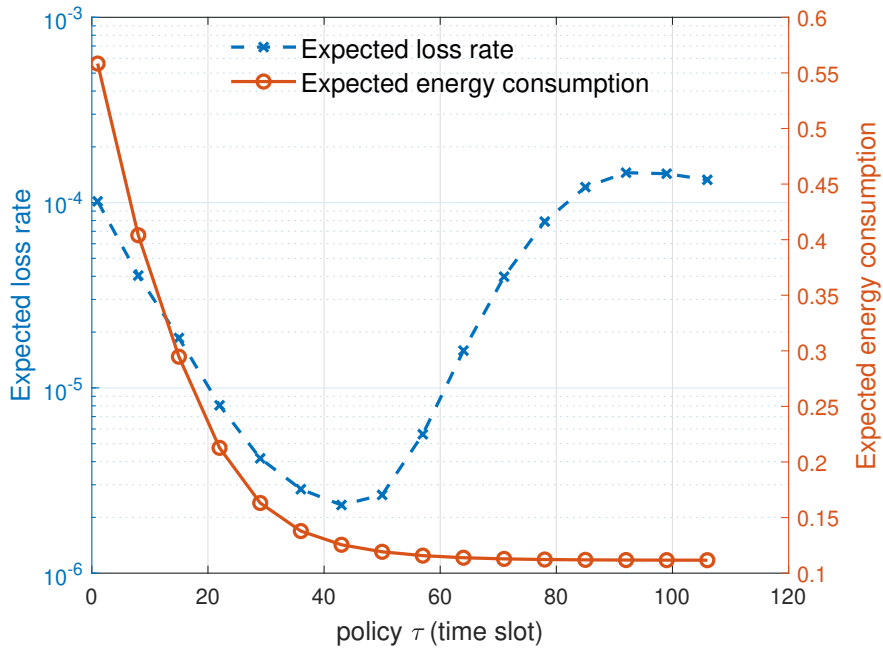


Figure 5.4: Expected loss rate and energy consumption for a field of stations using LBT, $N = 100$, $W = 16$, $T = 1$ ms, $\rho = 7$, $P_1 = 0.1$, $P_2 = 0.5$, time slot of $9 \mu\text{s}$ (τ in slots)

We show in Figure 5.4 the energy and loss rate for a field of stations using LBT protocol, with a common policy τ . The behavior is similar to that observed for Aloha systems in Figure 5.3. Loss is minimal when τ has a medium value, and increases when P_2 is not sufficiently used or is used extensively.

5.5 Learning optimal policies

We now move to an online implementation of the system, where the station has to learn the optimal transmission strategy for URLLC reliability and delay objectives. We make use of a Multi-Armed Bandit (MAB) framework [36].

5.5.1 MAB algorithms

In MAB, policies are called arms. We denote the set of all possible arms by $K = \{0, 1, \dots, T\}$, where arm k is associated to policy $\tau = k$. Each arm has a reward distribution that is unknown to the learner whose aim is to estimate its expected value over a horizon of rounds. Every packet generation represents a round, and at the beginning of each round, the station chooses an arm and then receives one observation of its reward distribution. The choice

of arms is divided into two phases, exploration and exploitation. In the exploration phase, arms are chosen in order to collect more information about their reward distributions, while in the exploitation one, the station chooses the empirically best arm explored so far in order to maximize its cumulative reward.

These two phases can be totally separated like in the *explore-first* algorithm which explores all arms uniformly (in a round robin fashion) for a given number of rounds, denoted by N_{explore} , then chooses the empirically best arm for the rest of the rounds, or mixed as for the ϵ -greedy algorithm which, in every round, explores the arms randomly with probability ϵ and exploits the best identified arm so far with probability $1 - \epsilon$. The ϵ -greedy algorithm can be preceded by a uniform exploration phase for a number of rounds denoted by N_{greedy} .

The aforementioned algorithms represent the basic forms of MAB, where exploration is deterministic. More advanced algorithms use adaptive exploration methods based on the uncertainty of estimation (the number of times each arm has been picked), as in so-called *Upper Confidence Bound* (UCB) and its variants [36]

5.5.2 MAB implementation

In the following, we use the notation (i, k) to designate “round i using arm k ”.

The energy consumed in (i, k) is given by equation (5.22) where $n_1(i, k)$ and $n_2(i, k)$ denote the number of transmission opportunities in (i, k) with power levels P_1 and P_2 , respectively. We divide by the number of (re-)transmissions so that $P(i, k) \in [0, 1] \quad \forall i, k, \text{ if } P_1 + P_2 \in [0, 1]$.

$$P(i, k) = \frac{n_1(i, k)P_1 + n_2(i, k)P_2}{n_1(i, k) + n_2(i, k)} \quad (5.22)$$

Accordingly, the expected energy consumption of arm k over a horizon of n rounds is given by equation (5.23), where $\mathbb{1}_{k_i=k}$ indicates the rounds in which arm k was picked.

$$\bar{P}(k) = \frac{\sum_{i=1}^n P(i, k) \mathbb{1}_{k_i=k}}{\sum_{i=1}^n \mathbb{1}_{k_i=k}} \quad (5.23)$$

The expected loss rate of arm k over a horizon of n rounds is given by equation (5.24), where $L(i, k)$ is a boolean indicating the loss of the packet in (i, k) .

$$\bar{L}(k) = \frac{\sum_{i=1}^n L(i, k) \mathbb{1}_{k_i=k}}{\sum_{i=1}^n \mathbb{1}_{k_i=k}} \quad (5.24)$$

We express the reward distributions of arms by their “penalty”. We define the expected penalty of arm k over a horizon of n rounds as follows:

$$\Psi_{URLLC}(k) = \bar{P}(k) \times |\bar{L}(k) - (1 - \Theta)| \quad (5.25)$$

In equation (5.25), we transformed the constrained optimization problem to a function which captures the behaviour of the original problem, where $|\bar{L}(k) - (1 - \Theta)|$ is a convex function in the practical case when $(1 - \Theta) \in [\min(\bar{L}(k)), \max(\bar{L}(k))]$, and $\bar{P}(k)$ is a decreasing one. Hence there exists at least one optimal arm which has a minimum penalty, denoted by k^* .

5.5.3 Performance evaluation

The most widely used measure to evaluate the performance of a MAB algorithm is the regret, defined as the difference between the effective cumulative reward obtained from the real realization of the algorithm and the cumulative reward obtained from constantly choosing the best arm, over a given horizon of rounds. The regret reflects also the speed of learning of an algorithm, where algorithms with higher regrets mean that they spent a large number of rounds exploring and not exploiting.

The regret of different algorithms is very dependent on the application and context. For the explore-first algorithm, it is hard to know when to stop the exploration phase, because committing to a non-optimal arm due to lack of exploration increases the regret. Likewise when exploring for a larger number of rounds than the necessary one. The regret of ϵ -greedy algorithm is shown to be smaller than the explore-first one as exploration is performed with a controlled probability. However, the choice of ϵ depends also on the application and its choice affects the regret. The widely used value is $\epsilon = 0.2$.

For this reason, we choose to measure the performance by the convergence time, which we define as the number of rounds needed for the algorithm to converge and stabilize to the optimal arm. For explore-first, this

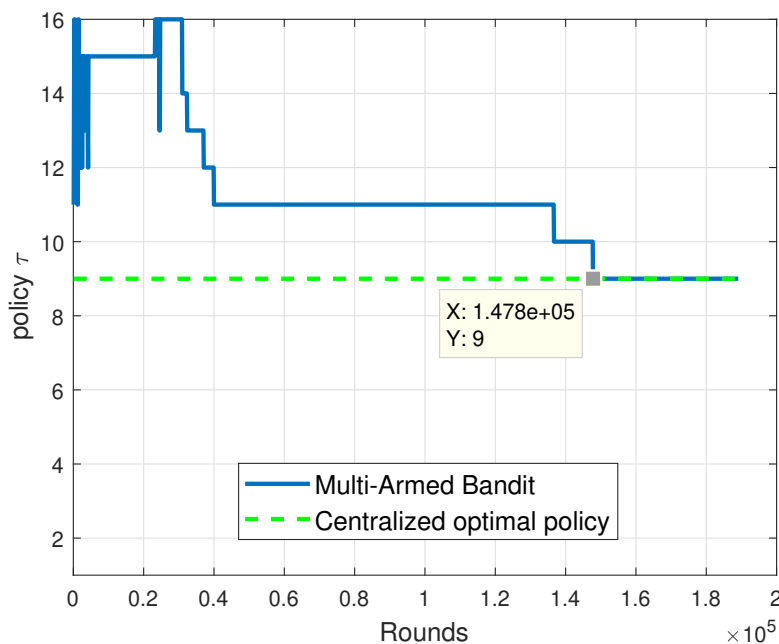


Figure 5.5: Convergence time of the ϵ -greedy MAB algorithm for URLLC case in LBT system, $\epsilon = 0.2$

corresponds to the number of rounds needed for the exploration phase to identify the optimal arm.

Using the derived penalty $\Psi_{URLLC}(k)$ in any MAB algorithm (Explore-First, ϵ -greedy, UCB, etc) [36], leads to the best arm identification after a finite number of rounds.

We develop a system-level Monte-Carlo simulator where a number of stations contend for a wireless access using an LBT protocol. We consider the following parameters: $N = 100$, $W = 16$, $\rho = 7$, $T = 111$, $P_1 = 0.1$, $P_2 = 0.5$, $\Theta = 1 - 10^{-5}$ and $\lambda = 0.001$. Temporal values are expressed in time slot unit, where the considered time slot is of $9 \mu s$. For the sake of convergence acceleration to the optimal policy, we consider the arms spaced by ρ , which reduces the arm selection space.

We illustrate in Figure 5.5 the convergence of the ϵ -greedy algorithm for the URLLC case in LBT system, with $\epsilon = 0.2$. We observe that the algorithm converges to the same optimal policy calculated by a central entity knowing the environment parameters, illustrated in subsection 5.4. However, we also observe that convergence is very slow and takes around 10^5 rounds (packet generations).

5.5.4 Model-aided learning

For our illustrated case in Figure 5.5, and as indicated previously, the measure which causes slow convergence is the loss rate, as our system has to operate in traffic regions where the loss event is rare. We hence propose a model-aided learning where the reward distribution is inferred from observations of the environment, which does not require as many rounds as when the reward distribution is exclusively estimated from the observed long term loss rate.

We make use of the model proposed in subsection 5.4, where we notice that by estimating q_1 , q_2 , f_{n_1} and f_{n_2} , the loss rate can be calculated from equation (5.16). As estimating f_{n_1} and f_{n_2} accurately requires a large number of rounds, we instead apply renewal theory as stated before to obtain the needed distributions.

The learner can acquire estimations of the parameters from the reaction of the environment to its transmissions. For instance, we can assess the following estimates:

$$\hat{q}_1(k) = \frac{N_{collision}(k)}{N_{transmit}(k)}; \quad \hat{q}_2(k) = \frac{N_{collision}^H(k)}{N_{transmit}^H(k)},$$

$$f_{\hat{\theta}}(l) = \mathbb{P}(\hat{\theta} = l) = \frac{N(\hat{\theta} = l)}{\sum_l N(\hat{\theta} = l)}$$

where $\hat{q}_1(k)$, $\hat{q}_2(k)$ and $f_{\hat{\theta}}$ denote the estimates of $q_1(k)$, $q_2(k)$ and f_{θ} , respectively, $N_{collision}(k)$ and $N_{collision}^H(k)$ denote the number of collisions when transmitting with low and high power levels using arm k , respectively, $N_{transmit}(k)$ and $N_{transmit}^H(k)$ denote the number of transmissions with low and high power levels using arm k , respectively, and $N(\hat{\theta} = l)$ denotes the number of sensed inter-transmission times $\hat{\theta}$ equal to l , where $\hat{\theta}$ is calculated from the packet generation until the reception of feedback from the receiver. $f_{\hat{\theta}}$ expresses also the histogram of the inter-transmission delays.

Note that $\hat{q}_1(k)$ and $\hat{q}_2(k)$ are calculated for each arm assuming the general case of a field of stations.

We show in Figure 5.6 the convergence time to the optimal policy for one realization of the model-aided MAB, for the same system parameters used in Figure 5.5. We observe a convergence time of the order of thousand rounds, which is significantly smaller than that of the non model-based case (of the

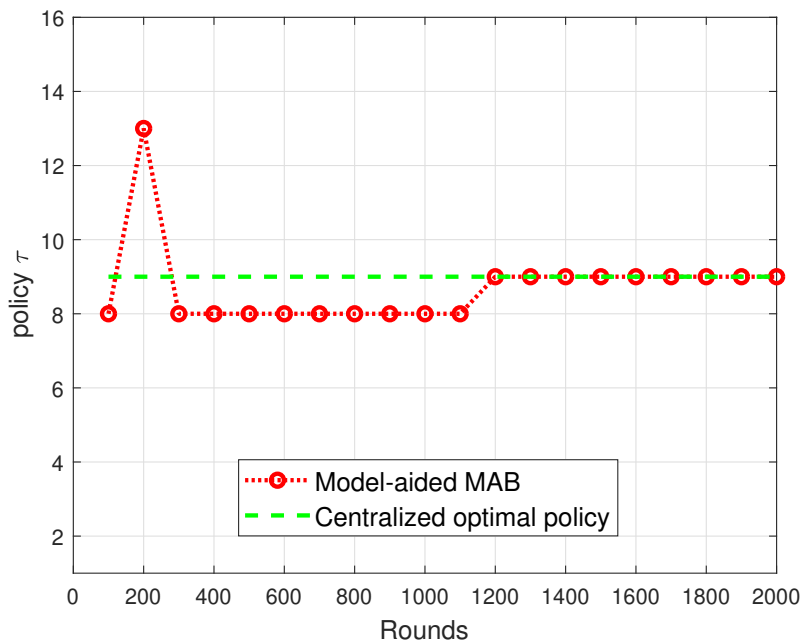


Figure 5.6: Convergence time of model-aided MAB

order of 10^5 rounds) as observed in Figure 5.5.

5.6 Conclusion

We developed in this chapter an online learning approach to allow stations to adapt their transmission policies in a distributed manner. We showed that a mild start, i.e., starting with low power level transmission then increasing it after a time threshold, minimizes the energy consumption while reaching reliability and delay requirements.

Our model-aided learning approach allows for a considerable acceleration of convergence to the optimal transmission policy by exploiting the knowledge about the system model, compared to a non model-aided learning algorithms which suffers from very slow convergence due to the time required to track the rare loss event.

A question that arises when designing such transmission schemes: *in what scenarios an aggressive start strategy could outperform a mild start one?* This question is discussed in the following chapter, where we consider transmission under different QoS constraints, other than the stringent, deterministic reliability and delay ones considered so far.

Chapter 6

Revisiting transmission policies for packet age minimization objective

6.1 Introduction

We were interested so far by the transport of URLLC class of services, based on meeting stringent requirements on latency and reliability. While these stringent performance objectives make sense in some settings, for instance an industrial plant where machines/robots need to communicate regular information to a central controller, other applications, involving for instance sensors, need rather to report information on a dynamic environment where freshness of information is key to system characterization and control. Even in critical applications where Time Sensitive Networking (TSN) [46] is adopted for ensuring a strict reliability target, the authors of [47] proposed a framework that strives to reduce the average age instead of ensuring deterministic delays. This information freshness is measured by so-called Age of information (AoI) [48, 49], and is the focus of the present chapter, where we will specifically study the optimal transmission policies under AoI objective and compare them to the ones obtained under stringent, deterministic URLLC objectives.

Recently, some works studied AoI in relationship to URLLC. In [50], the authors addressed the issue of minimizing the long-term peak-AoI in the downlink for URLLC traffic in the presence or not of throughput-constrained enhanced mobile broadband (eMBB) traffic. In [51], the authors studied and controlled the tail distribution of the AoI distribution in a vehicular network, with the objective to minimize the transmit power while integrating AoI violation probability as a URLLC QoS objective. In [52], the authors analysed

the AoI for URLLC traffic in a stationary and ergodic channel modeled as an M/M/1 queue with packet deadline.

This set of works integrate AoI as an additional QoS component for URLLC, or analysed the AoI resulting from URLLC scheduling, while our work does not aim at integrating AoI in URLLC frameworks but rather to show how differently the same system behaves depending on the pursued objective: meeting URLLC's latency deadline versus minimizing AoI.

6.2 Minimizing depreciation related to age

We consider here scenarios where for instance a set of sensors are deployed so as to monitor their environment. Each time a sensor detects a significant change in its environment, it generates a packet and transmits it to a central monitor. An example of such scenarios is road monitoring in vehicular networks or environment monitoring in industrial sites. We assume that the environment changes occur following some stochastic process, and so does the packet generation. Such applications need packets that are as fresh as possible, and the depreciation of a packet value is proportional to its age, which we denote by a , i.e., it is modeled as an increasing function $D(a)$ of age a defined as the elapsed time between the packet generation and its effective reception by the controller.

The objective is to minimize the average “depreciation” of all received packets that depends on the age of information for these received packets, and at the same time reduce the energy consumption as sensors are in general battery-powered. A packet is naturally dropped after several stages as in WiFi, so we drop packets that are not correctly received when their age reaches some limit denoted by T .

Let n be the number of transmission opportunities within the interval $[0, T]$ and t_i the arrival moment of opportunity number i after the packet generation. The optimal transmission policy is the solution of the multi-objective stochastic optimization problem that minimizes jointly the average energy (given by equation (5.1)), and the average depreciation of packets, as follows:

$$\begin{aligned} & \min_{\pi \in \Pi} \mathbb{E}_{\{n, t_1, \dots, t_n\}} [D(t_1)(1 - L(P^{(\pi)}(t_1))) \\ & + \sum_{j=2}^n D(t_j)(1 - L(P^{(\pi)}(t_j))) \prod_{i=1}^{j-1} L(P^{(\pi)}(t_i))] \end{aligned} \quad (6.1)$$

Before moving to the derivation of the optimal policy, we link it to the AoI concept, even if the objective (6.1) can be viewed as a minimization of a function of the packet delay.

To this aim, let $T_j, j = 1, 2, \dots$ denote the arrival times of the packets generated by a sensor of interest, \hat{a}_j the delay before the correct delivery of packet j , i.e., its age when it is correctly received, and $\hat{i}(t)$, for all $t > 0$, the index of arrival times such that $T_{\hat{i}(t)} \leq t < T_{\hat{i}(t)+1}$, for all time $t > 0$. For $\nu(t)$ denoting the timestamp of the last packet correctly received, the AoI at time t from the receiver's point of view is calculated by [53]:

$$AoI(t) = t - \nu(t) = \begin{cases} t - T_{\hat{i}(t)-1}, & t < T_{\hat{i}(t)} + \hat{a}_{\hat{i}(t)}, \\ t - T_{\hat{i}(t)}, & t \geq T_{\hat{i}(t)} + \hat{a}_{\hat{i}(t)} \end{cases} \quad (6.2)$$

giving the well-known sawtooth pattern. A policy that leads to a minimal average packet delay will then also minimize this AoI, provided that the amount of new information brought by the packet does not depend on the inter-packet generation time of the source, i.e., a packet generated after a long period of time does not necessarily bring more information than a packet generated after a short one.

6.3 Policies that minimize the packet age

The objective here is to minimize the average depreciation of the packet value, function of its freshness, while preserving the battery of sensors. The optimal policy here depends on two scenario-specific preferences:

- We consider two cases for the depreciation function $D(a)$: linear and exponential, i.e., $D(a) = a$ and $D(a) = e^{\beta a}$, with $\beta > 0$.
- The relative importance of the battery preservation objective with respect to the age objective, that depends on the criticality of the application and the battery lifetime objective.

6.3.1 Formulation of the optimization objective

We have the following result:

Lemma 6.1. *The energy and age depreciation minimization problem (5.1,6.1) reduces in the exponential inter-opportunity case to the joint minimization of the*

average energy in equation (5.3) and of the average depreciation given by:

$$\begin{aligned} \min_{\tau} \bar{D}(\tau) &= \frac{1}{\alpha} \left[\frac{1 - [1 + q_1(1 - q_1)\alpha\tau]e^{\alpha\tau(q_1-1)}}{1 - q_1} \right. \\ &+ (q_1\alpha\tau e^{\alpha\tau(q_1-1)})(1 - e^{\alpha(T-\tau)(q_2-1)}) \\ &\left. + e^{\alpha\tau(q_1-1)} \frac{1 - [1 + q_2(1 - q_2)\alpha(T - \tau)]e^{\alpha(T-\tau)(q_2-1)}}{1 - q_2} \right] \end{aligned} \quad (6.3)$$

in the linear decay case, and

$$\begin{aligned} \min_{\tau} \bar{D}(\tau) &= \frac{\alpha}{\alpha - \beta} \left[(1 - q_1) \frac{(1 - e^{\alpha(\frac{\alpha q_1}{\alpha - \beta} - 1)\tau})}{(1 - \frac{\alpha q_1}{\alpha - \beta})} \right. \\ &\left. + (1 - q_2) e^{\alpha(\frac{\alpha q_1}{\alpha - \beta} - 1)\tau} \frac{(1 - e^{\alpha(\frac{\alpha q_2}{\alpha - \beta} - 1)(T - \tau)})}{(1 - \frac{\alpha q_2}{\alpha - \beta})} \right] \end{aligned} \quad (6.4)$$

in the exponential decay case.

Proof. The power consumption is calculated as for the case where stringent, deterministic requirements were to be for URLLC, given by equation (5.3).

Let us now compute the depreciation of a packet. If the packet is correctly received at the j -th attempt, its age $a = t_j$ is an Erlang variable of parameters (j, α) . The depreciation of a packet knowing the numbers of opportunities n_1 and n_2 is computed as

$$\begin{aligned} &\mathbb{E}[t_1(1 - L(P^{(\tau)}(t_1)))] \\ &+ \sum_{j=2}^n t_j(1 - L(P^{(\tau)}(t_j))) \prod_{i=1}^{j-1} L(P^{(\tau)}(t_i)) | n_1, n_2] = \\ &\sum_{j=1}^{n_1} \mathbb{E}[D(a)](1 - q_1)q_1^{j-1} + q_1^{n_1} \sum_{j=1}^{n_2} \mathbb{E}[D(a)](1 - q_2)q_2^{j-1} \end{aligned} \quad (6.5)$$

For the linear case, $\mathbb{E}[D(a)] = j/\alpha$, leading to:

$$\begin{aligned} &\sum_{j=1}^{n_1} \frac{j}{\alpha} (1 - q_1)q_1^{j-1} + q_1^{n_1} \sum_{j=1}^{n_2} \frac{n_1 + j}{\alpha} (1 - q_2)q_2^{j-1} \\ &= \frac{1}{\alpha} \left[\frac{1 - q_1^{n_1}(1 + n_1(1 - q_1))}{1 - q_1} + n_1 q_1^{n_1} (1 - q_2^{n_2}) \right. \\ &\quad \left. + \frac{1 - q_2^{n_2}(1 + n_2(1 - q_2))}{1 - q_2} \right] \end{aligned} \quad (6.6)$$

Averaging over the Poisson distributions of n_1 and n_2 , we obtain equation (6.3). For the exponential case, the expectation of $D(a) = e^{\beta a}$ is computed by:

$$\begin{aligned}\mathbb{E}[D(a)] &= \int_0^\infty D(a) \frac{\alpha^j a^{j-1} e^{-\alpha a}}{(j-1)!} da \\ &= \frac{\alpha^j}{(\alpha - \beta)^j} \int_0^\infty \frac{(\alpha - \beta)^j a^{j-1} e^{-(\alpha - \beta)a}}{(j-1)!} da \\ &= \left(\frac{\alpha}{\alpha - \beta}\right)^j\end{aligned}$$

The term in the second integral being the probability density function of an $Erlang(j, \alpha - \beta)$ random variable, with $\alpha > \beta$ and denoting $c = \alpha/(\alpha - \beta)$, this transforms equation (6.5) into:

$$\begin{aligned}(1 - q_1) \sum_{j=1}^{n_1} c^j q_1^{j-1} + (1 - q_2) q_1^{n_1} \sum_{j=1}^{n_2} c^{n_1+j} q_2^{j-1} \\ = c \left[(1 - q_1) \frac{1 - (cq_1)^{n_1}}{(1 - cq_1)} + (1 - q_2) (cq_1)^{n_1} \frac{1 - (cq_2)^{n_2}}{(1 - cq_2)} \right]\end{aligned}\quad (6.7)$$

Averaging over the Poisson distributions of n_1 and n_2 , we obtain equation (6.4). \square

Note that for the LBT case, $a = j(\theta + \delta)$, and the expected value depreciation is calculated in equation (6.8) then plugged into equation (6.5). The resulting equation is averaged over the distributions f_{n_1} and f_{n_2} from equations (5.14-5.15), to obtain the functions $\bar{P}(\tau)$ and $\bar{D}(\tau)$.

$$\mathbb{E}[D(a)] = \begin{cases} j[\delta + \sum_{i=1}^\infty i f_\theta(i)] & : D(a) = a \\ e^{\beta j \delta} \sum_{i=1}^\infty e^{j \beta i} f_\theta(i) & : D(a) = e^{\beta a} \end{cases}\quad (6.8)$$

6.3.2 Solving the optimization problem

The behaviour of the objective functions $\bar{P}(\tau)$ and $\bar{D}(\tau)$ depends directly on the choice of P_1 and P_2 , however, the two functions are opposite in the sense of increasing and decreasing with τ .

To solve such a problem, linear scalarization method can be used to transform the multi-objective optimization problem to a single-objective one by combining the objective functions into a weighted sum, with priority given to the objectives with higher weights. Solving the resulting optimization

problem leads to Pareto optimal solutions to the multi-objective optimization problem. Recall that Pareto optimal solutions are the set of policies which satisfy all objectives for the given weights, and no other policy can improve one objective without degrading the others.

For our bi-objective case, we reformulate the optimization problem as:

$$\min_{\tau} \gamma \bar{P}(\tau) + (1 - \gamma) \bar{D}(\tau) \quad (6.9)$$

where $0 \leq \gamma \leq 1$ determines the priority given to the energy with respect to the value depreciation. $\bar{P}(\tau)$ and $\bar{D}(\tau)$ are normalized to 1 in order to illustrate the trade-off.

Figure 6.1 illustrates the performance for the age minimization case for an Aloha system. For each value of γ , the corresponding τ^* that minimizes equation (6.9) for an aggressive start policy is derived and the corresponding energy consumption and loss rate are obtained. When γ increases, the energy component becomes more important, and so it is reduced, while the age increases.

In order to validate the intuition of an aggressive start, we plot in Figure 6.2 the objective function (6.9) for the best aggressive start policy and the best mild start one. We observe that an aggressive start policy leads to a lower combined energy/age function than a mild start one, showing an opposite trend than the case where stringent requirements were to be met for URLLC transport. Note that both functions are normalized to 1.

6.3.3 Fixed point analysis for a field of sensors

When there are several sensors competing for the channel access, the same fixed point approach as for meeting the stringent URLLC requirements case can be followed, leading to the common policy τ^* that minimizes the objective function for all devices, when γ is fixed.

Figure 6.3 shows the average energy and value depreciation for a common policy to all sensors. The depreciation related to age decreases as expected when the policy is more aggressive, but then increases again as many sensors become aggressive, leading to a high packet repetition rate.

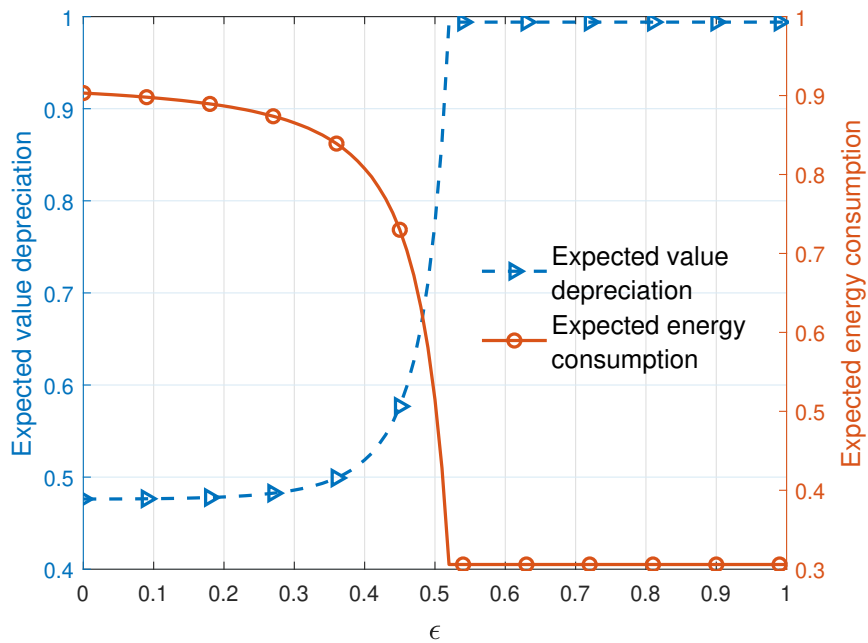


Figure 6.1: Energy consumption and value depreciation for Aloha and exponential value depreciation with $\beta = 2.4$, $\alpha = 5$, $P_1 = 0.5$, $P_2 = 0.1$, $q_1 = 0.1$, $q_2 = 0.5$

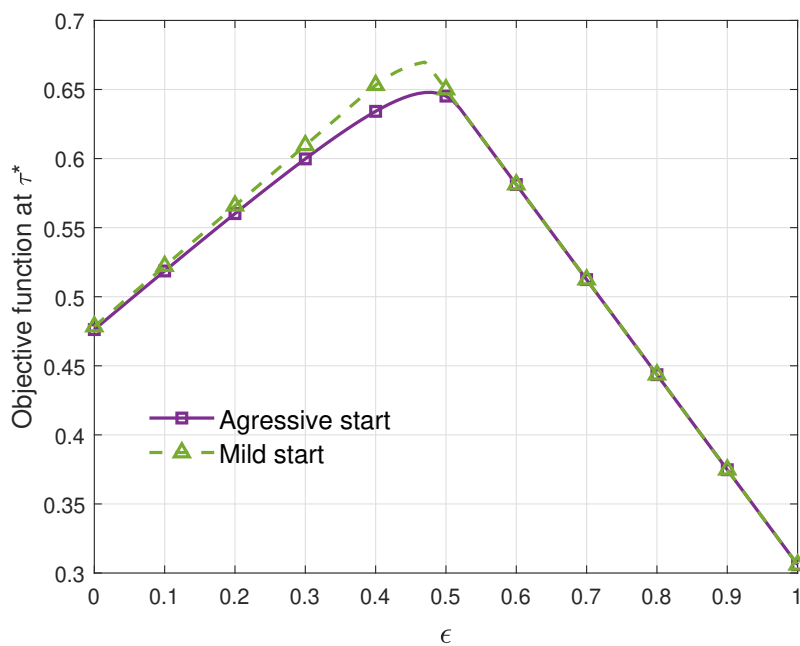


Figure 6.2: Comparing aggressive versus mild start for Aloha

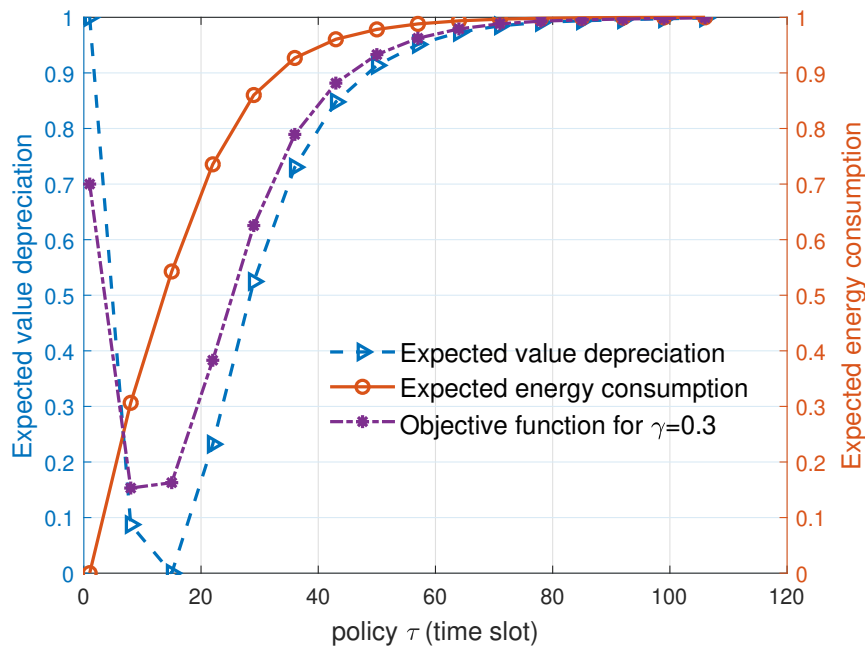


Figure 6.3: Energy consumption, value depreciation and objective function at $\gamma = 0.3$ for LBT in a field of sensors and exponential value depreciation with $\beta = 2$

6.4 Conclusion

We considered in this chapter scenarios where the freshness of information is essential and the value of a packet depreciates with its age. The optimal policy in this case is to start aggressively, in terms of transmission power, so as to ensure a better freshness performance as opposed to starting mildly which we showed in the previous chapter to be optimal for the case where the objective was to meet URLLC stringent delay and reliability constraints, as it allows to preserve energy. Note that a distributed learning approach can be implemented in the age minimization case as well, without requiring a prior knowledge of the system model, as in previous chapter, since optimal policies in the age minimization case does not suffer from rare events.

Chapter 7

General Conclusion and Perspectives

We focused in this thesis on the transport of critical services over unlicensed spectrum, since licensed spectrum is scarce and expensive. Our goal was to develop novel MAC techniques for optimal transmission of URLLC traffic with minimal cost.

We started, in Chapter 2, by studying the transport of URLLC over standalone unlicensed system. We proposed a Markov chain model that quantifies the reliability of the transmission under delay constraints. We also derived the capacity of the standalone unlicensed system in terms of the maximum number of stations verifying the stringent URLLC requirements.

Aiming to dimension the system capacity, we proposed in Chapter 3 the joint transmission of URLLC over unlicensed and licensed spectrum. The latter being an expensive asset, it is used only as a last resort when the former fails to transmit the packet within a fraction of the delay budget. This method requires a fine optimization of the fraction of the delay allocated to each system in order to minimize the cost, which is measured in terms of the additional licensed frequency resources needed to meet URLLC's requirements. This analysis was extended to a multi-tenant environment where tenants compete over the unlicensed resources, which may result in a tragedy of the commons type of situation. We proved the existence of at least one equilibrium point which minimizes the cost for all tenants.

We then studied the coexistence of URLLC with eMBB in unlicensed spectrum, in Chapter 4. As stated above, licensed resources being scarce and expensive, we proposed two transmission approaches based on the use of diversity in the power domain: URLLC is prioritized by transmitting at higher power than eMBB. The first method makes use of preemption using high power transmission when the URLLC delay budget is about to expire, which

violates LBT. The second one respects LBT and makes use of a time threshold within the delay budget, after which transmission power is switched from low to high.

Afterwards, we considered in Chapter 5 a decentralized setting, with no central entity to decide for the optimal policy to be followed by the URLLC stations. We focused on the time threshold method developed in the previous chapter, and analysed its performance in Aloha-like and LBT systems. We used an online learning approach to enable each station to achieve the optimal policy in a distributed manner. We also made use of our prior knowledge of the system model so as to accelerate the convergence of the learning algorithm.

In Chapter 6, we considered a different setting, for instance monitoring of a dynamic environment, where minimization of the age of the packets, or equivalently maximization of the freshness of information, is more valuable than meeting URLLC's strict reliability and delay constraints. We showed in the previous chapters that in the case of meeting URLLC stringent requirement, the optimal policies tend to start transmission with normal power level and then increase it as the packet delay approaches the allowed budget. However, when the objective is to minimize the delay of the packet, we show in this chapter that optimal policies favor starting at high power level.

Future work perspectives

In this thesis, we demonstrated the importance of unlicensed spectrum for 5G networks, and its ability of handling critical services in different scenarios. Some of the possible directions to continue this work are listed below.

- Following the line of the work done in Chapter 3, a thorough study of redundancy schemes in licensed spectrum can further reduce the cost of the joint transmission system. Indeed, 5G enables the integration of several Radio Access Technologies (RAT), for instance New Radio (NR) and legacy 4G, in addition to the unlicensed spectrum bands, and the packets can be duplicated in time, frequency and space dimensions.
- The coexistence of URLLC and eMBB in unlicensed spectrum introduced in Chapter 4 can be further investigated. In our work, we assumed that packets transmitted with normal power are totally lost in

case of collision. A possible approach is using Successive Interference Cancellation (SIC) [54], where it is possible to recover two packets transmitted simultaneously by first decoding the stronger signal, then subtracting it from the combined signal. This is possible in the case where one high-power URLLC packet is transmitted simultaneously with one normal-power eMBB packet, this can allow the receiver to recover both packets.

- A dynamic slicing technique [55] can extend the works in Chapters 3 and 4, where the reserved URLLC resources can be adapted depending on the traffic load and external interference. This adaptation may be performed using learning algorithms, where stations can adapt their policies depending on the sensed interference and hence the central entity responsible for reserving the URLLC resources can learn the environment based on the feedback from the stations and adapt its share of spectrum accordingly [56]. As tenants need to adapt their share of the spectrum, the operator can hence deploy some pricing policies based on the tenants' demands [57].
- We limited ourselves in Chapters 4, 5 and 6 to two power level policies. This work can be extended to include multiple power levels, which helps in reducing the energy consumption where the transmission power can be adapted depending on the channel conditions of each transmitter for instance.
- The distributed learning approach in Chapter 5 paves the way for interesting extensions. For instance, federated learning [58], also known as collaborative learning, can be considered. In this case, learners exchange their knowledge about the system and help accelerate the learning process. This can also be deployed in dynamic environments, i.e., when the number of stations and traffic intensity change "rapidly" in time. This allows a faster learning and adaptation to the optimal policy.
- The thesis focused principally on critical services meeting reliability and delay constraints, in a URLLC QoS framework. We briefly studied in Chapter 6 another type of critical services, which concentrates on the freshness of the information more than the reliability within a given delay for packets. This AoI framework can be extended to different types of applications, for example, where sources monitor a very

dynamic environments and have to decide, not only the power transmission strategy, but also the packet generation time. The history of transmissions is hence important for the source, as well as the behavior of the monitored system.

Bibliography

- [1] International Telecommunication Union (ITU). Imt vision–framework and overall objectives of the future development of imt for 2020 and beyond. *Recommendation ITU*, 2083, 2015.
- [2] *5G; Study on Scenarios and Requirements for Next Generation Access Technologies*. 3GPP, 5 2017. version 14.2.0 Release 14.
- [3] French state to raise 2.8 billion euros from 5g spectrum sale. *Reuters*, 2020. URL <https://www.reuters.com/article/us-france-telecoms-5g-exclusive/exclusive-french-state-to-raise-2-8-billion-euros-from-5g-spectrum-sale-source>
- [4] *Feasibility Study on Licensed-Assisted Access to Unlicensed Spectrum*. 3GPP, 5 2015. version 13.0.0 Release 13.
- [5] *5G; Study on New Radio (NR) access technology*. 3GPP, 9 2018. version 15.0.0 Release 15.
- [6] Jianping Song, Song Han, Al Mok, Deji Chen, Mike Lucas, Mark Nixon, and Wally Pratt. Wirelesshart: Applying wireless technology in real-time industrial process control. In *2008 IEEE Real-Time and Embedded Technology and Applications Symposium*, pages 377–386. IEEE, 2008.
- [7] Claudio Rosa, Markku Kuusela, Frank Frederiksen, and Klaus I Pederesen. Standalone lte in unlicensed spectrum: Radio challenges, solutions, and performance of multefire. *IEEE Communications Magazine*, 56(10): 170–177, 2018.
- [8] Daniel Jiang and Luca Delgrossi. Ieee 802.11 p: Towards an international standard for wireless access in vehicular environments. In *VTC Spring 2008-IEEE Vehicular Technology Conference*, pages 2036–2040. IEEE, 2008.

- [9] Nikita Lyamin, Qichen Deng, and Alexey Vinel. Study of the platooning fuel efficiency under etsi its-g5 communications. In *2016 IEEE 19th International Conference on Intelligent Transportation Systems (ITSC)*, pages 551–556. IEEE, 2016.
- [10] Aloÿs Augustin, Jiazi Yi, Thomas Clausen, and William Mark Townsley. A study of lora: Long range & low power networks for the internet of things. *Sensors*, 16(9):1466, 2016.
- [11] Juan Carlos Zuniga and Benoit Ponsard. Sigfox system description. *LP-WAN@ IETF97, Nov. 14th*, 25, 2016.
- [12] IEEE. Ieee standard for wireless lan medium access control (mac) and physical layer (phy) specifications. November 1997.
- [13] Gordon J Sutton, Jie Zeng, Ren Ping Liu, Wei Ni, Diep N Nguyen, Beeshanga A Jayawickrama, Xiaojing Huang, Mehran Abolhasan, and Zhang Zhang. Enabling ultra-reliable and low-latency communications through unlicensed spectrum. *IEEE Network*, 32(2):70–77, 2018.
- [14] Roberto Maldonado Cuevas, Claudio Rosa, Frank Frederiksen, and Klaus I Pedersen. On the impact of listen-before-talk on ultra-reliable low-latency communications. In *2018 IEEE Global Communications Conference (GLOBECOM)*, pages 1–6. IEEE, 2018.
- [15] Gordon J Sutton, Ren Ping Liu, and Y Jay Guo. Delay and reliability of load-based listen-before-talk in laa. *IEEE Access*, 6:6171–6182, 2017.
- [16] Giuseppe Bianchi. Performance analysis of the ieee 802.11 distributed coordination function. *IEEE Journal on selected areas in communications*, 18(3):535–547, 2000.
- [17] *Physical layer procedures*. 3GPP, 7 2018. version 15.1.0 Release 15.
- [18] Periklis Chatzimisios, Anthony C Boucouvalas, and Vasileios Vitsas. Ieee 802.11 packet delay-a finite retry limit analysis. In *GLOBECOM'03. IEEE Global Telecommunications Conference (IEEE Cat. No. 03CH37489)*, volume 2, pages 950–954. IEEE, 2003.
- [19] Ren Ping Liu, Gordon Sutton, and Iain B Collings. A 3-d markov chain queueing model of ieee 802.11 dcf with finite buffer and load. In *2009 IEEE International Conference on Communications*, pages 1–5. IEEE, 2009.

- [20] Gabriel Martorell, Guillem Femenias, and Felip Riera-Palou. A refined 3d markov model for non-saturated ieee 802.11 dcf networks. In *2013 IFIP Wireless Days (WD)*, pages 1–8. IEEE, 2013.
- [21] Yuan Gao, Xiaoli Chu, and Jie Zhang. Performance analysis of laa and wifi coexistence in unlicensed spectrum based on markov chain. In *2016 IEEE Global Communications Conference (GLOBECOM)*, pages 1–6. IEEE, 2016.
- [22] Ieee standard for information technology– local and metropolitan area networks– specific requirements– part 11: Wireless lan medium access control (mac)and physical layer (phy) specifications amendment 5: Enhancements for higher throughput. *IEEE Std 802.11n-2009 (Amendment to IEEE Std 802.11-2007 as amended by IEEE Std 802.11k-2008, IEEE Std 802.11r-2008, IEEE Std 802.11y-2008, and IEEE Std 802.11w-2009)*, pages 1–565, 2009.
- [23] Zhiyi Zhou, Dongning Guo, and Michael L Honig. Licensed and unlicensed spectrum allocation in heterogeneous networks. *IEEE Transactions on Communications*, 65(4):1815–1827, 2017.
- [24] Georg Hampel, Chong Li, and Junyi Li. 5g ultra-reliable low-latency communications in factory automation leveraging licensed and unlicensed bands. *IEEE Communications Magazine*, 57(5):117–123, 2019.
- [25] Bikramjit Singh, Olav Tirkkonen, Zexian Li, and Mikko A Uusitalo. Contention-based access for ultra-reliable low latency uplink transmissions. *IEEE Wireless Communications Letters*, 7(2):182–185, 2017.
- [26] 3GPP. Study on latency reduction techniques for LTE. 3GPP TR 36.881 v14.0.0, Tech. Rep., June 2016.
- [27] Jocelyne Elias, Fabio Martignon, Antonio Capone, and Eitan Altman. Non-cooperative spectrum access in cognitive radio networks: A game theoretical model. *Computer Networks*, 55(17):3832–3846, 2011.
- [28] Samson Lasaulce, Merouane Debbah, and Eitan Altman. Methodologies for analyzing equilibria in wireless games. *IEEE Signal Processing Magazine*, 26(5):41–52, 2009.

- [29] John Nash. Non-cooperative games. *Annals of mathematics*, pages 286–295, 1951.
- [30] Petar Popovski, Kasper Fløe Trillingsgaard, Osvaldo Simeone, and Giuseppe Durisi. 5g wireless network slicing for embb, urllc, and mmhc: A communication-theoretic view. *IEEE Access*, 6:55765–55779, 2018.
- [31] Yuanwei Liu, Zhijin Qin, Maged Elkhshlan, Zhiguo Ding, Arumugam Nallanathan, and Lajos Hanzo. Non-orthogonal multiple access for 5g and beyond. *arXiv preprint arXiv:1808.00277*, 2018.
- [32] Klaus I Pedersen, Guillermo Pocovi, Jens Steiner, and Saeed R Khosravirad. Punctured scheduling for critical low latency data on a shared channel with mobile broadband. In *2017 IEEE 86th Vehicular Technology Conference (VTC-Fall)*, pages 1–6. IEEE, 2017.
- [33] Arjun Anand, Gustavo De Veciana, and Sanjay Shakkottai. Joint scheduling of urllc and embb traffic in 5g wireless networks. In *IEEE INFOCOM 2018-IEEE Conference on Computer Communications*, pages 1970–1978. IEEE, 2018.
- [34] Anupam Kumar Bairagi, Md Shirajum Munir, Sarder Fakhrul Abedin, and Choong Seon Hong. Utilization of unlicensed spectrum in effective coexistence of embb and urllc. pages 1058–1060, 2018.
- [35] Renato Abreu, Thomas Jacobsen, Gilberto Berardinelli, Klaus Pedersen, István Z Kovács, and Preben Mogensen. Power control optimization for uplink grant-free urllc. In *2018 IEEE Wireless Communications and Networking Conference (WCNC)*, pages 1–6. IEEE, 2018.
- [36] Richard S Sutton and Andrew G Barto. Reinforcement learning: An introduction. 2011.
- [37] Mark Eisen, Clark Zhang, Luiz FO Chamon, Daniel D Lee, and Alejandro Ribeiro. Learning optimal resource allocations in wireless systems. *IEEE Transactions on Signal Processing*, 67(10):2775–2790, 2019.
- [38] Ioan-Sorin Comşa, Sijing Zhang, Mehmet Emin Aydin, Pierre Kuonen, Yao Lu, Ramona Trestian, and Gheorghiu Ghinea. Towards 5g: A reinforcement learning-based scheduling solution for data traffic management. *IEEE Transactions on Network and Service Management*, 15(4):1661–1675, 2018.

- [39] Medhat Elsayed and Melike Erol-Kantarci. Reinforcement learning-based joint power and resource allocation for urllc in 5g. In *2019 IEEE Global Communications Conference (GLOBECOM)*, pages 1–6. IEEE, 2019.
- [40] Madyan Alsenwi, Nguyen H Tran, Mehdi Bennis, Shashi Raj Pandey, Anupam Kumar Bairagi, and Choong Seon Hong. Intelligent resource slicing for embb and urllc coexistence in 5g and beyond: A deep reinforcement learning based approach. *arXiv preprint arXiv:2003.07651*, 2020.
- [41] Amin Azari, Mustafa Ozger, and Cicek Cavdar. Risk-aware resource allocation for urllc: Challenges and strategies with machine learning. *IEEE Communications Magazine*, 57(3):42–48, 2019.
- [42] Jordan Frank, Shie Mannor, and Doina Precup. Reinforcement learning in the presence of rare events. In *Proceedings of the 25th international conference on Machine learning*, pages 336–343, 2008.
- [43] Robby Goetschalckx. The use of domain knowledge in reinforcement learning (het gebruik van domeinkennis in reinforcement learning). 2009.
- [44] Gordon J Sutton, Ren Ping Liu, and Y Jay Guo. Delay and reliability of load-based listen-before-talk in laa. *IEEE Access*, 6, 2018.
- [45] Sheldon M. Ross. *Introduction to Probability Models, 12th Edition*. 2019. ISBN 978-0-12-814346-9.
- [46] Rachana Ashok Gupta and Mo-Yuen Chow. Networked control system: Overview and research trends. *IEEE transactions on industrial electronics*, 57(7):2527–2535, 2009.
- [47] Zonghui Li, Hai Wan, Boxu Zhao, Yangdong Deng, and Ming Gu. Dynamically optimizing end-to-end latency for time-triggered networks. In *Proceedings of the ACM SIGCOMM 2019 Workshop on Networking for Emerging Applications and Technologies*, pages 36–42, 2019.
- [48] Sanjit Kaul, Marco Gruteser, Vinuth Rai, and John Kenney. Minimizing age of information in vehicular networks. In *2011 8th Annual IEEE Communications Society Conference on Sensor, Mesh and Ad Hoc Communications and Networks*, pages 350–358. IEEE, 2011.

- [49] Antzela Kosta, Nikolaos Pappas, and Vangelis Angelakis. Age of information: A new concept, metric, and tool. *Foundations and Trends in Networking*, 12(3):162–259, 2017.
- [50] Arunabh Srivastava, Abhishek Sinha, and Krishna Jagannathan. On minimizing the maximum age-of-information for wireless erasure channels. *arXiv preprint arXiv:1904.00647*, 2019.
- [51] Mohamed K Abdel-Aziz, Sumudu Samarakoon, Chen-Feng Liu, Mehdi Bennis, and Walid Saad. Optimized age of information tail for ultra-reliable low-latency communications in vehicular networks. *IEEE Transactions on Communications*, 68(3):1911–1924, 2019.
- [52] Xi Zhang, Qixuan Zhu, and H Vincent Poor. Analyses for age of information supporting urlc over multimedia wireless networks. In *2020 IEEE 21st International Workshop on Signal Processing Advances in Wireless Communications (SPAWC)*, pages 1–5. IEEE, 2020.
- [53] Ali Maatouk, Saad Kriouile, Mohamad Assaad, and Anthony Ephremides. The age of incorrect information: A new performance metric for status updates. *arXiv preprint arXiv:1907.06604*, 2019.
- [54] Souvik Sen, Naveen Santhapuri, Romit Roy Choudhury, and Srihari Nelakuditi. Successive interference cancellation: A back-of-the-envelope perspective. In *Proceedings of the 9th ACM SIGCOMM Workshop on Hot Topics in Networks*, pages 1–6, 2010.
- [55] Alessandro Lieto, Ilaria Malanchini, Anwar Walid, and Antonio Capone. Quantifying the gain of dynamic network slicing under stringent constraints. In *2019 IEEE Global Communications Conference (GLOBECOM)*, pages 1–6. IEEE, 2019.
- [56] Francesca Fossati, Stefano Moretti, Stephane Rovedakis, and Stefano Secci. Decentralization of 5g slice resource allocation. In *NOMS 2020-2020 IEEE/IFIP Network Operations and Management Symposium*, pages 1–9. IEEE, 2020.
- [57] Haïkel Yaïche, Ravi R Mazumdar, and Catherine Rosenberg. A game theoretic framework for bandwidth allocation and pricing in broadband networks. *IEEE/ACM transactions on networking*, 8(5):667–678, 2000.

-
- [58] Qiang Yang, Yang Liu, Tianjian Chen, and Yongxin Tong. Federated machine learning: Concept and applications. *ACM Transactions on Intelligent Systems and Technology (TIST)*, 10(2):1–19, 2019.

Titre: Transport des services critiques dans le spectre non-licencié des réseaux 5G

Mots clés: 5G, services critiques, spectre non-licencié, URLLC

Résumé:

Cette thèse étudie le transport de services critiques dans les réseaux 5G, où le spectre non-licencié est préconisé pour minimiser le coût et faire face à la forte demande de ressources en fréquences. Nous évaluons d'abord les performances des services critiques type URLLC (Ultra-Reliable Low-Latency Communication) qui a des exigences strictes en matière de fiabilité et de latence, de l'ordre de 99,999% et 1 ms, respectivement, transporté dans le spectre non-licencié. Nous proposons un modèle basé sur une chaîne de Markov pour quantifier la fiabilité sous contrainte de délai, sous procédure d'accès au support Listen-Before-Talk (LBT), puis nous en déduisons le nombre maximum de stations pouvant être servies en même temps, tout en respectant l'URLLC contraintes. Cette analyse est ensuite utilisée pour étudier de nouvelles méthodes pour la transmission conjointe d'URLLC sur les spectres non-licencié et licencié. Nous proposons trois méthodes pour l'accès conjoint aux ressources disponibles et démontrons que la méthode optimale pour accéder aux ressources consiste à utiliser des ressources licenciées, uniquement lorsque la transmission dans le système non-licencié échoue dans un budget de temps donné. Cette méthode est ensuite étudiée dans le cas de plusieurs tenants à proximité en concurrence sur le même canal non-licencié. Si tous les tenants essaient de maximiser leur utilisation des ressources non-licenciées, tout le monde se retrouvera dans une situation type "tragédie des biens communs". Nous montrons qu'au moins un point d'équilibre existe pour ce système qui minimise le coût pour tous les tenants. Nous étudions ensuite la coexistence d'URLLC avec d'autres services 5G, tels que le haut débit mobile amélioré eMBB (enhanced Mobile Broadband), dans le spectre non-licencié. eMBB a de grandes paquets et son multiplexage avec URLLC peut entraîner une forte dégradation des performances d'URLLC.

Pour cela, nous proposons une nouvelle technique pour prioriser les paquets URLLC en les transmettant avec une puissance plus élevée. Cependant, la transmission à haute puissance n'est pas systématiquement effectuée afin de réduire les interférences sur les autres utilisateurs et aussi pour réduire la consommation d'énergie, ce qui est très important pour les appareils alimentés par batterie. Dans ce cas, deux méthodes ont été proposées pour transmettre avec une puissance élevée, en ne le laissant qu'en dernier recours. L'un est indépendant du LBT et transmet une fois le délai de paquet approche de l'expiration, tandis que l'autre respecte le LBT et n'utilise une puissance élevée que lorsque les opportunités de transmission se produisent au-delà d'un seuil de temps. Nous proposons ensuite une mise en œuvre décentralisée de l'approche par seuil de temps décrit ci-dessus. Nous formulons le problème dans le cadre d'optimisation où les émetteurs doivent choisir la politique optimale (seuil de temps) qui minimise la consommation d'énergie tout en préservant les exigences d'URLLC. Nous résolvons ensuite le problème d'optimisation en utilisant une approche d'apprentissage et montrons une lente convergence vers la politique optimale du fait que les pertes sont des événements rares. Pour y remédier, nous utilisons le cadre d'optimisation et la connaissance préalable du système pour accélérer cet apprentissage. Nous étudions enfin l'approche décentralisée pour un type différent de services critiques qui met l'accent sur la fraîcheur de l'information, connue sous le nom d'Age de l'Information (AoI). Dans ce contexte, au lieu de garantir une cible de fiabilité dans un délai, le paquet doit être livré dès sa génération, sinon sa valeur se dégrade. Nous démontrons que les politiques optimales dans le contexte AoI ont tendance à démarrer de manière agressive et à réduire la puissance de transmission lorsque l'âge du paquet augmente.

Title: Transport of critical services over unlicensed spectrum in 5G networks

Keywords: 5G, critical services, Unlicensed spectrum, URLLC

Abstract: We study in this thesis the transport of critical services in 5G networks, where unlicensed spectrum is advocated so as to minimize the cost and to cope with the high demand for frequency resources. We first evaluate the performance of Ultra-Reliable Low-Latency Communication (URLLC) which has stringent requirements on reliability and delay, on the order of 99.999% and 1 ms, respectively, transported in unlicensed spectrum. We propose a model based on a Markov chain that quantifies the reliability within a delay constraint under Listen-Before-Talk (LBT) medium access procedure, and deduce the maximum number of stations that can be handled at the same time, while respecting URLLC constraints. This analysis is then used to investigate novel methods for the joint transmission of URLLC over unlicensed and licensed spectrum. We propose three methods for the joint access to available resources, and demonstrate that the optimal method to access the resources is by using licensed ones only when unlicensed transmission fails within a given time budget. This method is then studied in the case of multiple tenants in proximity competing over the same unlicensed channel. If all tenants try to maximize their usage of unlicensed resources then everyone will end up in a tragedy of the commons type of situation. We show that at least one equilibrium point exists for this system which minimizes the cost for all tenants. We study next the coexistence of URLLC with other 5G services, such as enhanced Mobile Broadband (eMBB), in unlicensed spectrum. eMBB has large packets and its multiplexing with URLLC may entail a large degradation in the latter's performance. We then propose a new

technique to prioritize URLLC packets by transmitting them with higher power. However, high power transmission is not systematically performed so as to reduce the interference on other users and also to minimize energy consumption, which is very important for battery-powered devices. In this case, we propose two methods to transmit with high power, as a last resort: one that is LBT-agnostic and transmits whenever the packet delay approaches time-out, and another one which respects LBT and uses high power only when transmission opportunities occur beyond a time threshold. We then propose a decentralized implementation of the time-threshold approach. We formulate the problem as an optimization problem where transmitters are to choose the optimal policy (time threshold) which minimizes the energy consumption while preserving URLLC requirements. We then solve the optimization problem using a learning approach, which suffers from slow convergence to the optimal policy due to the fact that losses are rare events. To remedy to this, we make use of our optimization framework and the prior knowledge of the system model to accelerate this learning. We finally study the decentralized approach for a different type of critical services which focuses on the freshness of the information, known as the Age of Information (AoI). In this context, instead of guaranteeing URLLC's reliability target within a delay, the packet must be delivered as soon as it is generated, or else it loses its value. We demonstrate that optimal policies in the AoI context tend to start aggressively, and reduce the transmission power when the age of the packet increases.